
Nonlinear Maneuver Autopilot for the F-15 Aircraft

P.K.A. Menon, M.E. Badgett, and R.A. Walker

Contract NAS 2-11877
June 1989

(NASA-CR-179442) NONLINEAR MANEUVER
AUTOPILOT FOR THE F-15 AIRCRAFT Final Report
(Integrated Systems) 90 p CSCL 09B

N90-11487

G3/63 Unclass
0235687



Nonlinear Maneuver Autopilot for the F-15 Aircraft

P.K.A. Menon, M.E. Badgett, and R.A. Walker
Integrated Systems, Inc., 101 University Avenue, Palo Alto, CA 94301

Prepared for
Ames Research Center
Dryden Flight Research Facility
Edwards, California
Under Contract NAS 2-11877

1989



National Aeronautics and
Space Administration
Ames Research Center
Dryden Flight Research Facility
Edwards, California 93523-5000

TABLE OF CONTENTS

Chapter I Introduction	1
1.1 Background	1
1.2 Summary of Results	3
1.3 Report Organization	3
Chapter II Flight Test Trajectory Controller Synthesis	4
2.1 Aircraft Model	4
2.2 Command Augmentation System	6
2.3 Controller Synthesis	7
2.3.1 Controller for the Airspeed V	7
2.3.2 Controller for Altitude h	9
2.3.3 Controller for Angle of Attack α	11
2.3.4 Controller for the Roll Attitude ϕ	13
2.3.5 Maneuver Control with Pilot-in-the-loop	14
Chapter III Controller Evaluation	15
3.1 Simulation	15
3.2 System Build simulation of Aircraft and Controller	15
3.3 Flight Test Trajectory Control Simulation	17
3.3.1 Level Acceleration Flight Test Trajectory	17
3.3.2 Pushover/Pullup Trajectory	18
3.3.3 Zoom and Pushover Flight Test Trajectory	28
3.3.4 Excess Thrust Windup Turn	28
3.3.5 Constant Thrust Windup Turn	45
3.3.6 Constant Dynamic Pressure, Constant Load Factor Trajectory	45
3.4 Conclusions	58
Chapter IV Conclusions and Future Work	72
4.1 Future Work	72
References	73
Appendix A Nonlinear Flight Test Trajectory Controllers for Aircraft	A-1

Chapter I

Introduction

1.1. Background

The motivation for the development of flight test trajectory controllers is well documented in the literature [1 - 6]. In the past, several control system design techniques have been applied to this problem, viz, the LQR approach [4], the eigenstructure assignment technique [5], Kosut's suboptimal LQR design with guaranteed stability margin and minimum error excitation criterion [6]. In order to apply these approaches, one is required to linearize the aircraft model about the desired flight test trajectory. The linearized aircraft model is then a combination of a linear perturbation model and open-loop state-control histories along the desired flight test maneuver. A closed-loop perturbation controller can then be synthesized using one of the several techniques for linear system design. Since the linearized model changes as a function of the flight condition, gain scheduling is invariably required to obtain satisfactory control system response. Note that the linearized model generates only a part of the total control. The second component of control is provided by the trim values of the control variables along the desired trajectory. This part of control is open-loop. Thus the flight test trajectory controller is a combination of closed-loop linear perturbation control and the open-loop trim control. While such an approach can certainly be made to work for arbitrary nonlinear plants, the amount of data that has to be stored can sometimes be prohibitive. In such case, one is forced to compromise and store the gains and open-loop controls at sparser intervals. As a consequence, the control system suffers performance degradation. It is often possible to partially compensate for this performance loss by designing relatively parameter insensitive controllers. However, the performance degradation due to lack of fidelity in the trim control settings are often more difficult to correct. In addition to this, there is another mechanism responsible for the degradation of these controllers, viz, the effect of off-nominal conditions. This arises due to the inaccuracy of the linearized model when the aircraft is far from the desired trajectory. The trim controls as well as the closed-loop controls in this case would be in error. It is interesting to note here that this effect can arise even if the gains and open-loop settings are stored at close intervals. Several of these issues were addressed in an earlier contract with NASA Ames-Dryden Flight Research Facility [6].

Recently, an alternate approach for nonlinear control synthesis has emerged [7-13]. The development of this technique for flight controls is due to G. Meyer of NASA Ames Research Center. Much of the initial theoretical foundations in this area were laid by Brockett [14], Hunt, Su and Meyer [11-13]. In this work, the nonlinear dynamic model is assumed to be of the form

$$\dot{x} = f(x) + g(x)u \quad (1.1)$$

The simplest case arises when the number of states in the model are equal to the

number of controls. In this case, if $g(x)$ is invertible and x is perfectly known, the above system can be transformed to the form

$$\dot{x} = V \tag{1.2}$$

where,

$$V = f(x) + g(x)u, \tag{1.3}$$

are the pseudo control variables. A linear feedback controller can be designed for the system (1.2). This controller will be of the form

$$V = kx. \tag{1.4}$$

The expressions (1.3) and (1.4) can now be combined to obtain the nonlinear controller of the form

$$u = g(x)^{-1}[kx - f(x)] \tag{1.5}$$

It is clear that if $f(x)$ and $g(x)$ are perfectly known, the nonlinear controller (1.5) will have all the attributes of the pseudo linear controller (1.4). More often than not, this information is not perfect. As a result, one may have to compensate for this error by building-in extra margins in the controller (1.4) through the introduction of additional compensators. Note that in this development, only the control variables were transformed. In general, whenever the state-control excess is zero, the prelinearizing transformation will leave the original system states unaltered, modifying only the control variables.

In most practical situations, however, the number of controls are less than the number of states. In this case, a simple transformation such as the one described above is no longer feasible. A prelinearizing transformation may still be synthesized, but the states will not remain unaltered under this transformation. Moreover, the prelinearizing transformation would involve the partial derivatives of the right-hand-sides of the original nonlinear system. This would require one to impose certain other conditions on the functions $f(x)$ and $g(x)$. Such requirements are naturally handled in the language of Lie group germs and Lie algebras, see Guggenheimer [15] for an initial exposition and Hunt, Su and Meyer [11] for specific details.

In the cases where the number of controls exceed the number of states, one has freedom in choosing the combination of controls to be employed in a particular situation. This is a natural setting for system optimization. One such case has been discussed by Cicolani, Sridhar and Meyer [16].

Attempting to construct prelinearizing transformations in the case where the number of control variables are less than the number of states will invariably lead to the computation of several partial derivatives, which can sometimes make the problem ill-posed.

An alternate approach was proposed recently [17] using singular perturbation theory. Aircraft forms a natural system for the application of singular perturbation theory since, there clearly are slow and fast modes in the system. For example, the body rates evolve faster than other state variables. The use of singular perturbation theory in the aircraft control problem can eliminate the need for partial derivatives to a certain extent. This can improve the problem conditioning significantly. Moreover, the controller requires less computations, making it more efficient for on-line implementation. Reference [17] discusses the details of the approach. This paper is given in Appendix A.

Two modes of operation for the flight test trajectory controllers have been identified in the literature [2]. The first is that of trajectory tracking with pilot - in - the - loop and the second, a completely automatic operation. The attention will be focussed on the latter, though the manual flight test trajectory control aspect will be briefly examined.

1.2. Summary of Results

The results of the present study are summarized in the following.

1. A systematic approach for the development of flight control systems using singular perturbation theory and the theory of prelinearizing transformation was developed. A paper containing this work has been presented at the Guidance and Control Conference at Snow Mass, Co. which is appended at the end of this report.
2. The inclusion of the Command Augmentation System (CAS) in the aircraft model modifies the flight test trajectory control problem considerably. Specifically, the boundary layer corrections required in the original singular perturbation approach are no longer required. This simplifies the control system development considerably.
3. The performance of the synthesized controllers are evaluated along the six required flight test maneuvers using a complete simulation of the CAS and the aircraft.

In the next project phase, these controllers will be evaluated in a manned simulation before attempting a flight test.

1.3. Report Organization

A description of the flight test trajectory control system is given in Chapter II. This chapter also gives the details of the nonlinear controller synthesis. In Chapter III, the controller performance for the six required flight test maneuvers are given. Conclusions and future work are outlined in Chapter IV. Appendix A presents a paper describing the application of singular perturbation theory for synthesizing nonlinear controllers for aircraft.

Chapter II
Flight Test Trajectory Controller Synthesis

2.1. Aircraft Model

The six-degrees of freedom model for aircraft flight over a flat nonrotating earth is given by :

$$\dot{V} = [-D\cos\beta + S\sin\beta + (k_1\cos\alpha\cos\beta + k_3\sin\alpha\cos\beta)T - mg(\sin\theta\cos\alpha\cos\beta - \cos\theta\sin\phi\sin\beta - \cos\theta\cos\phi\sin\alpha\cos\beta)]/m \quad (2.1)$$

$$\dot{\alpha} = [-L + (k_3\cos\alpha - k_1\sin\alpha)T + mg(\cos\theta\cos\phi\cos\alpha + \sin\theta\sin\alpha)]/mV\cos\beta + q - \tan\beta(p\cos\alpha + r\sin\alpha) \quad (2.2)$$

$$\dot{\beta} = [D\sin\beta + S\cos\beta - (k_1\cos\alpha\sin\beta + k_3\sin\alpha\sin\beta)T + mg(\sin\theta\cos\alpha\sin\beta + \cos\theta\sin\phi\cos\beta - \cos\theta\cos\phi\sin\alpha\sin\beta)]/Vm + p\sin\alpha - r\cos\alpha \quad (2.3)$$

$$\dot{h} = V(\cos\beta\cos\alpha\sin\theta - \sin\beta\sin\phi\cos\theta - \cos\beta\sin\alpha\cos\phi\cos\theta) \quad (2.4)$$

$$\dot{\phi} = p + q\sin\phi\tan\theta + r\cos\phi\tan\theta \quad (2.5)$$

$$\dot{\theta} = q\cos\phi - r\sin\phi \quad (2.6)$$

$$\dot{p} = [PI_1 + RI_3 + e_1I_1\delta_e + e_2I_1\delta_a + e_3I_1\delta_r + pq(I_{xz}I_1 - D_xI_3) - qr(D_xI_1 + I_{xz}I_3)]/I \quad (2.7)$$

$$\dot{q} = [QI_4 + f_1I_4\delta_e + f_2I_4\delta_a + f_3I_4\delta_r + p^2I_{xz}I_4 - prD_yI_4 + r^2I_{xz}I_4]/I \quad (2.8)$$

$$\begin{aligned} \dot{r} = [PI_3 + RI_6 + g_1I_6\delta_e + g_2I_6\delta_a + g_3I_6\delta_r + pq(I_{xz}I_3 - D_xI_6) \\ - qr(D_xI_3 + I_{xz}I_6)]/I \end{aligned} \quad (2.9)$$

With

$$I_1 = I_yI_x$$

$$I_3 = I_yI_{xz}$$

$$I_4 = I_xI_x - I_{xz}$$

$$I_6 = I_xI_y$$

$$D_x = I_x - I_y$$

$$D_y = I_x - I_x$$

$$I = I_xI_yI_x - I_yI_{xz}^2$$

$$I_{xy} = I_{yx} = 0 \quad \text{for the Aircraft under consideration.}$$

The state variables in this model are V the airspeed, h the altitude, α the angle of attack, β the angle of sideslip, θ the pitch attitude, ϕ the roll attitude, p the roll body rate, q the pitch body rate, and r the yaw body rate. The yaw attitude ψ , down range x and the cross range y are ignorable in the flight test trajectory control problem. The control variables in this model are throttle, the elevator deflection δ_e , the rudder deflection δ_r and the differential tail δ_a . P , Q , and R are the total aerodynamic and thrust moments about the roll, pitch, and yaw body axes, not including the moments due to control surface deflections. The variables e_1 , e_2 , e_3 , f_1 , f_2 , f_3 , g_1 , g_2 , g_3 are the control surface influence coefficients for roll, pitch and yaw axes, respectively. Though the aircraft is equipped with ailerons, flaps and speed brake, these are accessible only through manual control. The

aircraft has a command augmentation system (CAS), which has inputs from the joystick and rudder pedals, and also from the autopilot. For automatic flight test maneuvering, it will be assumed that the pilot inputs are zero and that the autopilot input port will be connected to the flight test trajectory controller. In all that follows, for the sake of brevity, the flight test trajectory controller will be termed the Maneuver Autopilot (MAP). For a more detailed nomenclature, see the paper given in Appendix A.

In addition to this, the aircraft engine dynamics of the form

$$\dot{\eta} = \tau(\eta_c - \eta) \quad (2.10)$$

will be included in the analysis. In equation (2.10), η is the actual throttle setting while η_c is the commanded throttle setting. τ is the engine time constant. In reality, the engine dynamics is much more complex than that given by the expression (2.10). But inclusion of these in the analysis will complicate the development and may not lead to simple control laws. Earlier work [2] has shown that this model is adequate in the flight test trajectory controller development.

If the aircraft did not have a Command Augmentation system, the flight test trajectory controller may be designed by splitting the dynamics into slow and fast modes and applying the methods of singular perturbation theory and the theory of prelinearizing transformations as in [17].

On the otherhand, if a command augmentation system is integrated with the airframe, the maneuver autopilot should work through this system in order to access the aircraft control surfaces. In this case, the formal application of the singular perturbation theory is no longer feasible due to the noninvertible CAS dynamics. However, if we assume that the CAS dynamics is stable and sufficiently fast, one needs to construct only the slow controller, leaving the task of boundary layer corrections to the CAS. This approach will be followed in the present work.

2.2. Command Augmentation System

The CAS forms the interface between the pilot, the autopilot, and the aircraft control surfaces. Since the present effort is in generating a completely automatic maneuver autopilot, the MAP has to effect trajectory tracking through the autopilot inputs in the CAS.

The autopilot inputs of the command augmentation system consists of three control channels, the input commands of which are a_n the normal acceleration in g 's, p the roll rate and β the angle of sideslip. It is important to note that these inputs were not supplied by the aircraft manufacturer, but were identified after several simulations on the aircraft and CAS system. We assume here that the CAS system is capable of controlling these three quantities with a sufficient degree of accuracy and speed. Thus, if a MAP system generates these input quantities, we leave the burden of maintaining these at the desired value to the CAS system. It is to reasonable to assume that the CAS has stable, fast dynamics because, otherwise, the aircraft would have been difficult to fly in the

first place. If the resulting system is found to have an unacceptable performance, it may become necessary to provide additional feedback compensation for the CAS. Fortunately, this case did not arise in the present research.

The CAS generates the control surface deflections based on the commanded values of the normal acceleration in g 's, the angle of sideslip, and the roll rate. The feedback quantities for the CAS pitch channel are roll and pitch angular acceleration, pitch body rate, normal acceleration and angle of attack, and a stall limit. This channel has gains scheduled as functions of Mach number, static and total pressure. In the roll CAS channel, the autopilot provides the roll rate command while the feedback quantity is the actual aircraft roll rate. The yaw CAS channel command is the angle of sideslip β while the feedback quantities are the aircraft lateral acceleration, yaw and roll angular acceleration, and yaw and roll rates. This channel has a gain scheduled as a function of angle of attack. All the control surface actuators have position and rate limits in addition to freeplay and deadband nonlinearities.

2.3. Controller Synthesis

With the foregoing, in the following, the nonlinear controllers for this system will be developed. Since the CAS tracks the commanded values of normal acceleration a_n , in g 's, roll rate p and the angle of sideslip β , the MAP will be designed to generate the required commands in these quantities in order to track the commanded values of altitude, airspeed, angle of attack and roll attitude.

The nonlinear controllers will be developed for each of these quantities separately. The MAP for a particular maneuver may be synthesized by employing the appropriate combinations of these controllers.

2.3.1. Controller for the Airspeed V

The state equations for these quantities may next be used to develop this controller. Firstly, we shall consider the airspeed loop. The control variable in this case is the throttle, the other quantities on the right hand side of the state equation (2.1) being computed from the measurement of states. The prelinearizing transformation in this case is particularly simple, viz,

$$\dot{V} = U_1 \quad (2.11)$$

With,

$$U_1 = [-D \cos \beta + S \sin \beta + (k_1 \cos \alpha \cos \beta + k_3 \sin \alpha \cos \beta) T - mg(\sin \theta \cos \alpha \cos \beta - \cos \theta \sin \phi \sin \alpha \cos \beta)] / m \quad (2.12)$$

The aircraft drag D and the sideforce S can be computed using a simple nonlinear model or interpolated from stored tables. The thrust component coefficients k_1 and k_3 are known constants. Since other terms in (2.12) can be computed from feedback values of the states θ , ϕ , α , β , if the pseudo control U_1 is known, this expression may be inverted to obtain thrust T . The thrust may then be reverse interpolated to yield the throttle setting using a table lookup. The transformed linear dynamic model for airspeed is given by the expression (2.11). A simple proportional controller can stabilize the system. However, since the controller has to track ramp airspeed command and because the nonlinear functions on the right hand side of expression (2.12) cannot be computed exactly, an integral feedback will be used in this channel. With this, the pseudo control U_1 will be of the form

$$U_1 = G_1 e_V + G_2 \int_0^{t_f} e_V dt \quad (2.13)$$

Where

$$e_V = V_c - V \quad (2.14)$$

V_c is the desired value of airspeed, G_1 and G_2 are the feedback gains to be determined based on the maximum available thrust, and the desired speed of response. These gains may be determined without difficulty since the closed-loop transfer function of the airspeed control loop in the pseudo control variable U_1 is given by

$$\frac{V(s)}{V_c(s)} = \frac{G_1 s + G_2}{s^2 + G_1 s + G_2} \quad (2.15)$$

The gains G_1 and G_2 can be selected to provide adequate damping and speed of response. Note, however, that the dynamics given in (2.15) does not explicitly include the aircraft thrust limits. It is the designer's responsibility to pick the combination of gains that would lead to a satisfactory performance without violating the thrust limit.

Using equations (2.13) and (2.12), the actual control can be computed as

$$\frac{mU_1 + D \cos \beta - S \sin \beta + mg(\sin \theta \cos \alpha \cos \beta - \cos \theta \sin \phi \sin \alpha \cos \beta)}{(k_1 \cos \alpha \cos \beta + k_3 \sin \alpha \cos \beta)} = T \quad (2.16)$$

The thrust emerging from the expression (2.16) can next be used to determine the desired throttle setting η_c from a table. The thrust-throttle relationship for aircraft are often highly nonlinear, requiring an iterative algorithm to compute the throttle from the given thrust. In the present case, a modified linear interpolation method was used, see page 10 of Ref. 18 for details. In all the maneuvers studied here, this thrust-throttle iteration converged in four steps for an absolute thrust tolerance of 1×10^{-13} . In practice, a higher value of tolerance can be used. The computed throttle setting must satisfy

$$\eta_{min} \leq \eta_c \leq \eta_{max} \quad (2.17)$$

If the calculated throttle setting is larger than the maximum or less than the minimum, it may be fixed at the appropriate bound. Note that no explicit compensation for the engine time lag has been incorporated. If required, a lead-lag engine prefilter may be used to partially offset the engine lag effects. However, this was not found necessary for satisfactory operation in the present case. For the aircraft engine considered here, there is a small core thrust saturation region approximately between 83° and 98° of throttle setting. Since the slope of the throttle-thrust curve is ill defined in this region, a hysteresis safe guard logic was introduced. According to this logic, when the thrust is decreasing from the maximum afterburner value to that corresponding to less than 98° throttle, the throttle is held at this value, till the required thrust falls below that corresponding to 83° throttle. Reverse of this logic applies whenever the required thrust approaches the saturation value from the core thrust direction.

In some flight test trajectories such as the *constant thrust windup turn*, the throttle would have to be fixed while regulating the airspeed. This can be accomplished by introducing an altitude rate in the system. Since,

$$\dot{V} = [-D\cos\beta + S\sin\beta + (k_1\cos\alpha\cos\beta + k_3\sin\alpha\cos\beta)T - m(g/V)\dot{h}]/m \quad (2.18)$$

In this case, the right hand side of the expression (2.18) would be the pseudo control U_1 , and the actual control would be the altitude rate \dot{h} . The right hand side of expression (2.18) may then be equated to expression (2.13) to compute the altitude rate required to maintain the airspeed at the desired value. Therefore,

$$(V/mg)[-D\cos\beta + S\sin\beta + (k_1\cos\alpha\cos\beta + k_3\sin\alpha\cos\beta)T - mU_1] = \dot{h} \quad (2.19)$$

The task of generating this desired altitude rate would be that of the altitude control channel. In this situation, it is clear that one would not be able to track an arbitrary altitude history, unless it happens to be the same as that emerging from the controller. Note that this controller will perform satisfactorily only if the altitude control loop can produce the desired altitude rate sufficiently fast. Thus care should be taken to ensure that the airspeed control loop remains slower than the altitude loop in this maneuver.

2.3.2. Controller for Altitude h

Just as in the airspeed channel, two versions of this controller will be required to execute the flight test trajectories under consideration. This arises because in certain flight test maneuvers such as the *excess thrust windup turn* flight test trajectory, one would be

required to track an angle of attack history while maintaining the altitude at the desired value.

In order to develop the altitude controller, we shall use an alternate form of the state equation than that in (2.4). It can be verified that

$$\ddot{h} = a_x \sin\theta - a_y \sin\phi \cos\theta - a_z \cos\phi \cos\theta \quad (2.20)$$

In the above expression a_x , a_y , and a_z are the acceleration components along the X, Y, and Z body axes. Now, the normal acceleration a_n is related to a_x as

$$a_x = -a_n + (g/g_0) \cos\theta \cos\phi \quad (2.21)$$

With this, the equation (2.20) becomes,

$$\ddot{h} = a_x \sin\theta - a_y \sin\phi \cos\theta + a_n \cos\phi \cos\theta - (g/g_0) \cos^2\theta \cos^2\phi \quad (2.22)$$

Equation (2.22) is in the form suitable for the development of a nonlinear control law for altitude. The expression (2.22) may be written as

$$\ddot{h} = U_2 \quad (2.23)$$

With,

$$U_2 = a_x \sin\theta - a_y \sin\phi \cos\theta + a_n \cos\phi \cos\theta - (g/g_0) \cos^2\theta \cos^2\phi \quad (2.24)$$

A linear control law of the form

$$U_2 = G_3 e_h + G_4 \dot{e}_h + G_5 \int_0^{t_f} e_h dt \quad (2.25)$$

Where

$$e_h = (h_c - h) \quad (2.26)$$

may be set up to obtain desired time response for the transformed system (2.23). The calculated U_2 may then be used to compute the normal acceleration command to the CAS as

$$\frac{U_2 - a_x \sin\theta + a_y \sin\phi \cos\theta + (g/g_0) \cos^2\theta \cos^2\phi}{\cos\phi \cos\theta} = a_n \quad (2.27)$$

As in the airspeed control loop, the closed-loop transfer function for the altitude control loop in the pseudo control variable can be obtained as

$$\frac{h(s)}{h_c(s)} = \frac{G_3 s + G_4 s^2 + G_5}{s^3 + G_3 s + G_4 s^2 + G_5} \quad (2.28)$$

The choice of the gains G_3 , G_4 , and G_5 are a little more difficult in this case, because the expression (2.28) is a third order transfer function. However, this is straight forward.

As mentioned earlier, in certain flight test trajectories, one would be required to control the angle of attack and the altitude simultaneously. In this situation, the normal acceleration is no longer available as the control variable to maintain the altitude at the desired level. The above approach will then have to be modified.

Whenever the simultaneous control of angle of attack and angle of attack are desired, one can assign the roll attitude ϕ as the control variable in the altitude channel. If this is done, the roll attitude required to control the altitude can be computed as

$$\phi_c = \cos^{-1} \left[\frac{a_x \sin \theta - U_2}{\cos \theta \sqrt{a_y^2 + a_x^2}} \right] + \phi_0 \quad (2.29)$$

Where,

$$\phi_0 = \tan^{-1} \left[\frac{a_y}{a_x} \right] \quad (2.30)$$

The assumption here is that the dynamics of the roll attitude control loop is much faster than that of the altitude control loop, a reasonable assumption for high performance fighter aircraft. This commanded roll attitude ϕ_c must be tracked by the roll attitude control loop. Note that the commanded roll attitude emerging from the expression (2.29) is devoid of any sign. This indicates that the altitude control may be achieved through a roll attitude yielding either a right handed or left handed turn. In the present work, it will be assumed that positive values of ϕ_c will be used, leading always to a right-hand turn.

Before closing this section it is perhaps worthwhile to note that one should be careful in selecting too high altitude loop gains. Clearly, the aircraft has a maximum normal acceleration limit beyond which the control system performance cannot be predicted. Moreover, when the control law (2.29) is being used, trying to speed up the altitude control channel beyond a certain point will result in large changes in the commanded roll attitude ϕ_c which the roll attitude controller may not be able to track. This can lead to control system instability.

2.3.3. Controller for Angle of Attack α

A nonlinear controller for the angle of attack α can be set up in a manner analogous

to that of the airspeed control loop. As before, we define the right-hand-side of expression (2.2) as another pseudo control variable U_3 . Thus,

$$\dot{\alpha} = U_3 \quad (2.31)$$

With

$$U_3 = [-L + (k_3 \cos \alpha - k_1 \sin \alpha)T + mg(\cos \theta \cos \phi \cos \alpha + \sin \theta \sin \alpha)] / (mV \cos \beta) \\ + q - \tan \beta (p \cos \alpha + r \sin \alpha) \quad (2.32)$$

A linear control law of the form

$$U_3 = G_6 e_\alpha + G_7 \int_0^{t'} e_\alpha dt \quad (2.33)$$

Where,

$$e_\alpha = \alpha_c - \alpha \quad (2.34)$$

may be designed to obtain the desired time response from the prelinearized dynamic system (2.31). In expression (2.34), α_c is the commanded value of angle of attack. The gains G_6 and G_7 can be chosen based on the desired natural frequency and damping ratio. The closed-loop transfer function of the angle of attack loop in the pseudo controls is given by

$$\frac{\alpha(s)}{\alpha_c(s)} = \frac{G_6 s + G_7}{s^2 + G_6 s + G_7} \quad (2.35)$$

The actual control variable in the angle of attack channel is the normal acceleration. This variable can be obtained by using the expression (2.32) in conjunction with the expression for normal acceleration. Since the normal acceleration is given by

$$a_n = [-k_3 T + D \sin \alpha + L \cos \alpha - mg \cos \theta \cos \phi] / mg, \quad (2.36)$$

the expression (2.32) and (2.35) may be used to obtain the normal acceleration required to track a given angle of attack history as :

$$a_n = \left[\frac{V \cos \alpha \cos \beta}{g} \right] \left\{ [D \tan \alpha - k_1 T \sin \alpha + mg(\cos \theta \cos \phi \cos \alpha + \sin \theta \sin \alpha)] / (mV \cos \beta) + q - \tan \beta (p \cos \alpha + r \sin \alpha) - U_3 \right\} - \cos \theta \cos \phi \quad (2.37)$$

This completes the development of the angle of attack controller.

2.3.4. Controller for the Roll Attitude ϕ

The controller synthesis for the roll attitude ϕ follows the same steps as those described for airspeed and angle of attack channels. We first assign a pseudo control variable U_4 such that

$$\dot{\phi} = U_4 \quad (2.38)$$

With

$$U_4 = p + q \sin \phi \tan \theta + r \cos \phi \tan \theta \quad (2.39)$$

We next design a linear controller of the form

$$U_4 = G_8 e_\phi + G_9 \int_0^{t_f} e_\phi dt \quad (2.40)$$

Where,

$$e_\phi = \phi_c - \phi \quad (2.41)$$

The variable ϕ_c is the commanded value of roll attitude in expression (2.41). The closed-loop transfer function for the roll attitude control loop in the pseudo control variable is given by

$$\frac{\phi(s)}{\phi_c(s)} = \frac{G_8 s + G_9}{s^2 + G_8 s + G_9} \quad (2.42)$$

It is clear that the gains G_8 and G_9 can be chosen to meet the desired time response specifications. The pseudo control variable obtained from (2.40) may be used in the expression (2.39) to obtain the actual control variable p . Thus,

$$p = U_4 - q \sin \phi \tan \theta - r \cos \phi \tan \theta \quad (2.43)$$

It is clear that as long as the feedback state variables q , r , ϕ , and θ are close to their actual values, the nonlinear controller will have almost the same performance as that of the pseudo control loop.

This completes the closed-loop controller development. These control laws may be further simplified because all the maneuvers are to be carried out with $\beta = 0$. We note here that in order to implement these control laws, one needs to be able to compute the aircraft drag and the throttle setting from the calculated thrust. There are two ways to approach this problem. The first one consists of storing these as tables and the second, to construct simple approximate models for these quantities. The latter approach will be used in the present work. The state variables required are V , h , α , θ , ϕ , q , r , and the three accelerations a_x , a_y , and a_z . In the next Chapter, the controllers developed here will be combined together to form the maneuver autopilot to execute particular flight test trajectories.

In the following section, we shall briefly indicate how the synthesized closed-loop control laws may be modified for operation with pilot-in-the-loop.

2.3.5. Maneuver Control with Pilot-in-the-loop

In the foregoing, the technique for the synthesis of nonlinear control laws for flight test trajectory control was discussed. In order to enable manual control, these control laws may be modified in several different ways. One approach would be to assume that the errors e_v , e_h , e_α , and e_ϕ remain constant over a time interval to predict the pseudo controls U_1 , U_2 , U_3 , and U_4 . These control variables may be displayed to the pilot through devices such as the one described in [2]. This approach compensates only the observation and neuromuscular delay in the human pilot dynamics [4].

An alternate approach would be to include the pilot transfer function in the pseudo control loops and select the gains to achieve the desired time response. Mere gain stabilization may not always be feasible in this case. If the resulting control loop displays unacceptable behavior, appropriate dynamic compensation networks will then have to be introduced. In any case, the present methodology gives a systematic approach to handle the manual control problem also.

Chapter III Controller Evaluation

3.1. Simulation

In order to evaluate the performance of the nonlinear flight test trajectory controller, a Fortran implementation of this controller is mechanized on a complete CAS+Aircraft model developed at NASA Ames-Dryden Flight Research Facility. This section describes the details of controller implementation and the results of closed loop simulations with the nonlinear controller for the six required flight test maneuvers.

Specifically, the following maneuvers are simulated.

- Level Acceleration Trajectory
- Pushover Pullup Trajectory
- Zoom and Pushover Trajectory
- Excess Thrust Windup Turn Trajectory
- Constant Thrust Windup Turn Trajectory
- Constant Dynamic Pressure, Constant Load Factor Trajectory

For a detailed description of these maneuvers, see Ref. 17.

The simulations are mechanized on the SYSTEM_BUILD software of Integrated Systems Inc., some details of which are given in [19,20]. This proprietary software is block diagram oriented and is suitable for efficient generation of nonlinear, multi-rate simulations. This software incorporates several commonly encountered dynamic subsystems in a library. The cases where the dynamics is not representable with any of the available blocks in the library, Fortran blocks may be attached. This is often the situation in aircraft simulations wherein the aerodynamics and engine thrust are given as nonlinear functions of several state variables. In the next section we give a brief description of the aircraft and CAS simulation as it is mechanized on SYSTEM_BUILD.

3.2 SYSTEM_BUILD simulation of Aircraft and Controller

Airframe, Engine and command augmentation system models provided by NASA Ames-Dryden Flight Research Facility are linked with the Fortran code for the nonlinear flight test trajectory controller in the SYSTEM_BUILD environment. A block diagram of this implementation is given in Figure 3.2.1. In this figure, the CAS,AROMDL and ENGINE super blocks in the closed loop simulation were supplied NASA Ames-Dryden Flight Research Facility, while the CONT super block was developed and linked to the SYSTEM_BUILD model of the aircraft and CAS. The listing Fortran code implemented in the block CONT is given in Appendix B.

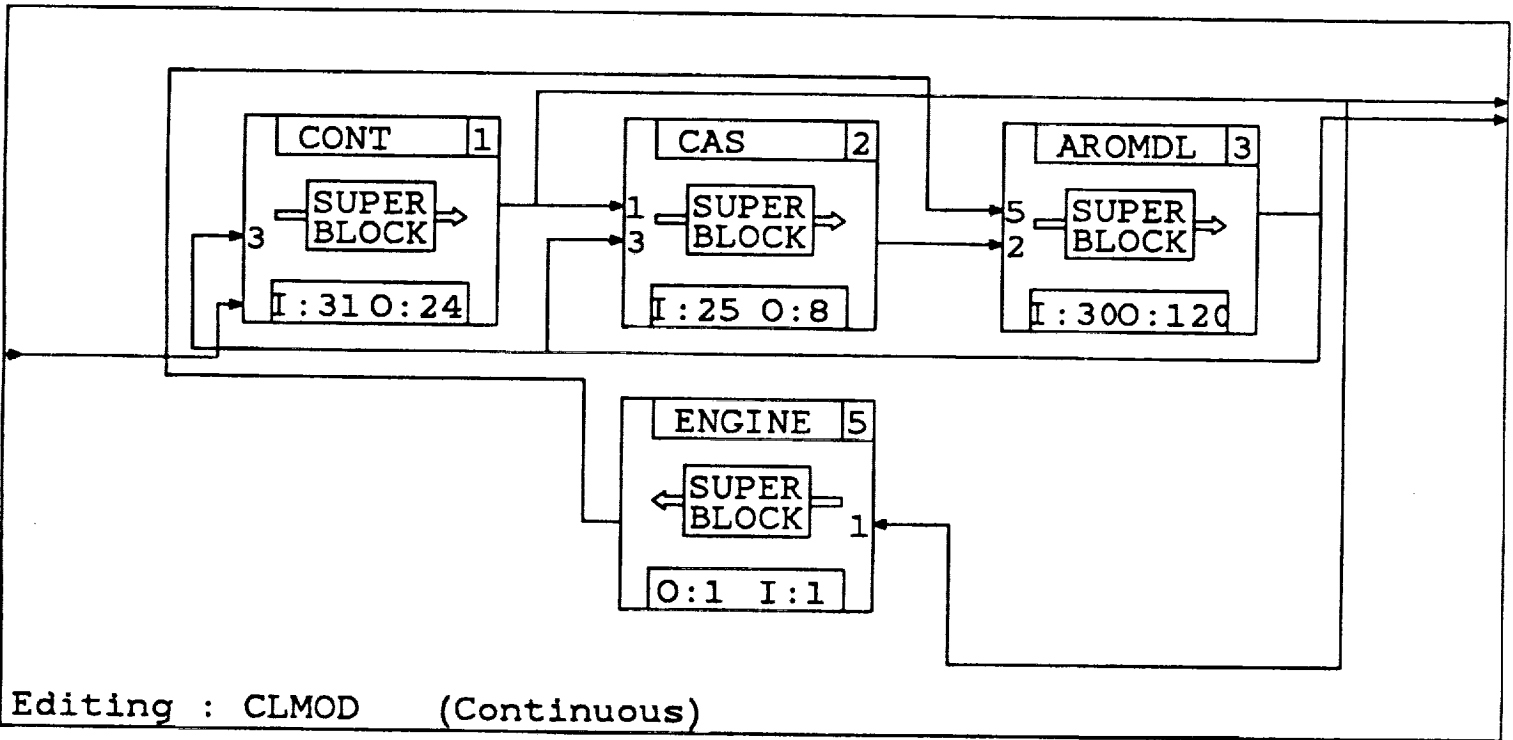


Figure 3.2.1. SYSTEM_BUILD Block Diagram of the Simulation.

The command augmentation system is implemented as a discrete Fortran block in the simulation. The sampling interval of 0.02 seconds has been fixed from previous simulations of the aircraft and CAS system. The nonlinear aircraft model is also implemented as Fortran block, but it is a continuous system.

Real time simulation and testing of the nonlinear flight test trajectory controller will require that the output of the controller be interfaced to the aircraft through the CAS system. This in turn requires that the output of the controller be the normal acceleration, angle of sideslip and the roll body rate rather than control surface deflections. Since the CAS nonlinear dynamics are not invertible, one has to either assume that the CAS is stable and sufficiently fast when compared with the MAP such that it tracks the input commands, or build-in a feedback compensation to ensure that it tracks the input commands. The present experience indicates that the former assumption is valid.

Time scale separation is a key feature of the nonlinear controller, and here, we briefly explain how this separation was implemented in the computer simulation of the closed - loop aircraft model. Given that the CAS model has been coded to run in the SYSTEM_BUILD simulation as a discrete time block with a fixed step size of 0.02 seconds, a second order Runge-Kutta algorithm was used for all simulations with a step size of 0.02 seconds. This time scaling is consistent with the dynamics of the continuous time airframe and engine models but much too fast for the nonlinear controller. In order to slow the command variables from the controller so that response times of the aircraft and CAS states were shorter than the dynamics of the controller commands, a flag internal to the controller code updates the command outputs every "i" integration steps. Response testing at straight and level flight conditions with $i = 5$ gave good results. Thus, the following simulations were all completed with the nonlinear controller running at 10 Hz.

3.3. Flight Test Trajectory Control Simulation

Six required flight test trajectories were simulated to evaluate the performance of the nonlinear controller. One of the major problems encountered during the simulation was that of finding a consistent set of initial conditions that would trim the aircraft at the desired altitude and airspeed. Though the NASA-DFRF linearization program produces consistent set of initial conditions, it was found that when these were introduced in the simulations, there was a significant starting transient. For now, this transient is attributed to the unknown initial conditions in the CAS, since this system contains several dynamic loops. Moreover, some repeatability problems were encountered in the initial phases which were traced to two undefined logical variables in the CAS model. As mentioned earlier, the CAS input variables were not clearly known at the outset, but had to be identified after several simulations.

In the following, the performance of the nonlinear controller along each of the six flight test maneuvers will be given separately.

3.3.1. Level Acceleration Flight Test Trajectory

The requirements in this maneuver are : track a ramp airspeed history while

maintaining constant altitude with wings level. To achieve this objective, the nonlinear controller for the airspeed given by the expressions (2.13),(2.14), and (2.16) is used in conjunction with the altitude controller expressions (2.25),(2.26) and (2.27), and the roll attitude controller expressions (2.40), (2.41) and (2.43). The commanded roll attitude ϕ_c is zero in this case.

A level acceleration flight test trajectory starting at 30000 feet and 0.9 Mach is given in Figures 3.1 through 3.4. In this maneuver, the aircraft was required to accelerate from 0.9 Mach to 1.2 Mach in about 40 seconds while maintaining the altitude within ± 50 feet. This represents a particularly stringent maneuver since the aircraft has to pass through the transonic region while maintaining the altitude. From Figure 3.1, it can be seen that the aircraft tracked the Mach number history with very little error, except in the vicinity of Mach 1. In this figure, the dotted line represents the commanded Mach number, while the solid line shows the tracked history. If a linear perturbation controller had to perform this task with an equivalent accuracy, it would have required atleast three sets of gains, the first set in the subsonic regime, the second in the transonic regime and the third one in the supersonic regime. The altitude history given in Figure 3.2. shows that the altitude was maintained within ± 15 feet, well within the require accuracy. The elevator history given in Figure 3.3 shows about 1 HZ oscillation in the transonic region getting rapidly damped out as the aircraft commences its supersonic flight. However, the elevator deflection is well within the saturation limits, the maximum deflection being about $\pm 5^\circ$. From Figure 3.4, it may be observed that the throttle saturates during the transonic region at its maximum afterburner value and continues to stay there for about 5 seconds. Subsequently, oscillations can be seen which rapidly damp out during the supersonic flight. Overall response of the control system is very good. Considering that this performance is achieved with a single set of gains, the performance is indeed remarkable.

3.3.2. Pushover/Pullup Trajectory

The requirement here is to track a saw tooth wave form in angle of attack while maintaining the constant Mach number. The maneuver autopilot for this trajectory consists of the airspeed controller given by the expressions (2.13), (2.14) and (2.16), the angle of attack controller given by the expressions (2.33), (2.34) and (2.37), and the expressions (2.40), (2.41) (2.43) for the roll attitude controller .

Figures 3.5 though 3.9 give the behavior of the controller along a typical pushover/pullup flight test trajectory. The commanded angle of attack history is shown in dotted line in this figure while the control system response is shown in solid line. The small amplitude oscillations in angle of attack at the begining of this maneuver is due to the initial conditions rather than due to the command. After the initial oscillations, the angle of attack history tracking is very good. The Mach number is maintained within 0.004 throughout the maneuver. The altitude is of no particular concern here, since it is an uncontrolled variable. However, for the sake of completeness, the resulting altitude is given in Figure 3.9. The controller performance is again very good.

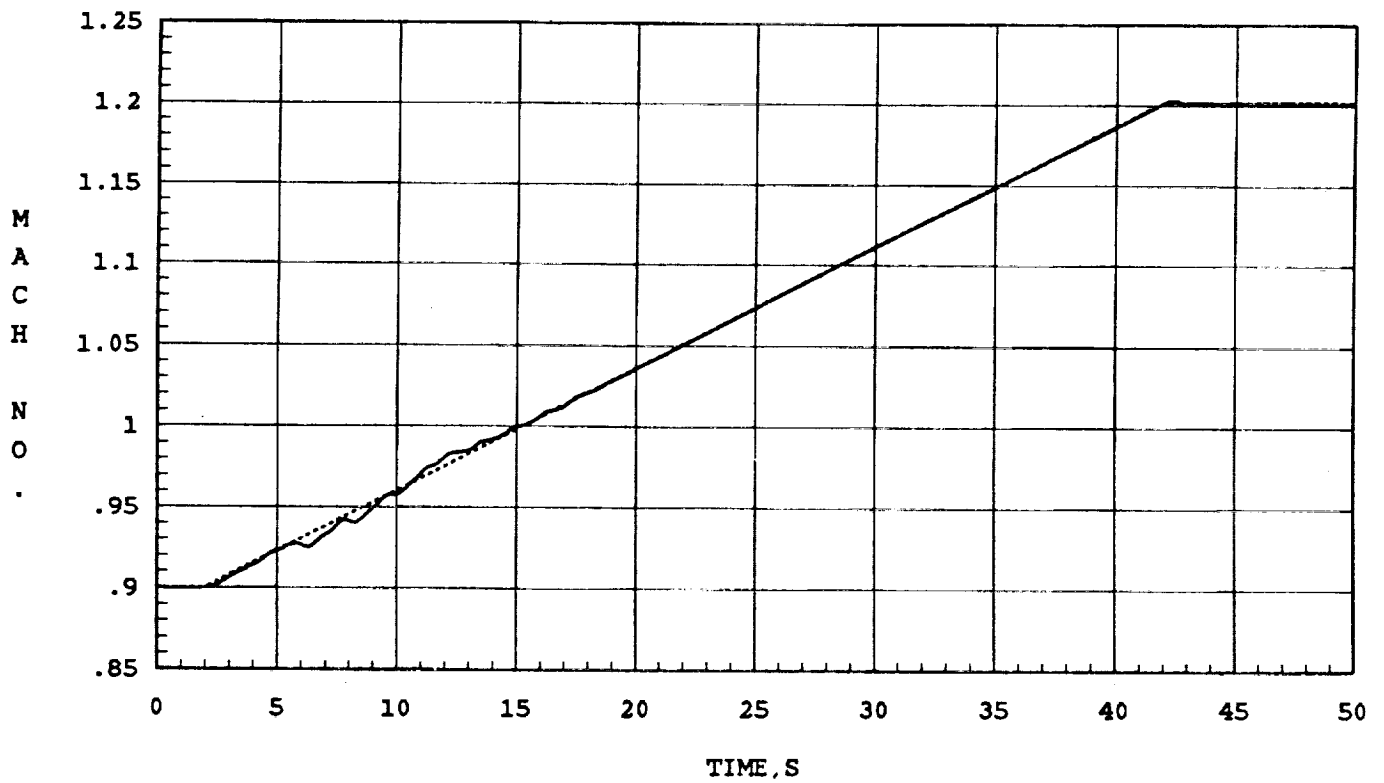


Figure 3.1. Mach Number vs. Time along the Level Acceleration Trajectory.

Dotted line: Commanded Mach number.

Solid line: Actual Mach number.

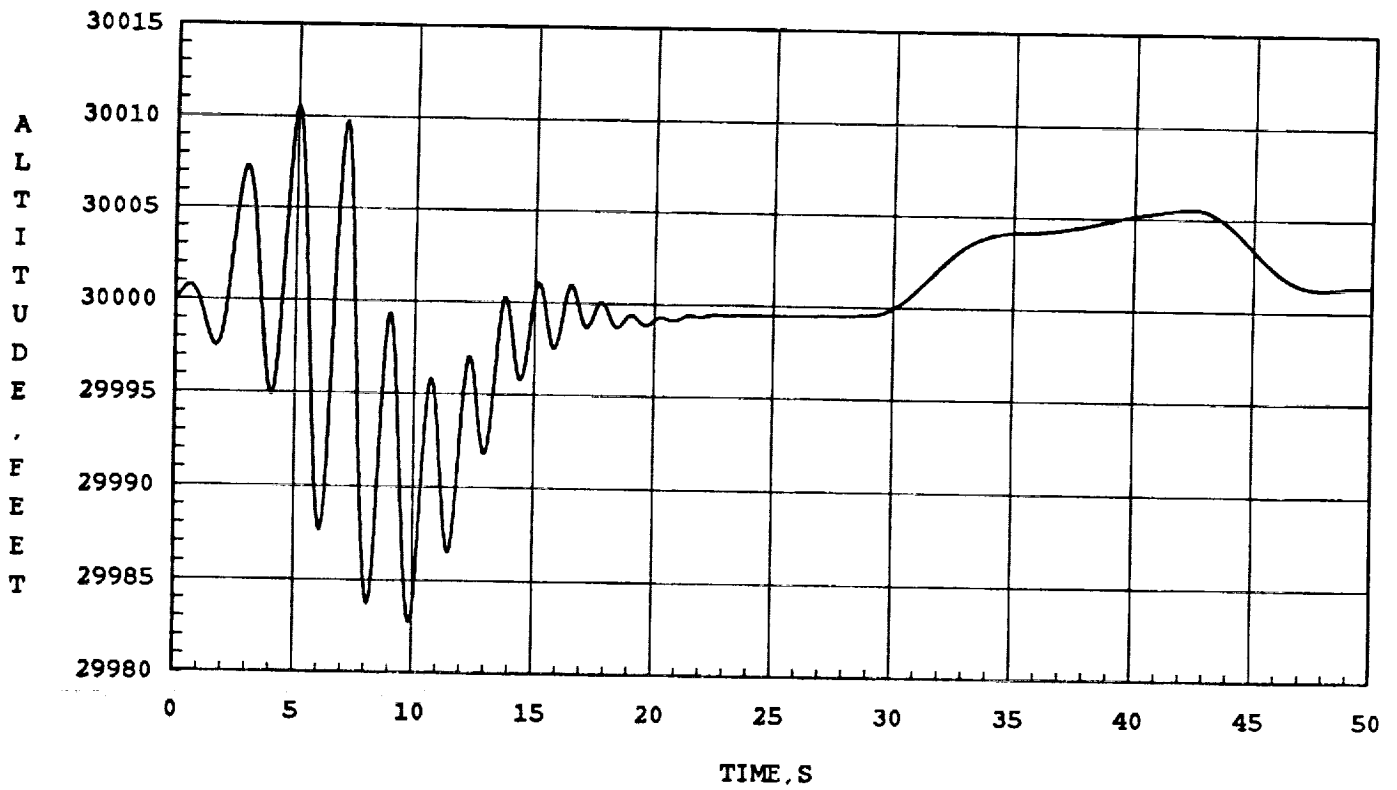


Figure 3.2. Altitude vs. Time along the Level Acceleration Trajectory.

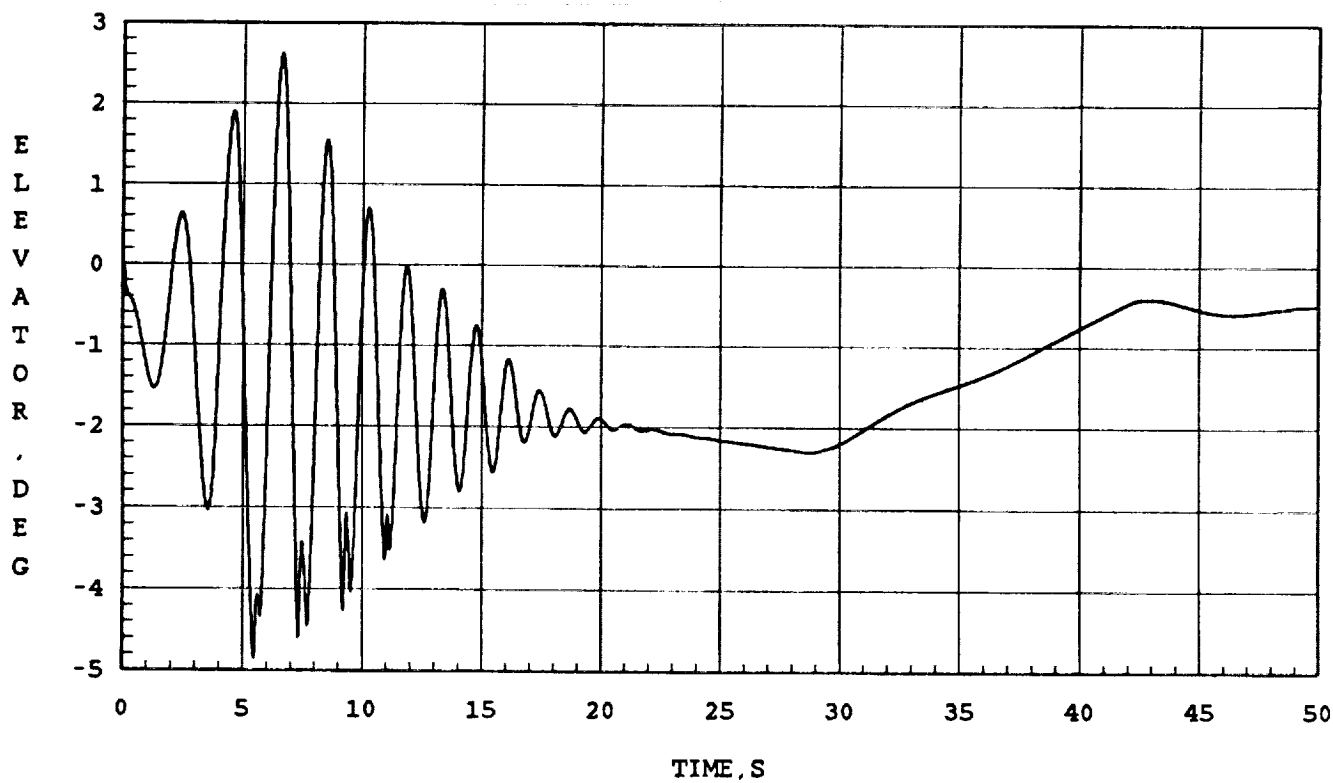


Figure 3.3. Elevator Deflection vs. Time along the Level Acceleration Trajectory.

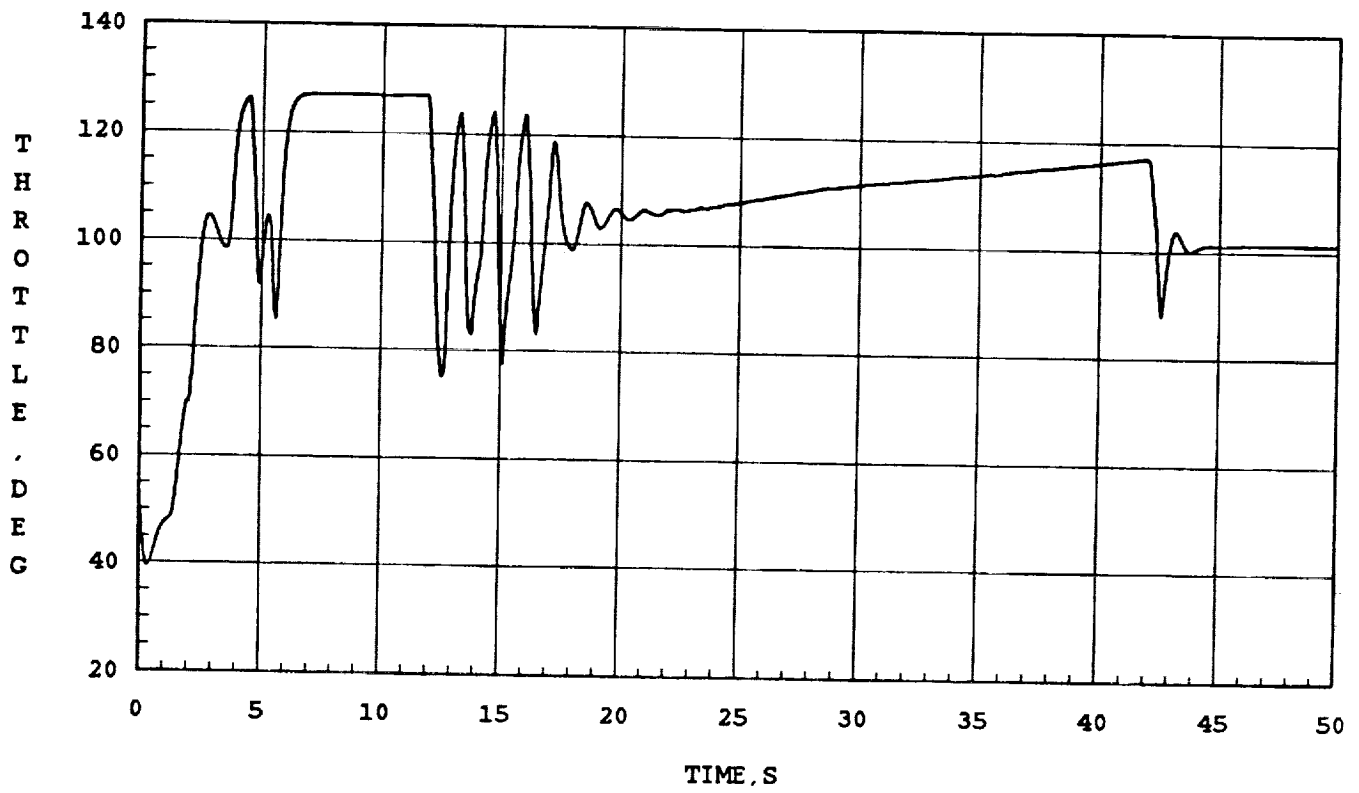


Figure 3.4. Throttle setting vs. Time along the Level Acceleration Trajectory.

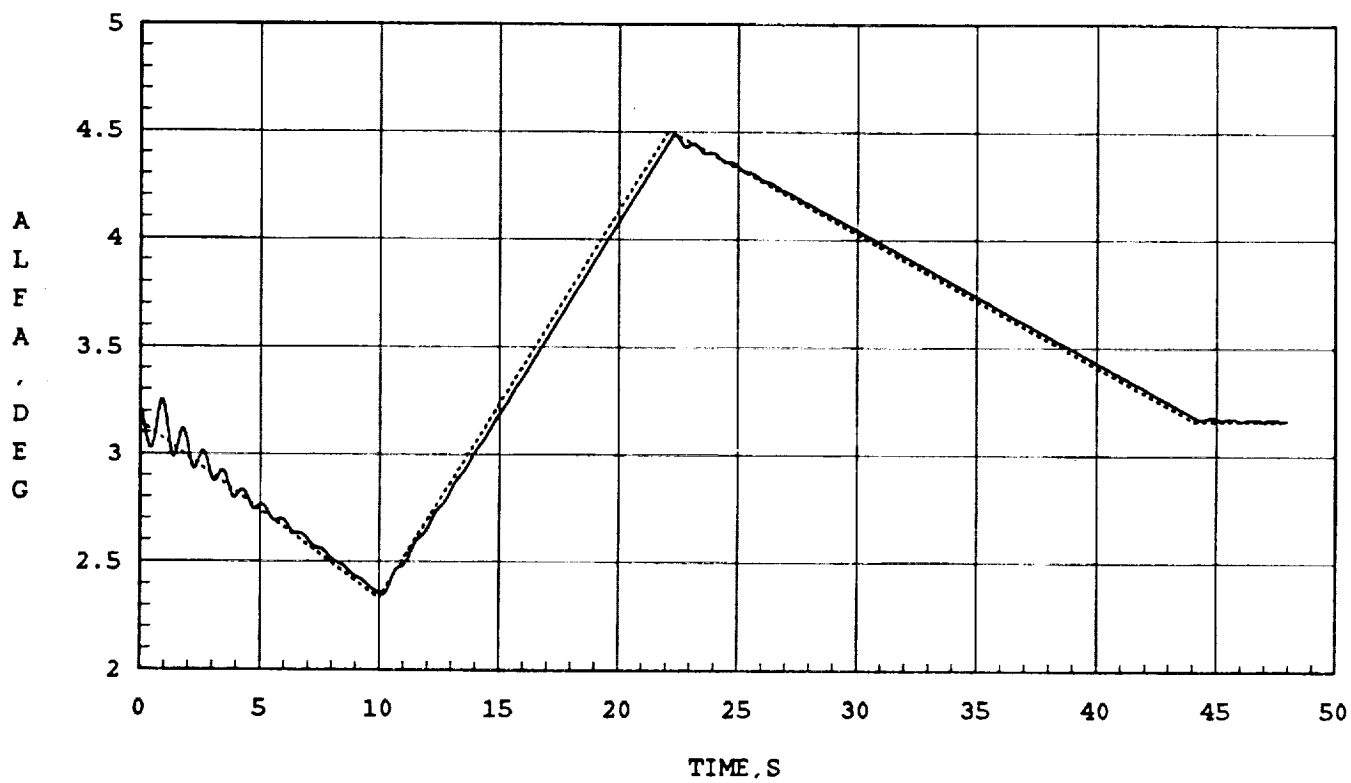


Figure 3.5. Angle of attack vs. Time along the Pushover/Pullup Maneuver.

Dotted Line: Command Angle of Attack.

Solid Line: Actual Angle of Attack.

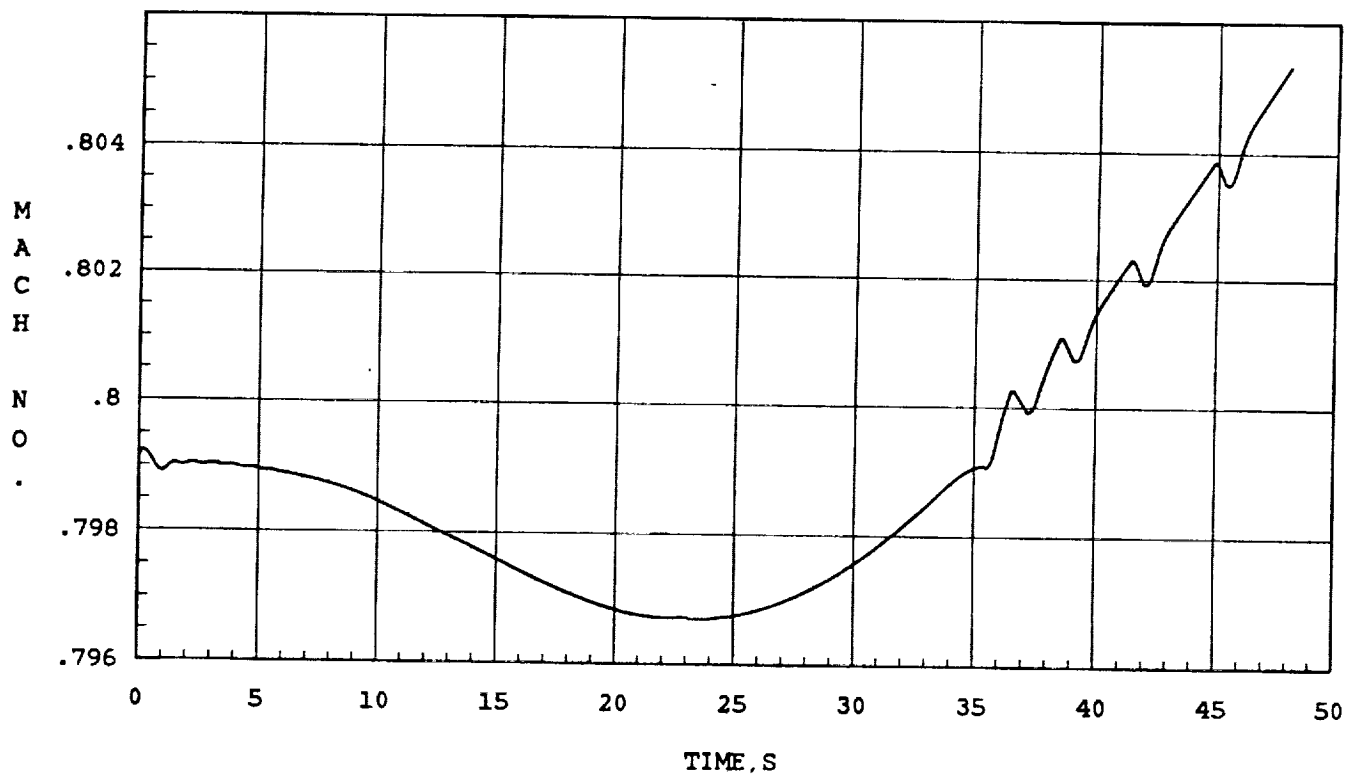


Figure 3.6. Mach number vs. Time along the Pushover/Pullup Maneuver.

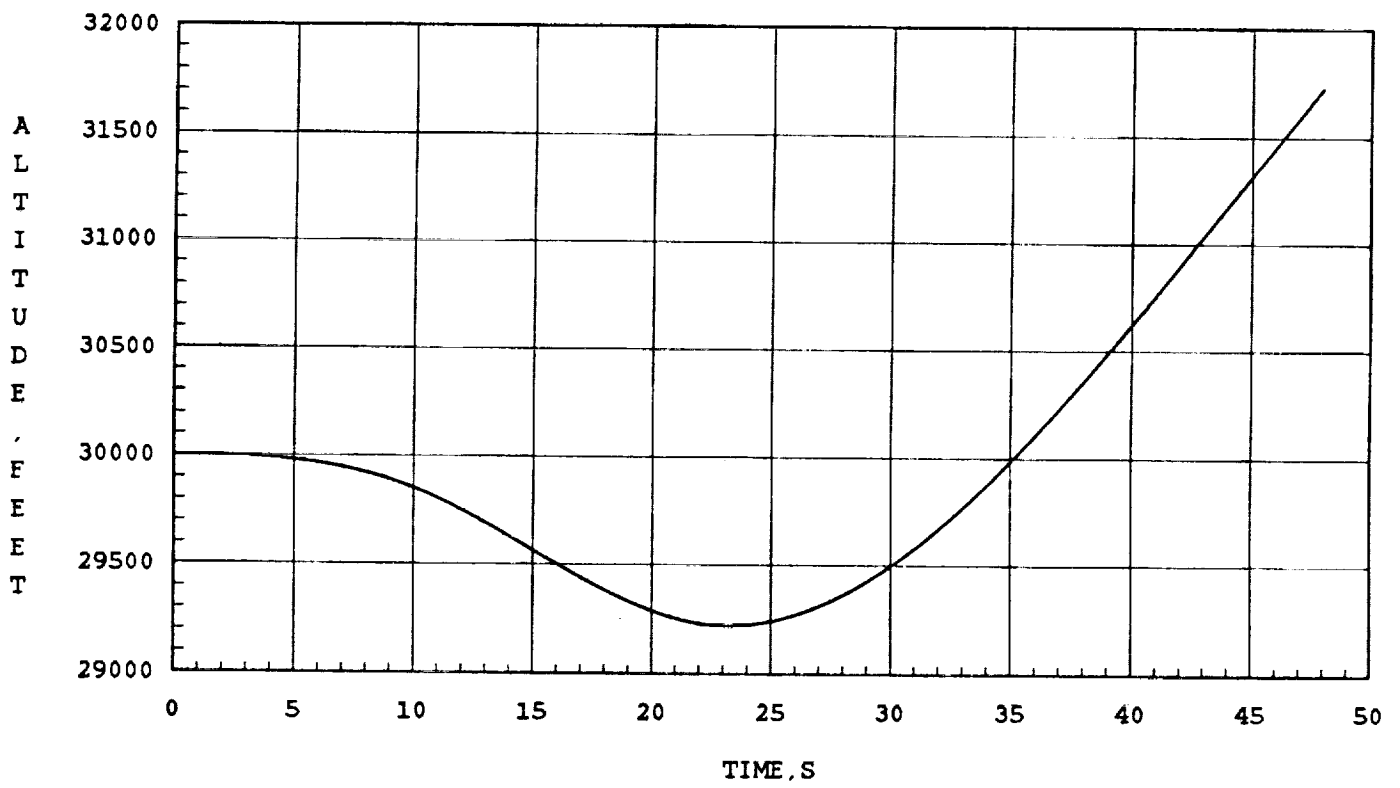


Figure 3.7. Altitude vs. Time along the Pushover/Pullup Maneuver.

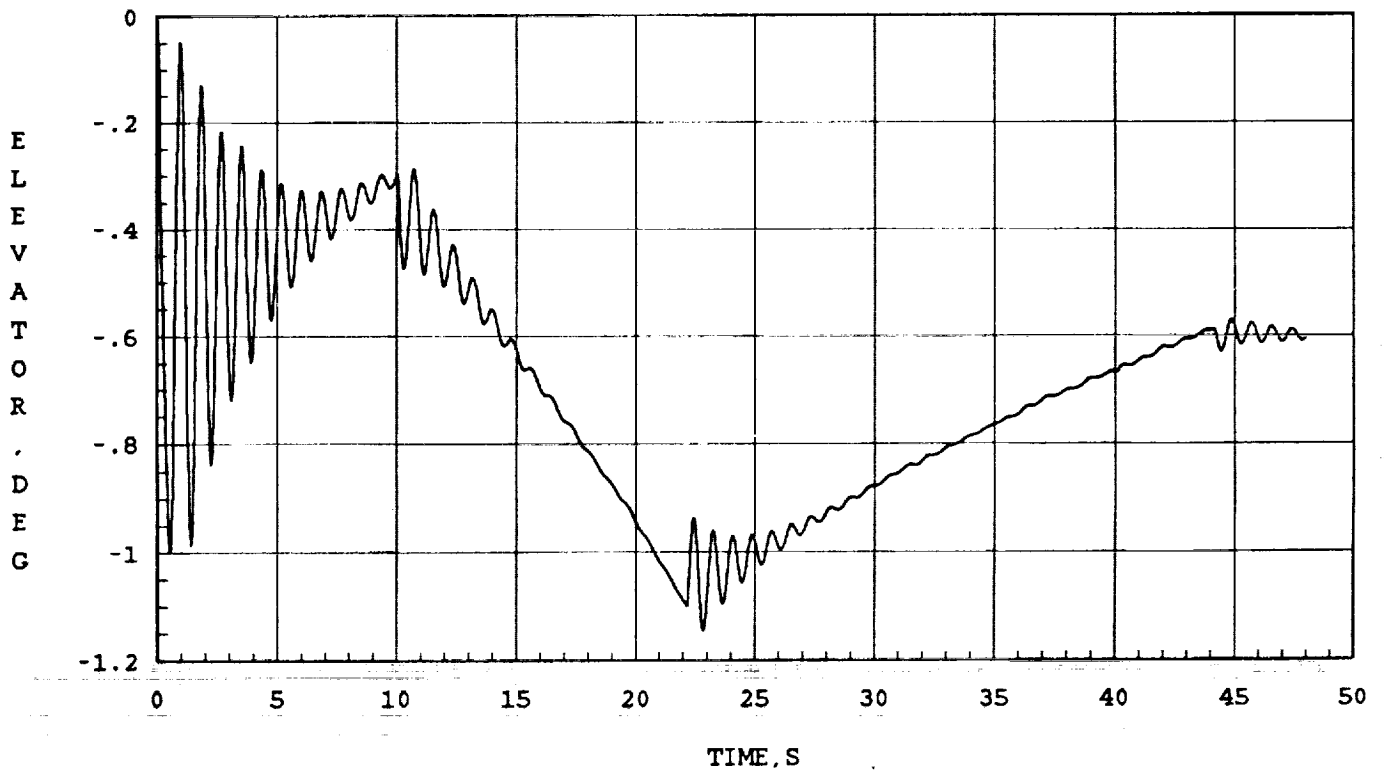


Figure 3.8. Elevator vs. Time along the Pushover/Pullup Maneuver.

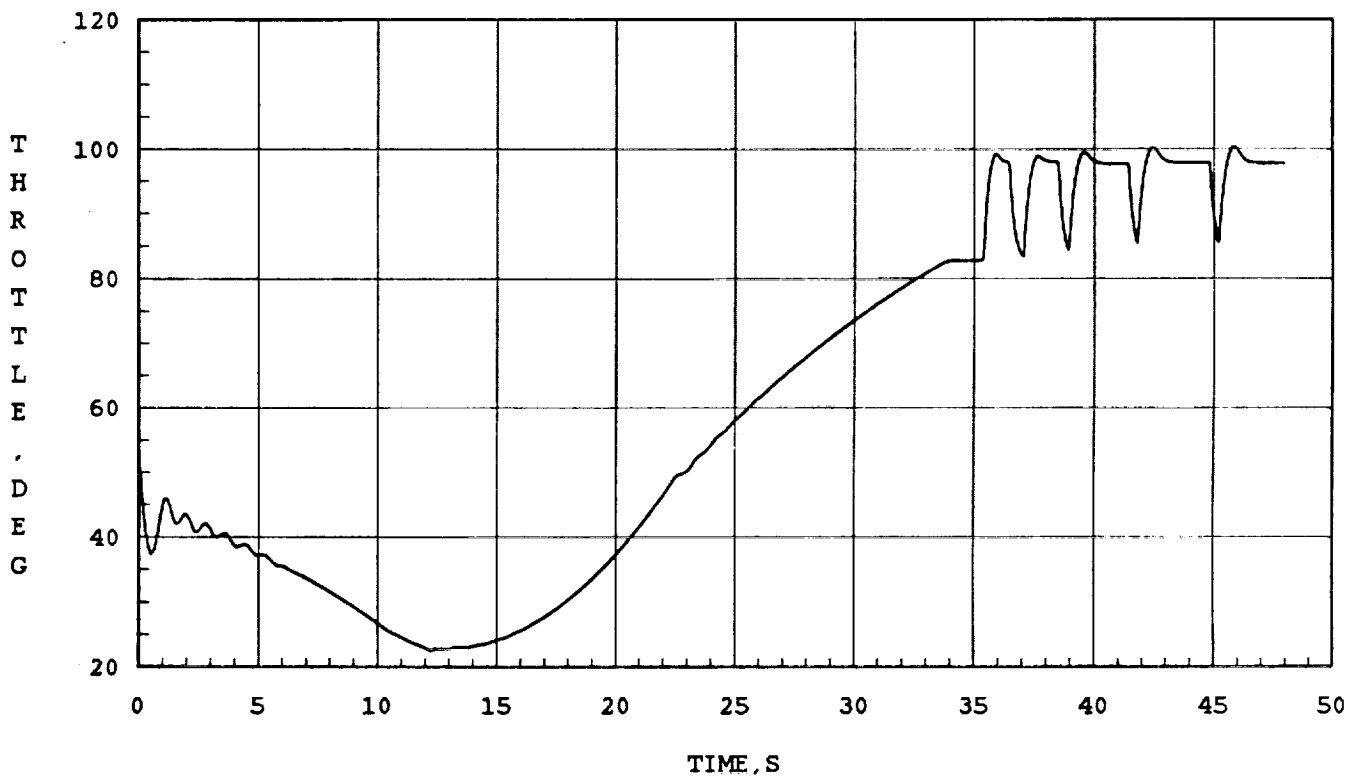


Figure 3.9. Throttle Setting vs. Time along the Pushover/Pullup Maneuver.

3.3.3. Zoom and Pushover Flight Test Trajectory

The zoom and pushover flight test trajectory requires flight along a parabolic flight path with a set of Mach/angle of attack/ altitude condition to be met at the apex of the parabola. The flight along the parabolic path occurs with constant thrust. A systematic approach for generating commands for such a flight test trajectory was discussed in the earlier contract phase [6]. In the present work, however, it was found that simply by stretching the angle of attack history in the pushover/pullup maneuver, one could obtain the zoom and pushover trajectory. The maneuver autopilot for this trajectory consists of the expressions for the airspeed controller (2.13), (2.14) and (2.16), the angle of attack controller expressions (2.33), (2.34) and (2.37), the roll attitude controller expressions (2.40), (2.41) and (2.43) in the initial transient phase. During the zoom and pushover phase, the airspeed control loop is disabled since this maneuver is required to be flown at constant throttle.

The desired conditions at the apex of the parabola in the present case was 30000 feet altitude, 0.7 Mach and 3° angle of attack. The actual values at the apex were, 30019.26 feet, 0.691 Mach and 3.17° angle of attack. The actual errors are well within the required specifications.

The trajectory variables for this maneuver are presented in Figures 3.10 through 3.14. The throttle was fixed at 20% during the zoom and pushover maneuver. The controller performance is found to meet the desired accuracy specifications.

3.3.4. Excess Thrust Windup Turn

The requirement here is to track a linear angle of attack history while maintaining the airspeed and altitude constant. This maneuver is highly coupled and potentially unstable because the aircraft can have bank angles very close to 90°.

The nonlinear controller uses the normal acceleration to track the desired angle of attack history, the throttle to maintain the airspeed and the roll attitude to maintain altitude. Thus, the maneuver autopilot consists of the airspeed controller expressions (2.13), (2.14), (2.16), the angle of attack controller expressions (2.33), (2.34), (2.37), the altitude controller equations (2.25), (2.26), (2.29), (2.30) in conjunction with the roll attitude controller equations (2.40), (2.41) and (2.43).

Alternately, the maneuver modeling scheme described in [6] may be used to generate a consistent set of angle of attack and roll attitude commands which may be tracked using the V , α , ϕ controllers to obtain the desired excess thrust windup turn trajectory. This approach is employed here in the interest of simplifying the controller. Note that with this approach, the altitude is not controlled, but is allowed to vary as it may throughout the maneuver.

The performance of the nonlinear controller along this maneuver is illustrated in Figures 3.15 through 3.26. There appears to be hang-off error in the angle of attack channel which increases with an increase in the roll attitude. Since there is an integral feedback in this channel, such a hang-off error can arise only if the CAS input in the pitch channel

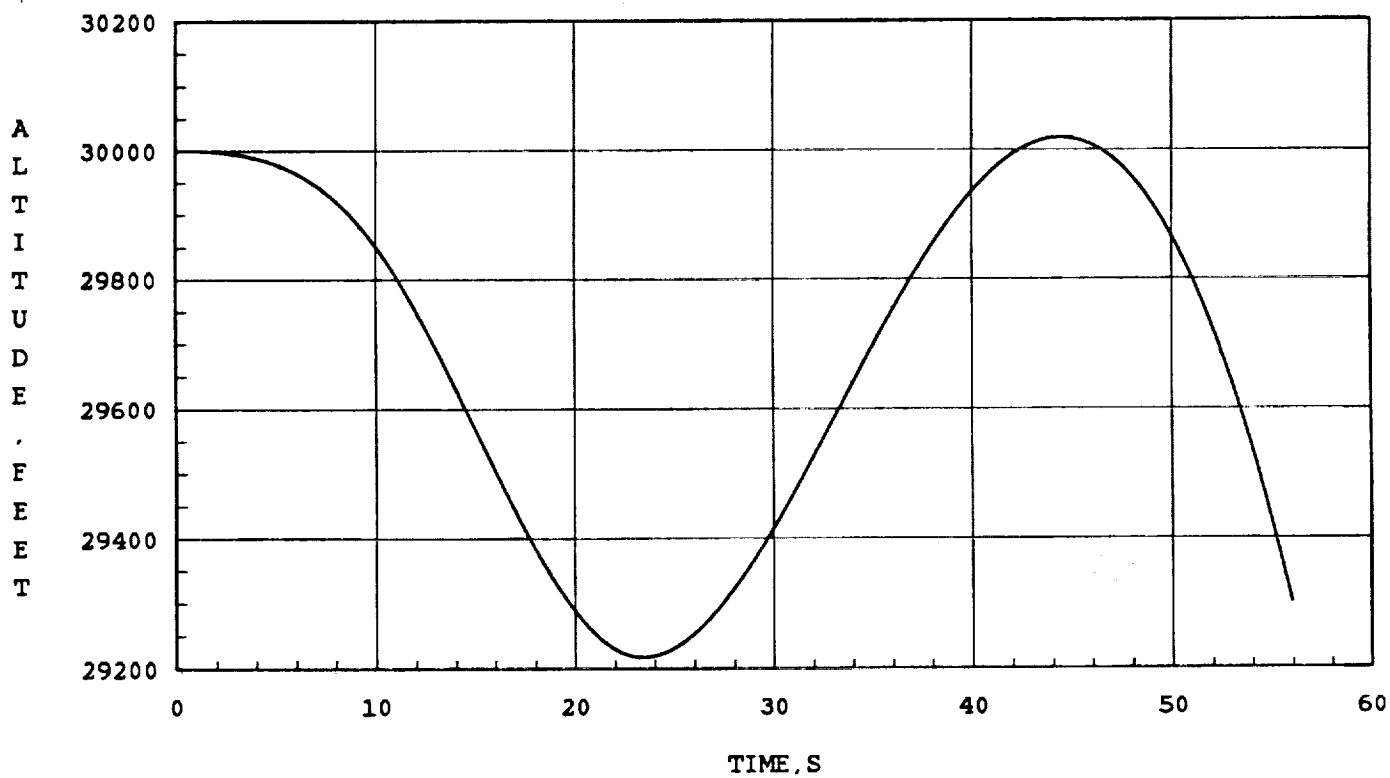


Figure 3.10. Altitude vs. Time along the Zoom and Pushover Maneuver.

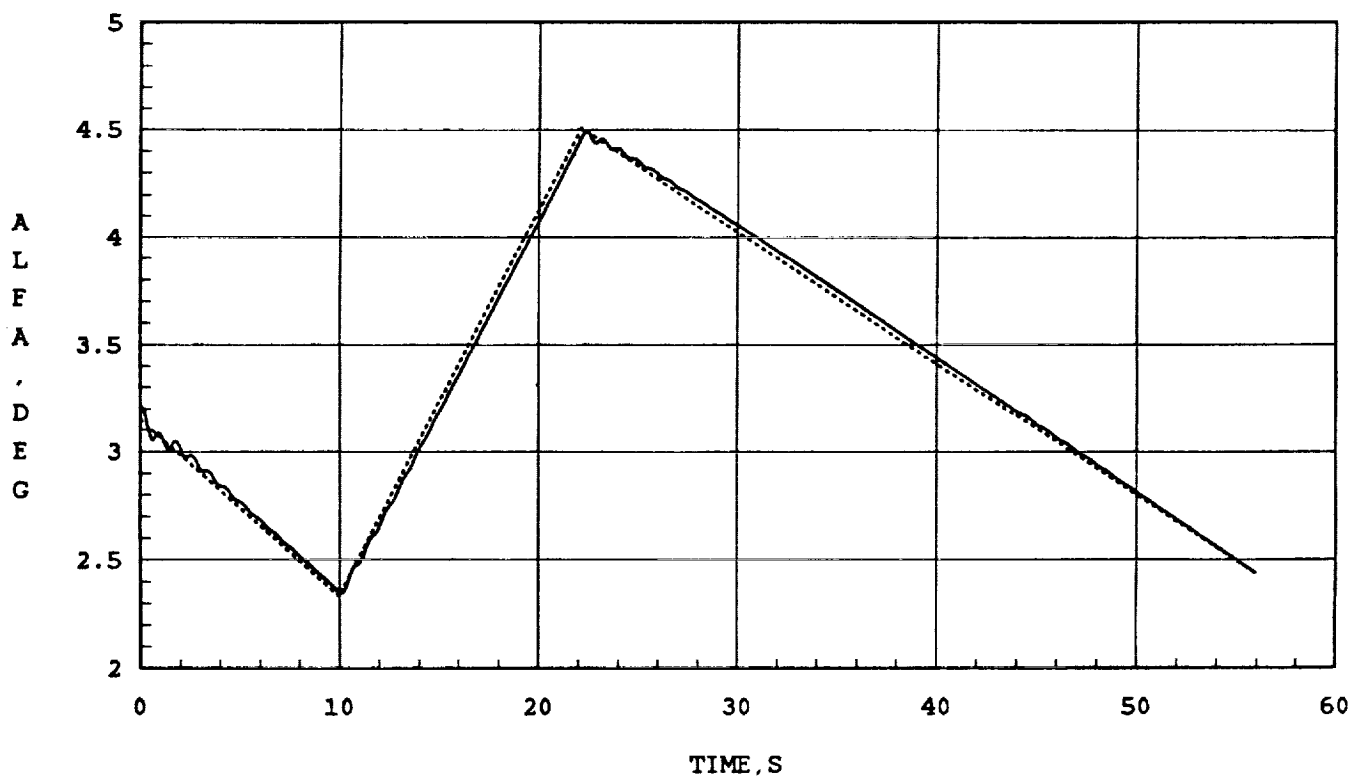


Figure 3.11. Angle of Attack vs. Time along the Zoom and Pushover Maneuver.

Dotted Line: Commanded Angle of Attack
 Solid Line: Actual Angle of Attack.

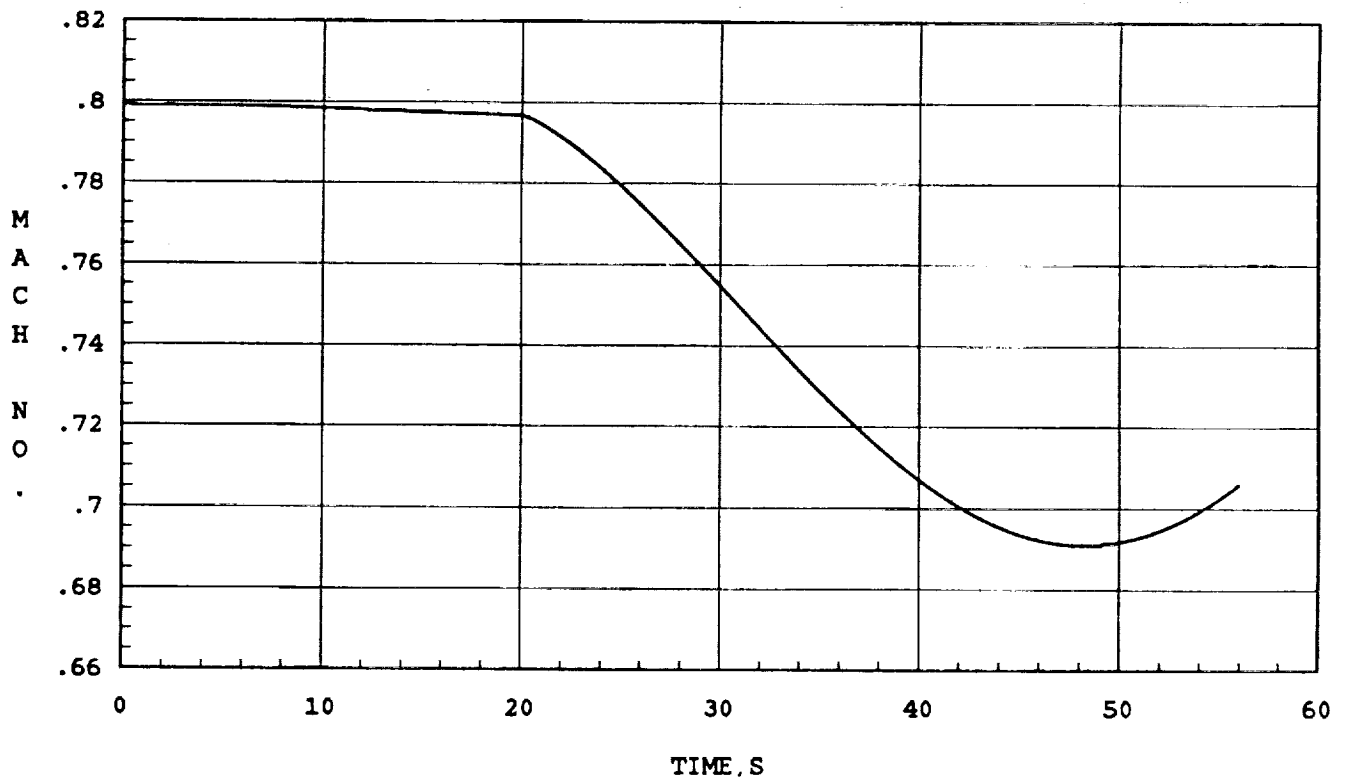


Figure 3.12. Mach number vs. Time along the Zoom and Pushover Maneuver.

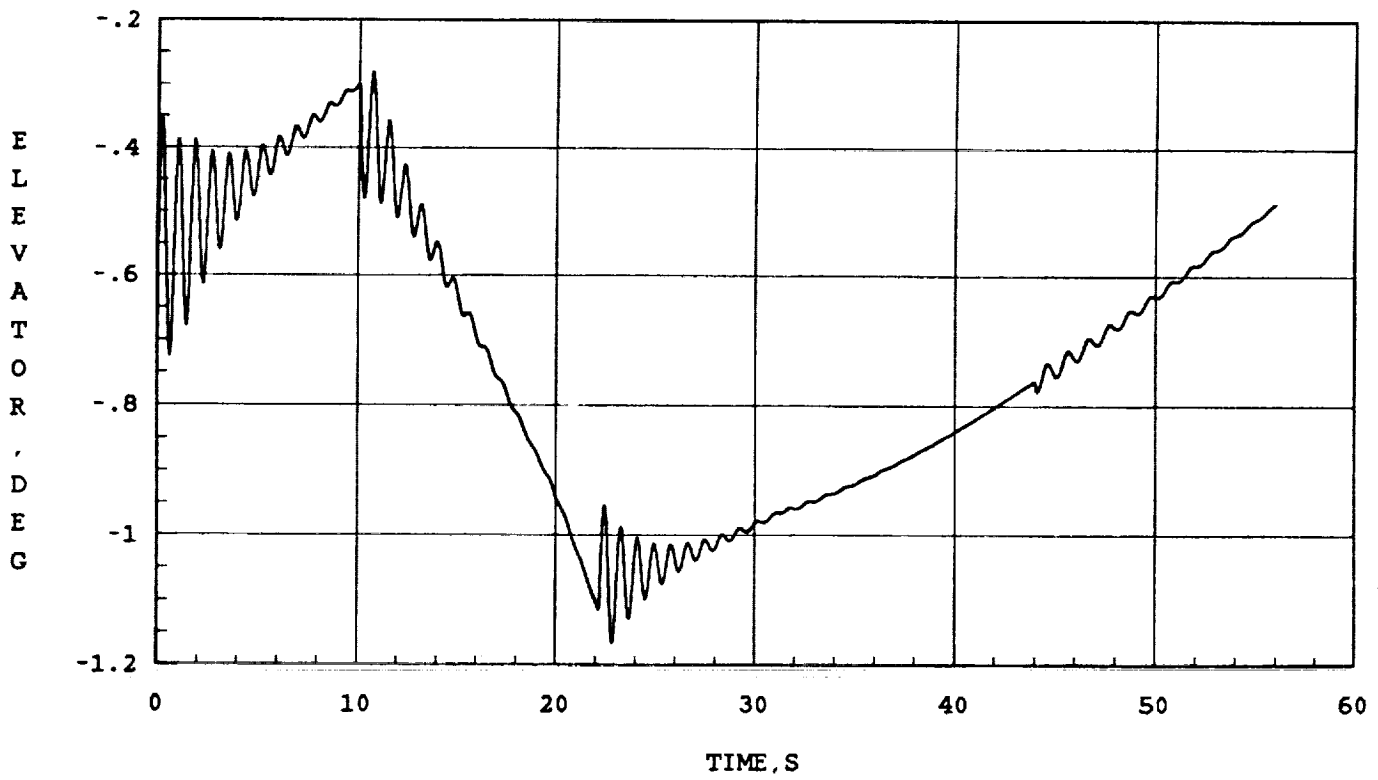


Figure 3.13. Elevator Deflection vs. Time along the Zoom and Pushover Maneuver.

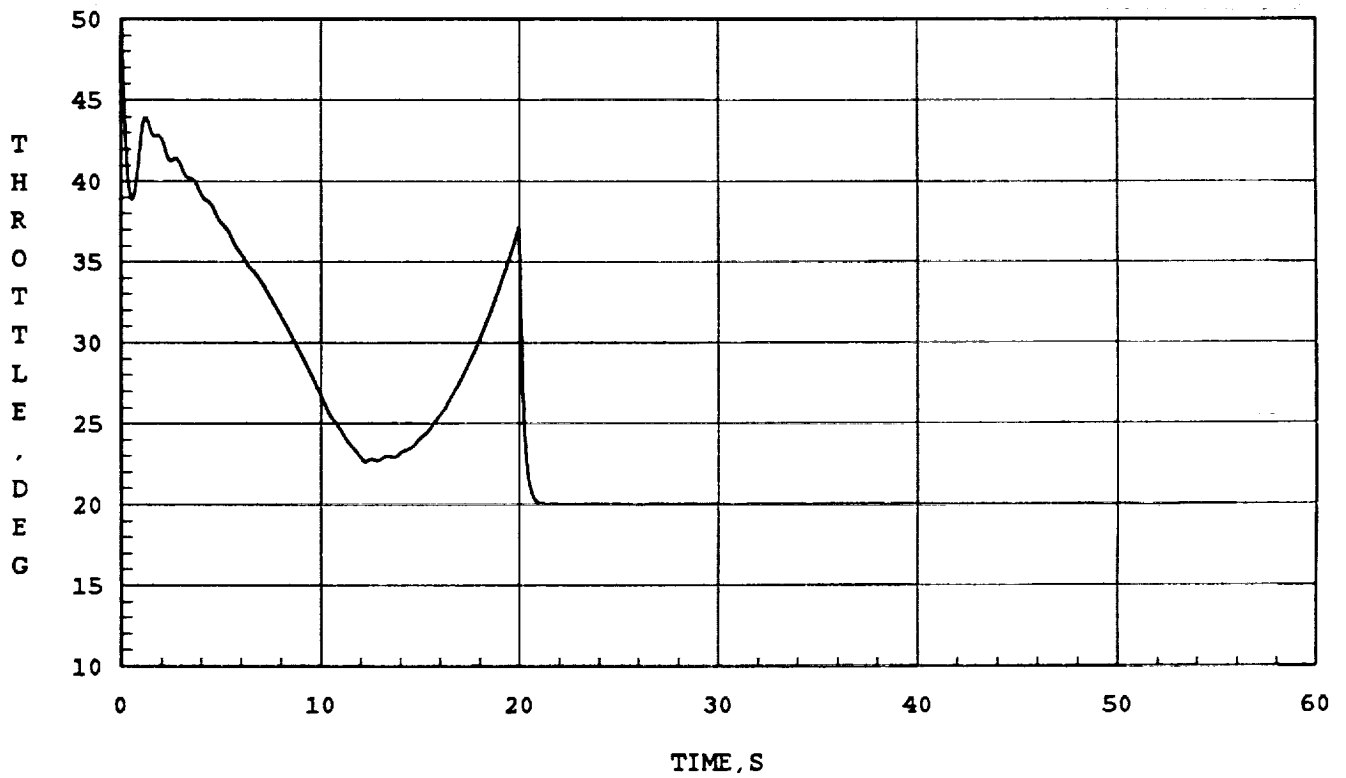


Figure 3.14. Throttle Setting vs. Time along the Zoom and Pushover Maneuver.

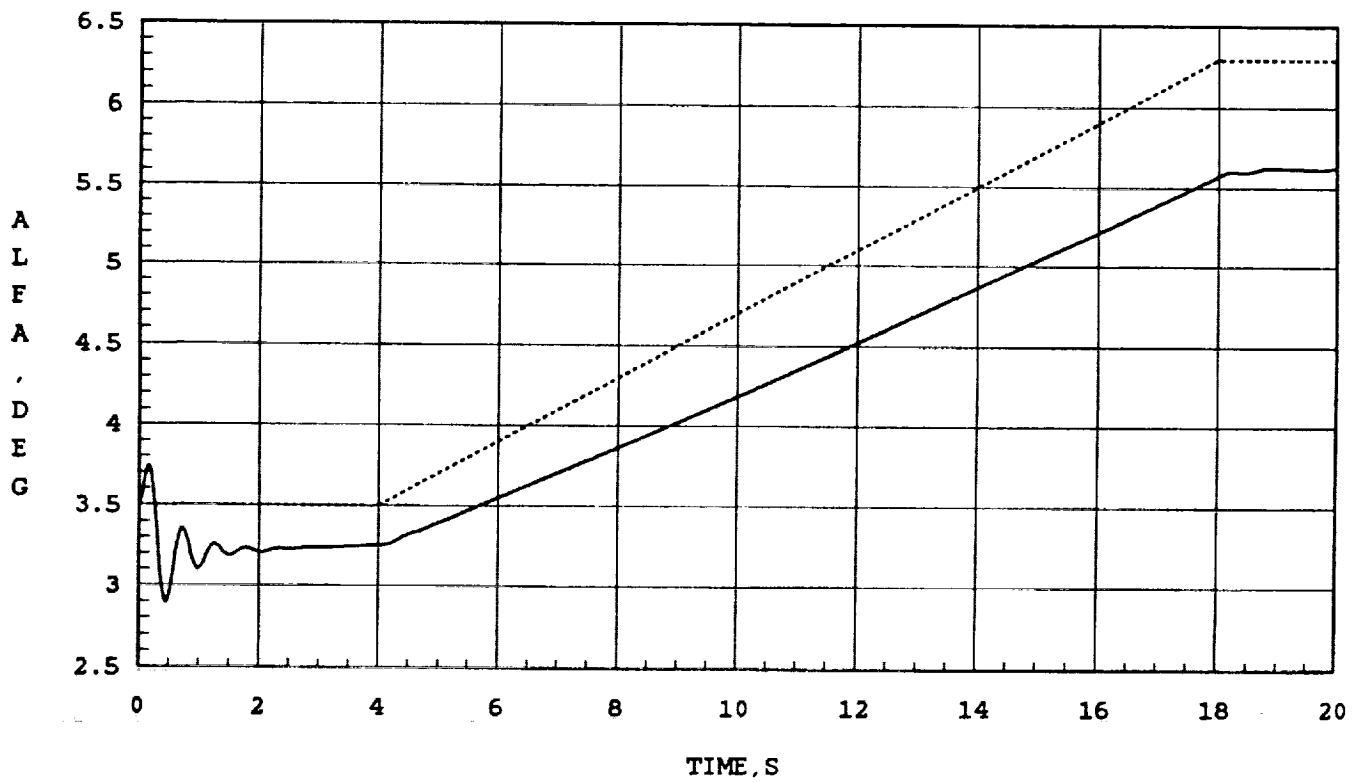
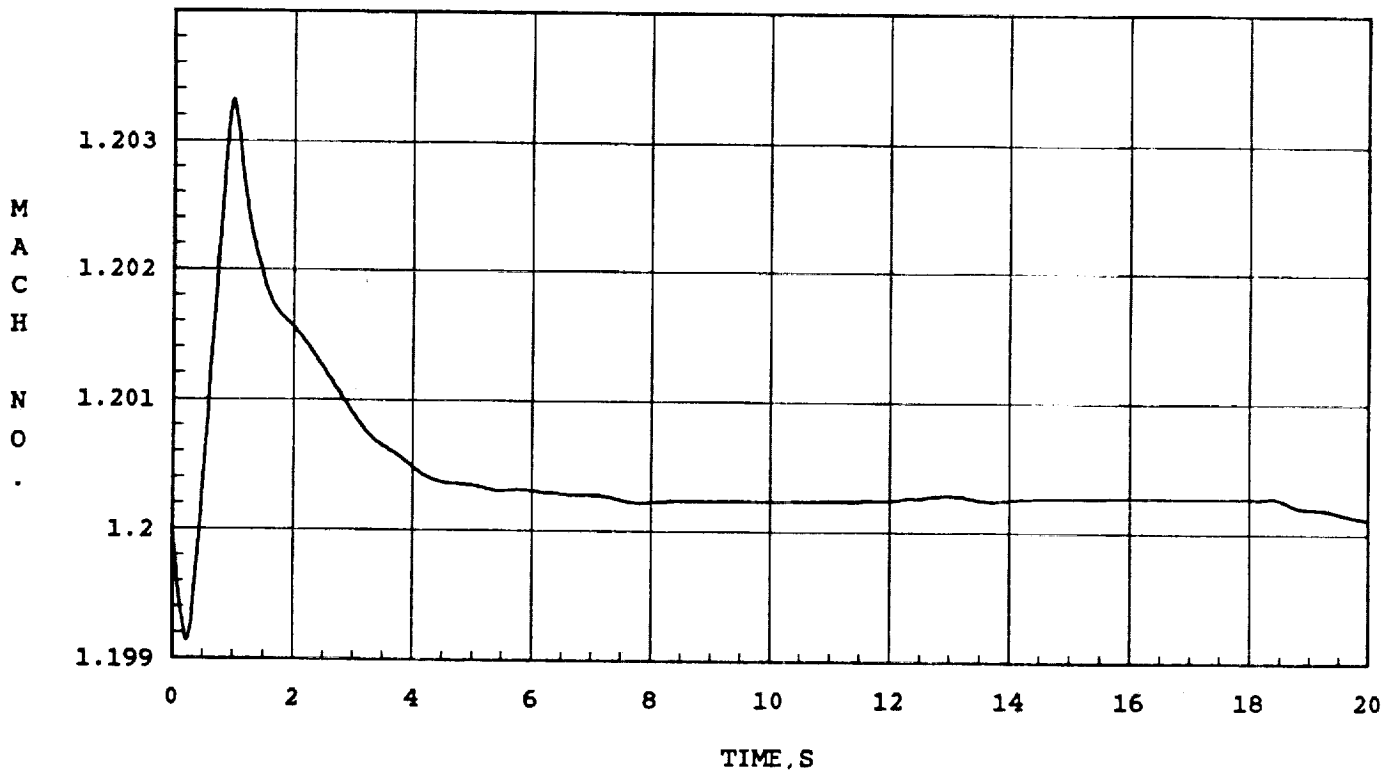


Figure 3.15. Angle of Attack vs. Time along the Excess Thrust Windup Turn Flight Test Trajectory.

Dotted Line: Command Angle of Attack.
 Solid Line: Actual Angle of Attack.



3.16. Mach Number vs. Time along the Excess Thrust Windup Turn Flight Test Trajectory.

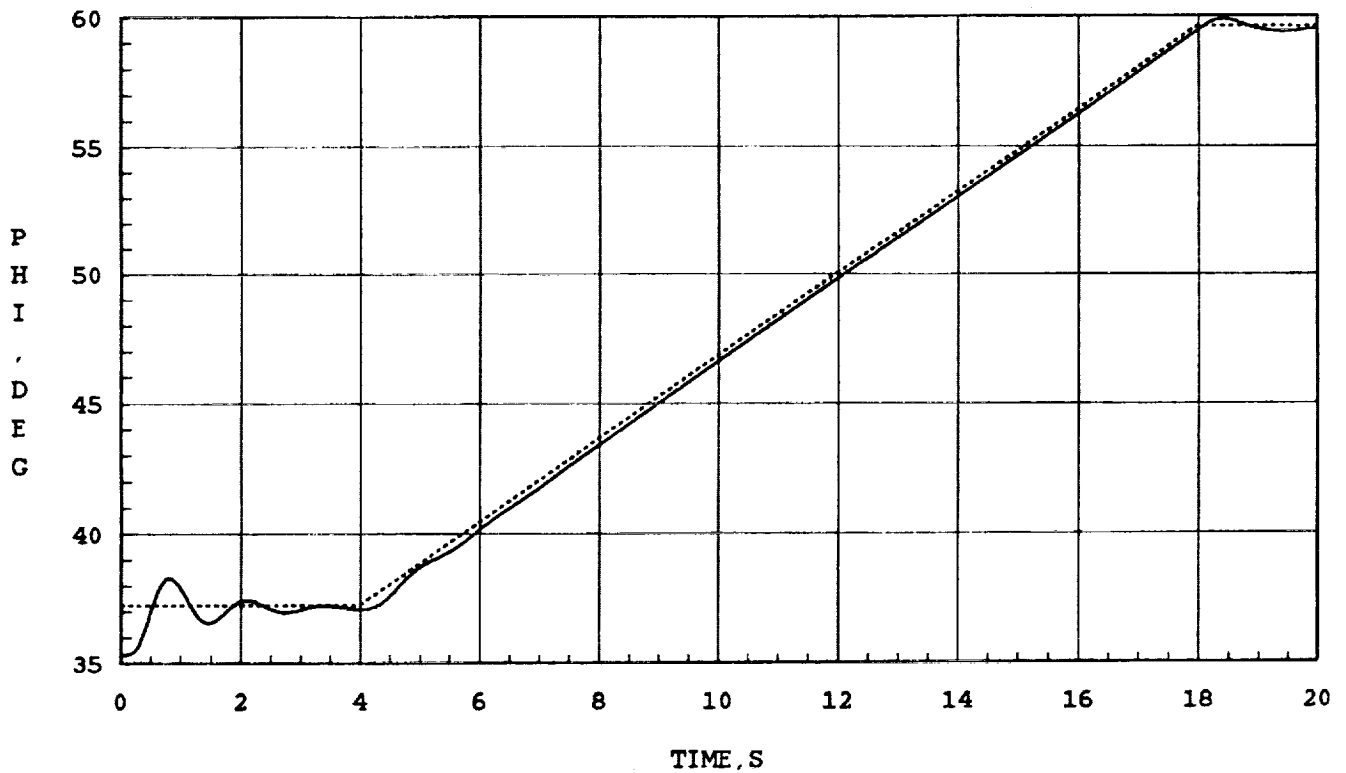


Figure 3.17 Roll Attitude vs. Time along the Excess Thrust Windup Turn Flight Test Trajectory.

Dotted Line: Commanded Roll Attitude.

Solid Line: Actual Roll Attitude.

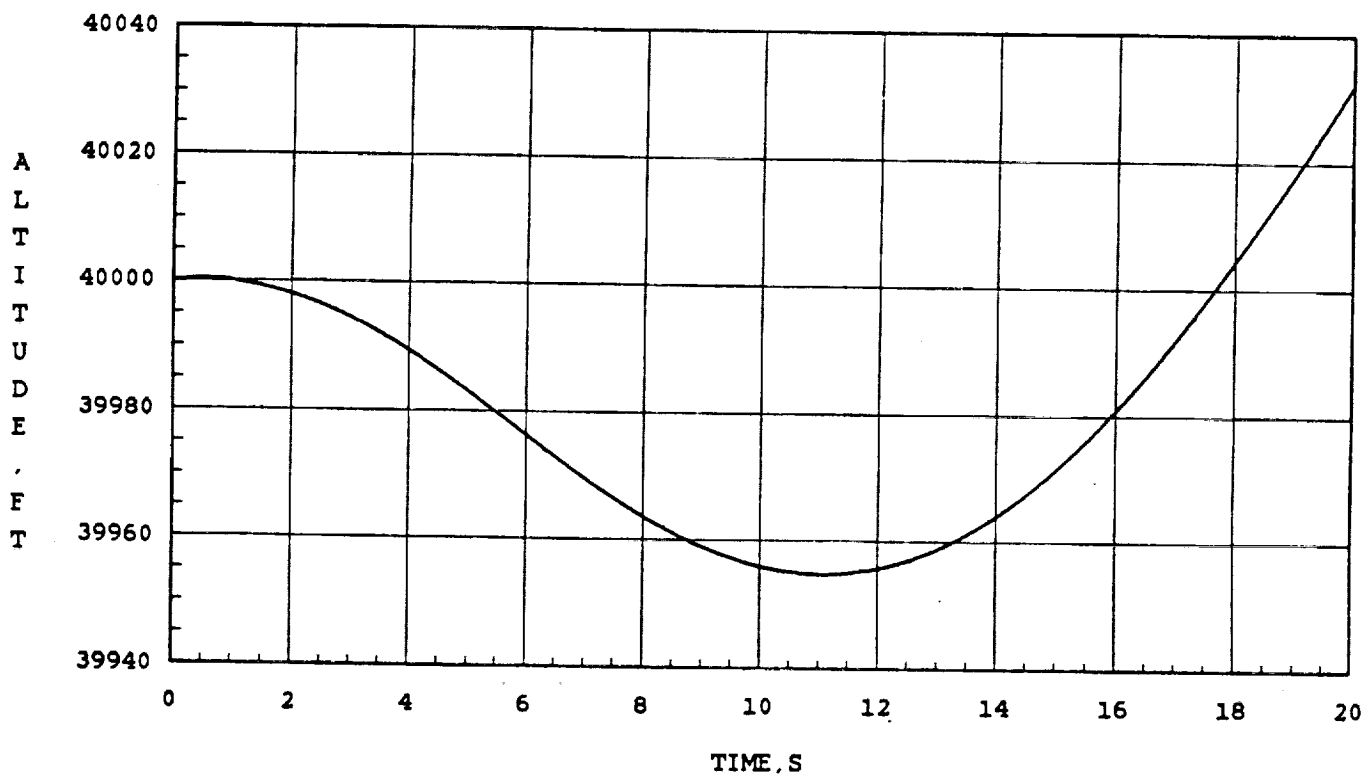


Figure 3.18. Altitude vs. Time along the Excess Thrust Windup Turn Flight Test Trajectory.

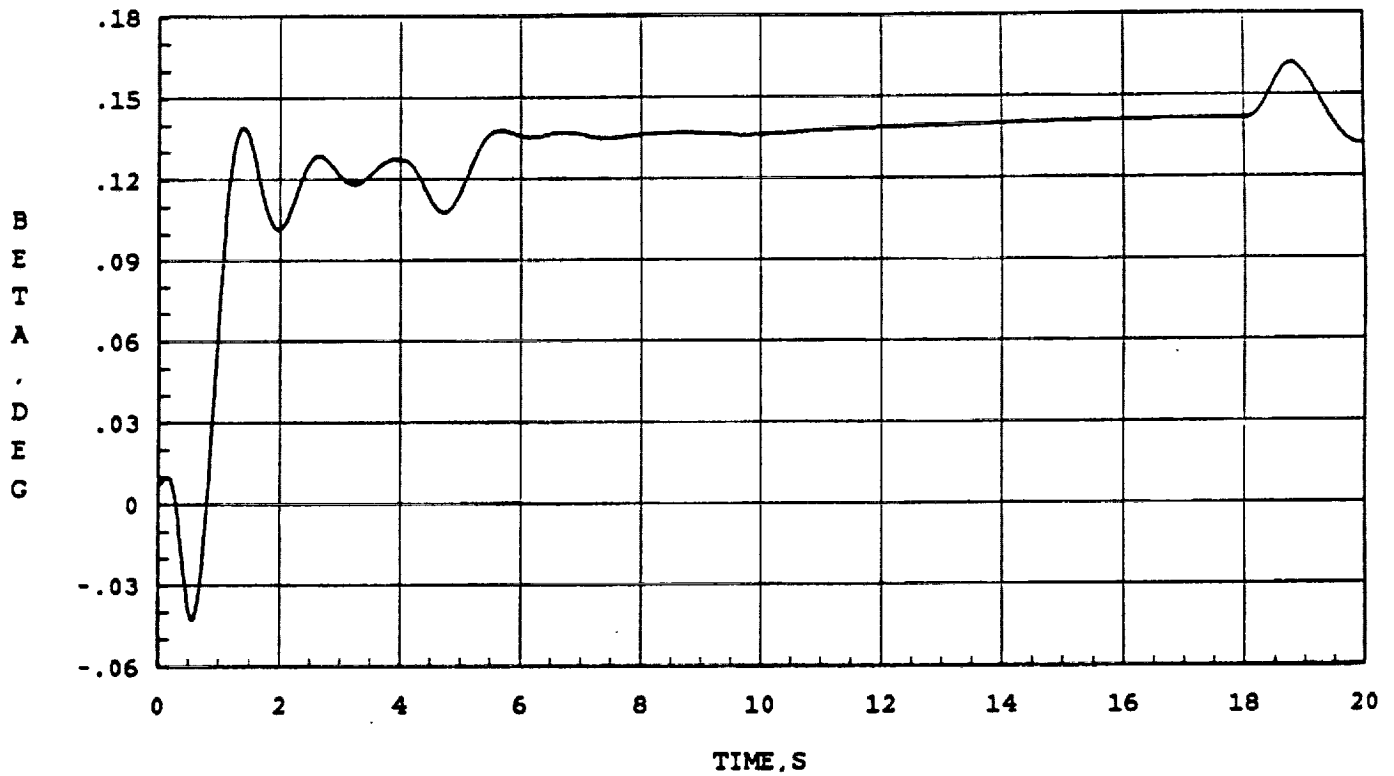


Figure 3.19. Angle of Sideslip vs. Time along the Excess Thrust Windup Turn Flight Test Trajectory.

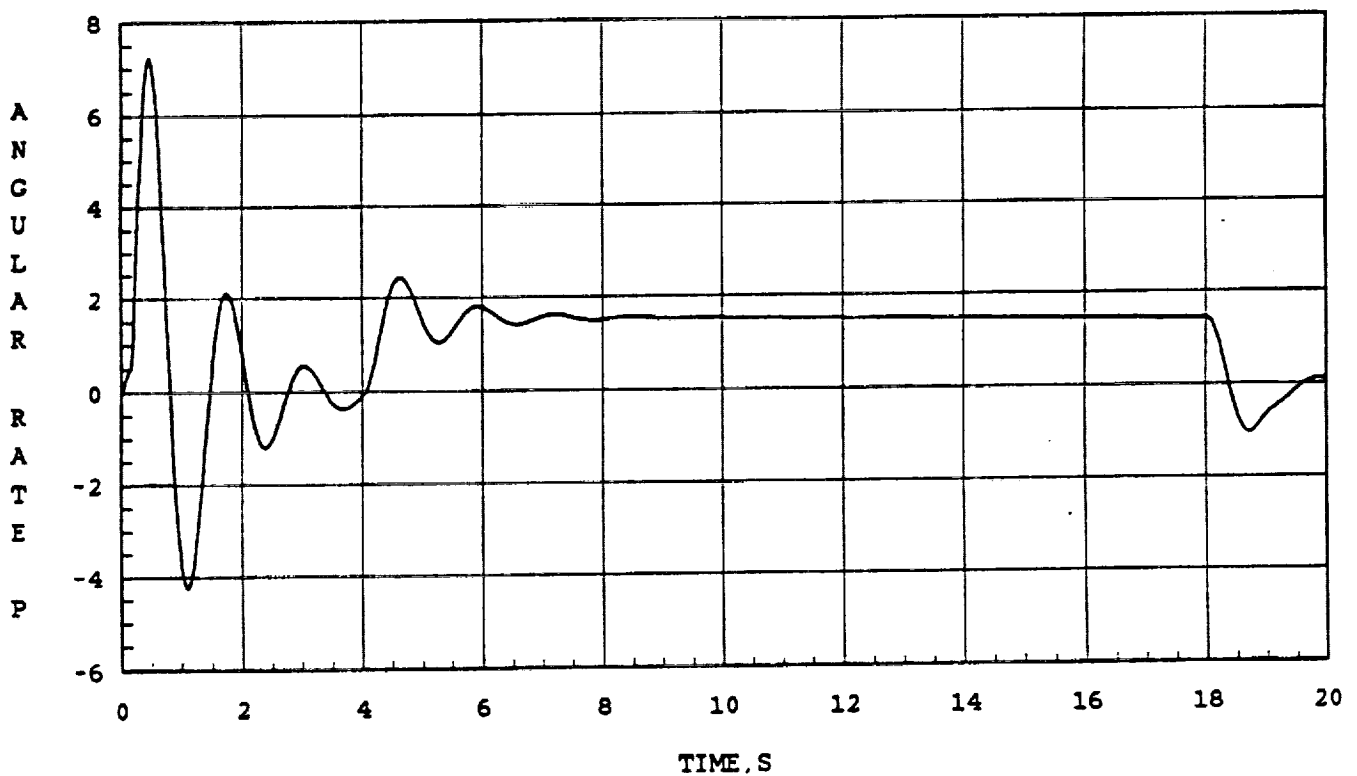


Figure 3.20. Roll Body Rate (Deg/s) vs. Time along the Excess Thrust Windup Turn Flight Test Trajectory.

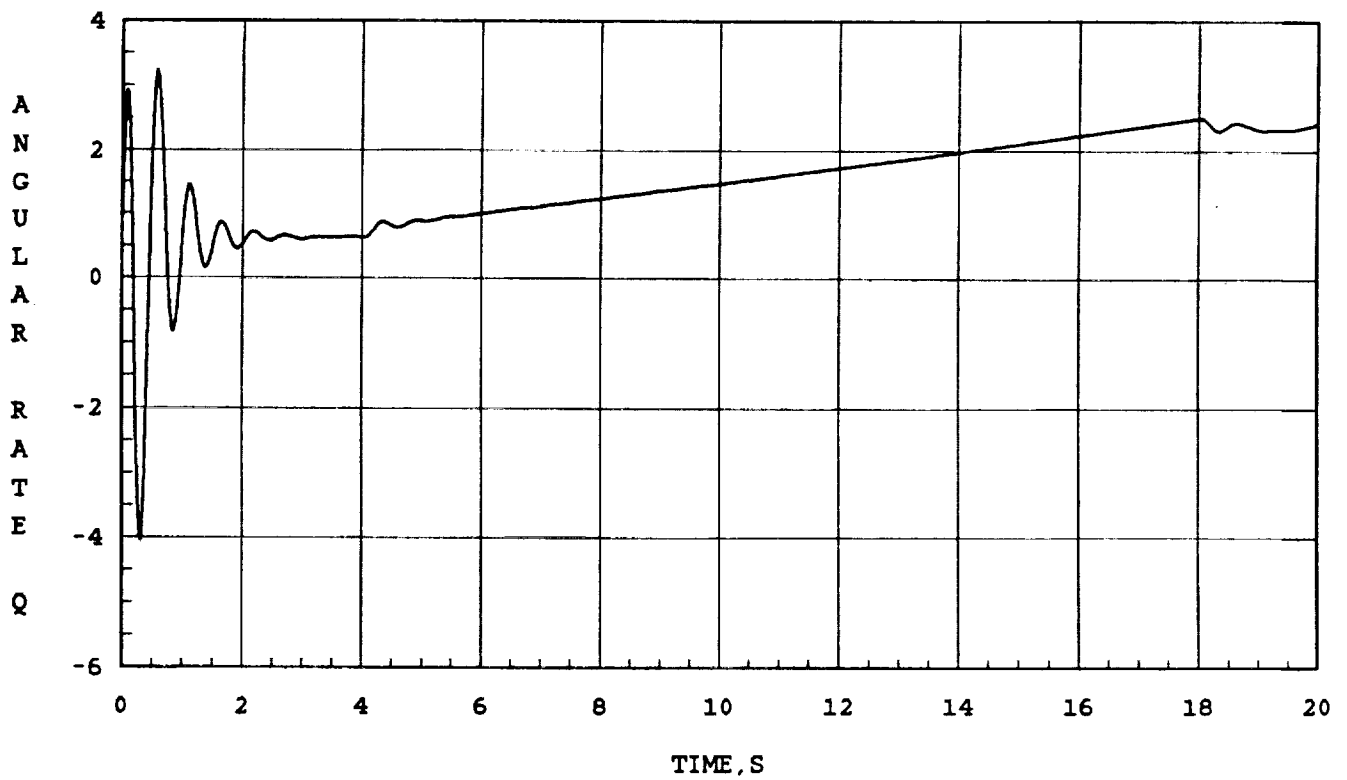


Figure 3.21. Pitch Body Rate (Deg/s) vs. Time along the Excess Thrust Windup Turn Flight Test Trajectory.

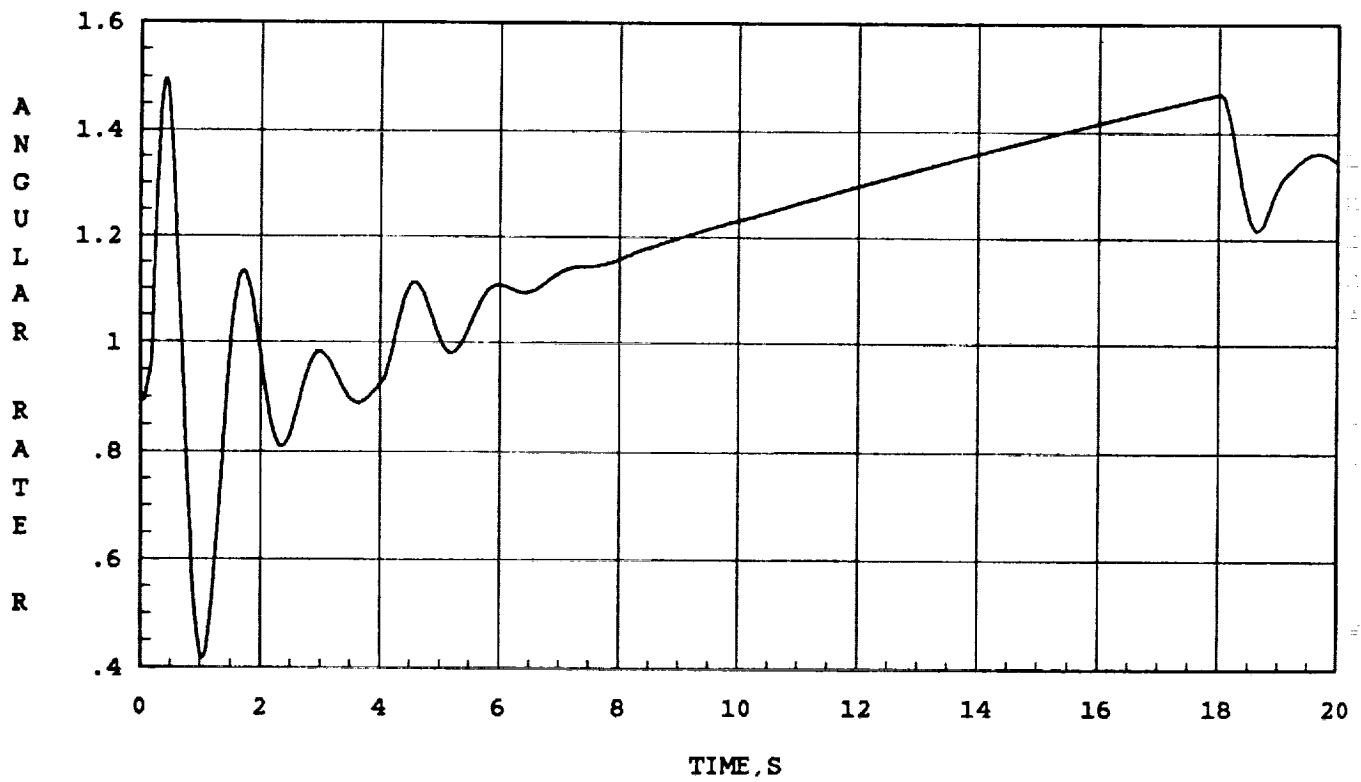


Figure 3.22. Yaw Body Rate (Deg/s) vs. Time along the Excess Thrust Windup Turn Flight Test Trajectory.

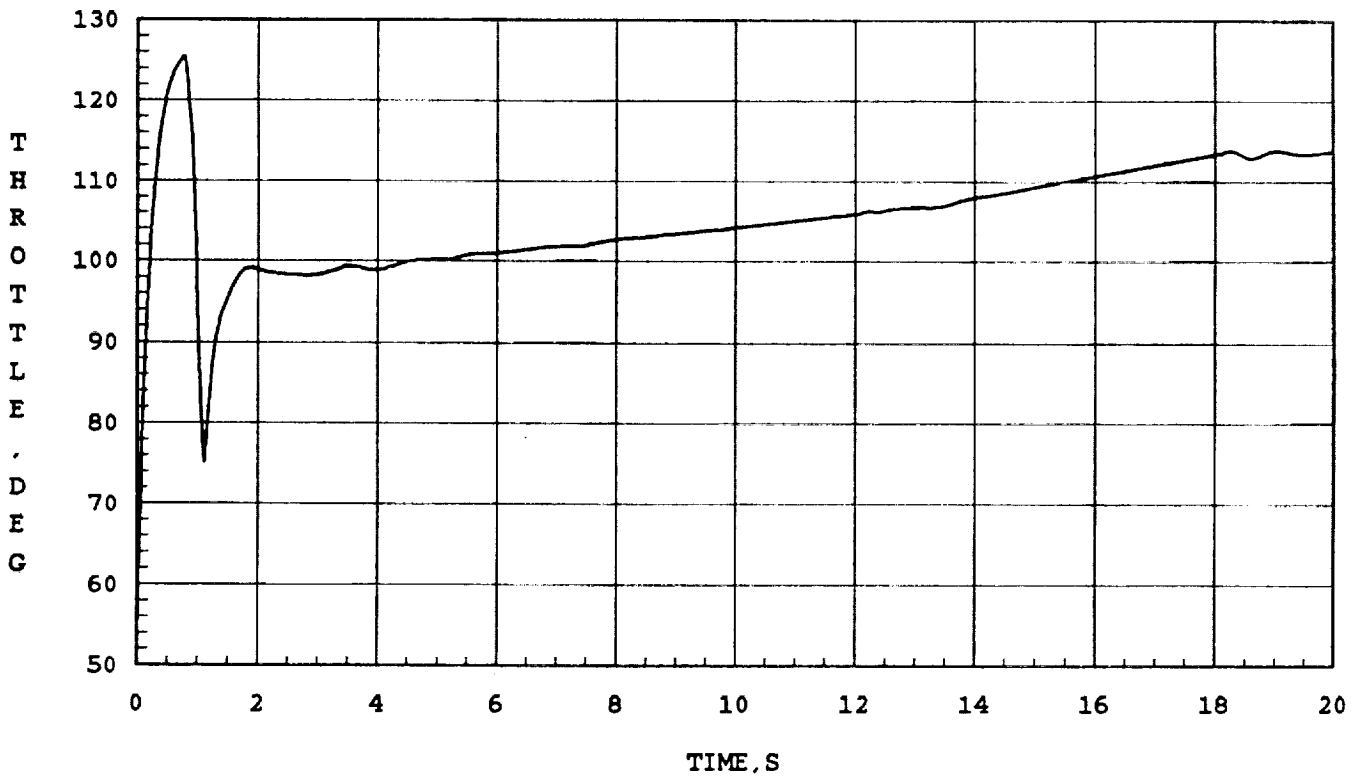


Figure 3.23. Throttle Setting vs. Time along the Excess Thrust Windup Turn Flight Test Trajectory.

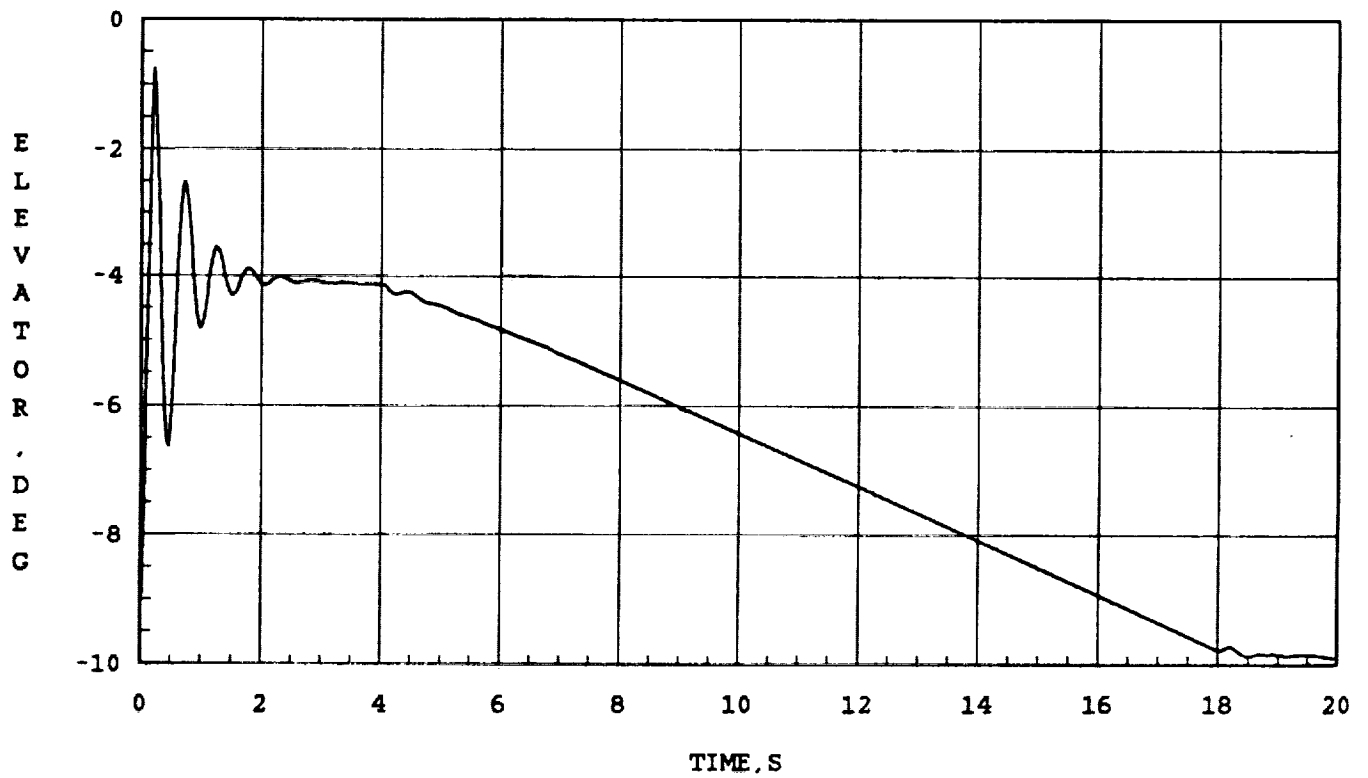


Figure 3.24. Elevator Deflection vs. Time along the Excess Thrust Windup Turn Flight Test Trajectory.

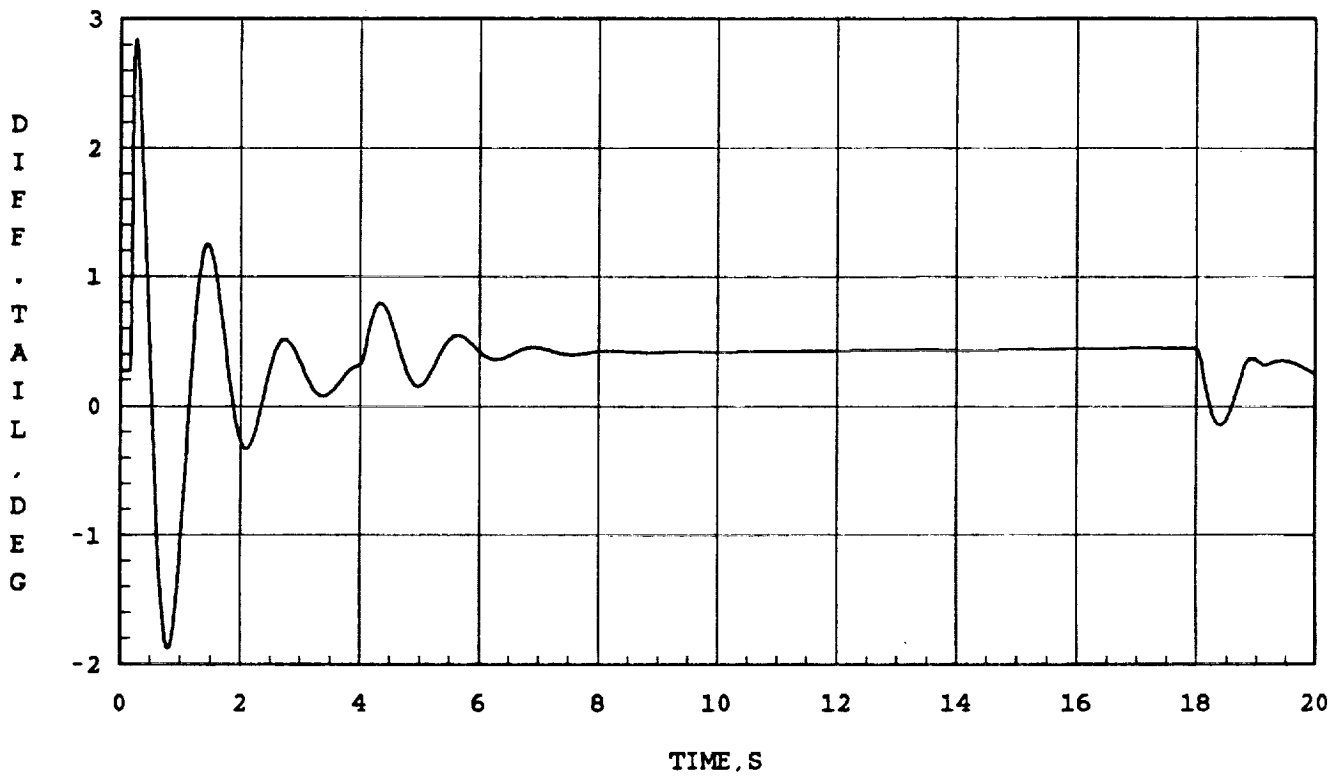


Figure 3.25. Differential Tail Deflection vs. Time along the Excess Thrust Windup Turn Flight Test Trajectory.

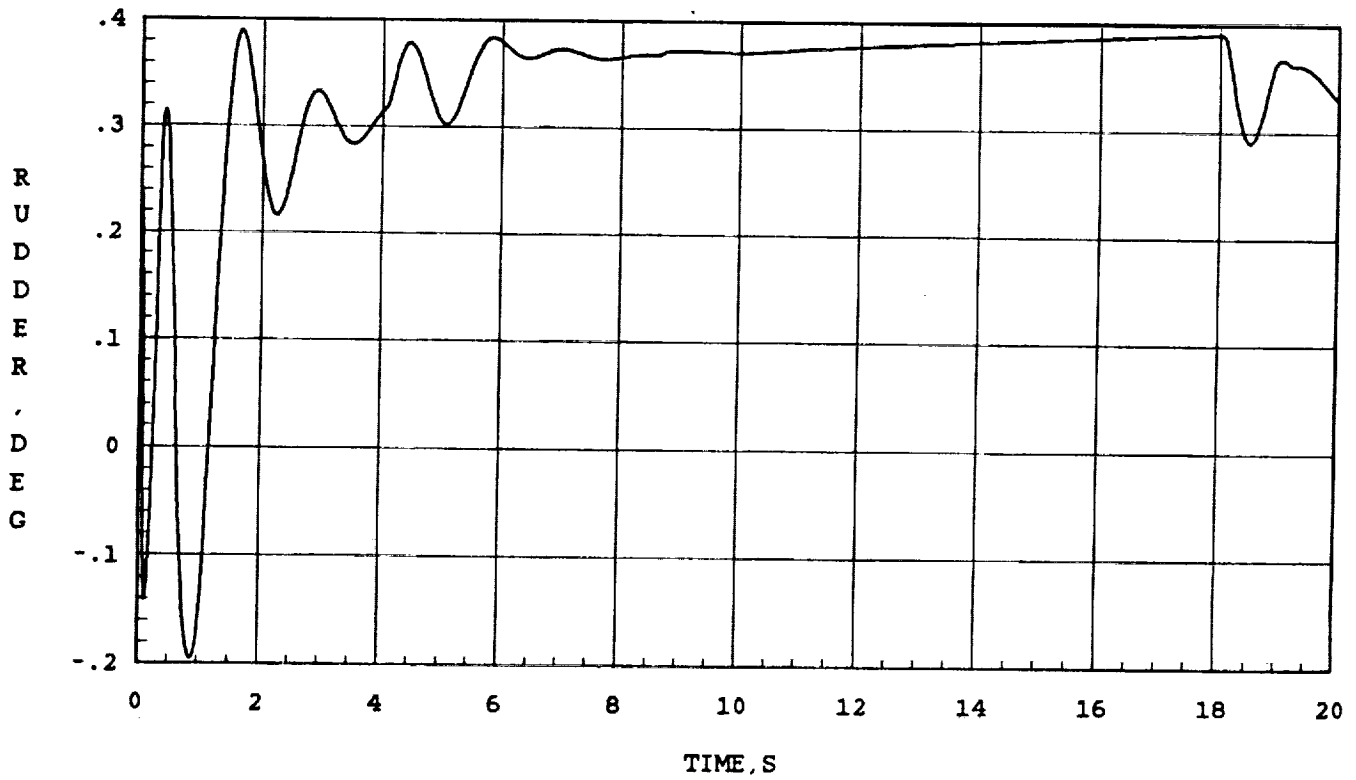


Figure 3.26. Rudder Deflection vs. Time along the Excess Thrust Windup Turn Flight Test Trajectory.

was a component of the normal acceleration rather than the pure normal acceleration. It is possible that this hang-off error arises due to angle of attack limit also. In any case, the angle of attack error is less than a degree throughout the maneuver. The important requirement in this maneuver, however, is that the angle of attack history be linear in time, which is certainly satisfied by the present nonlinear controller. The Mach number error is within 0.0005 throughout the maneuver. The roll attitude tracking is excellent, being less than 0.2 degrees throughout the maneuver. The altitude error throughout the maneuver is within ± 50 feet, which satisfies the specifications. It should be possible to decrease this error by using finer trim data in the maneuver modeling program.

3.3.5. Constant Thrust Windup Turn

In this maneuver, it is desired to track a linear angle of attack history with fixed throttle setting while maintaining constant Mach number. Since the throttle is fixed, the Mach number can be maintained only through an altitude rate. Moreover, since the normal acceleration channel is used to track the angle of attack history, the required altitude rate will have to be achieved through an appropriate roll attitude. Thus the maneuver autopilot consist of the airspeed controller (2.13), (2.14), (2.19) in conjunction with the altitude controller (2.25), (2.26), (2.29), (2.30) and the roll attitude controller (2.40), (2.41), and (2.43); and the angle of attack controller (2.33), (2.34) and (2.37). Note that this implementation relies on the fact that the airspeed control loop is driven slower than the altitude control loop which in turn is assumed to be slower than the roll attitude control loop.

Just as in the excess thrust windup turn flight test trajectory, in order to simplify the controller implementation, the maneuver modeling described in [16] is used to generate a consistent set of angle of attack and roll attitude commands to yield the desired constant thrust windup turn trajectory.

The performance of the controller along the constant thrust windup turn trajectory is given in Figures 3.27 through 3.38. Just as in the excess thrust windup turn case, there is a hang-off error in the angle of attack history, which appears to depend on the roll attitude. The tracking error is always less than about one degree throughout. The Mach number is maintained within 0.015 during the maneuver while the altitude is within 120 feet of the required value. Throughout this maneuver, the throttle is maintained at 105 degrees.

3.3.6. Constant Dynamic Pressure, Constant Load Factor Trajectory

Along this flight test trajectory, the load factor and the dynamic pressure should be constant, while maintaining a desired Mach rate. The load factor can be maintained by fixing the value of normal acceleration while the desired Mach rate can be sustained using the throttle. The dynamic pressure is maintained by an appropriate altitude rate depending on the desired Mach rate and ambient density. The altitude rate is generated through the vehicle roll attitude. It is clear that one cannot permit an arbitrary Mach rate in the system while maintaining the load factor and dynamic pressure constant since

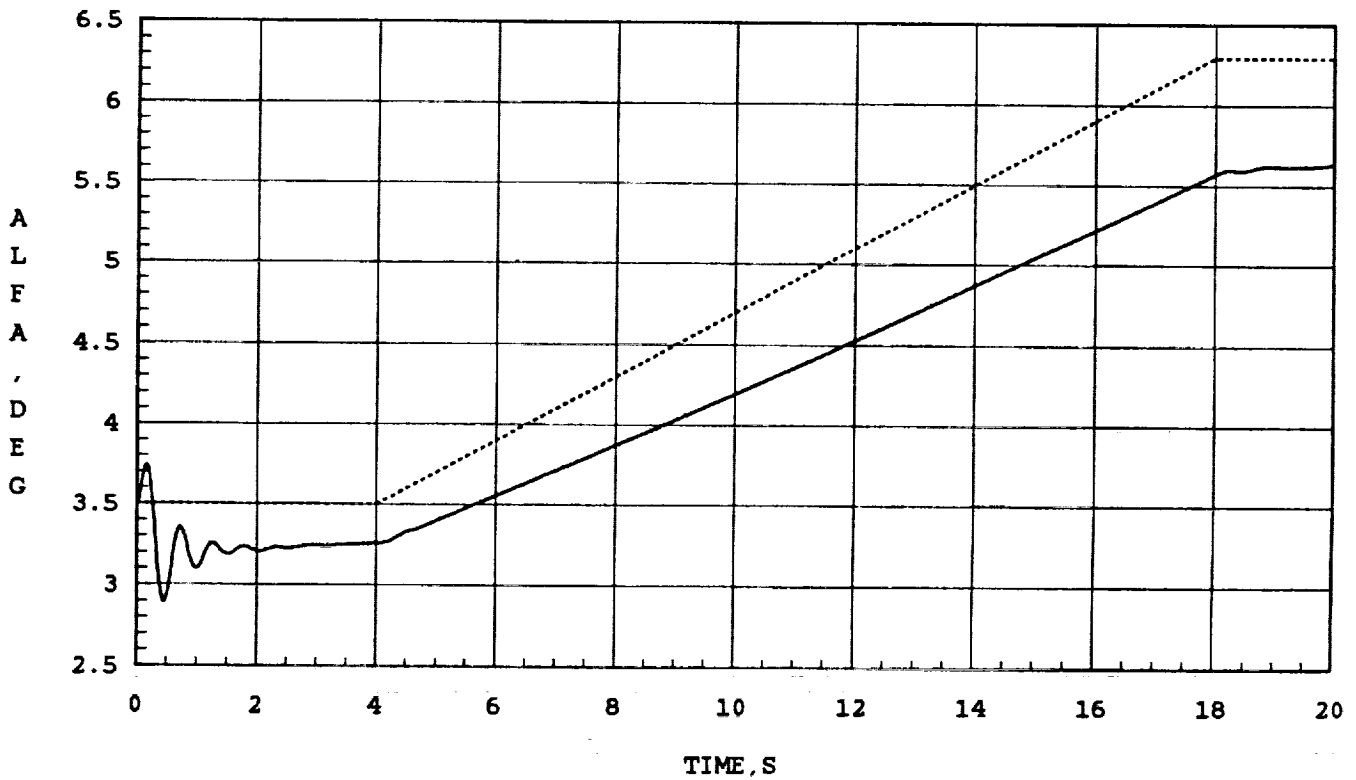


Figure 3.27. Angle of Attack vs. Time along the Constant Thrust Windup Turn Flight Test Trajectory.

**Dotted Line: Commanded Angle of Attack.
 Solid Line: Actual Angle of Attack.**

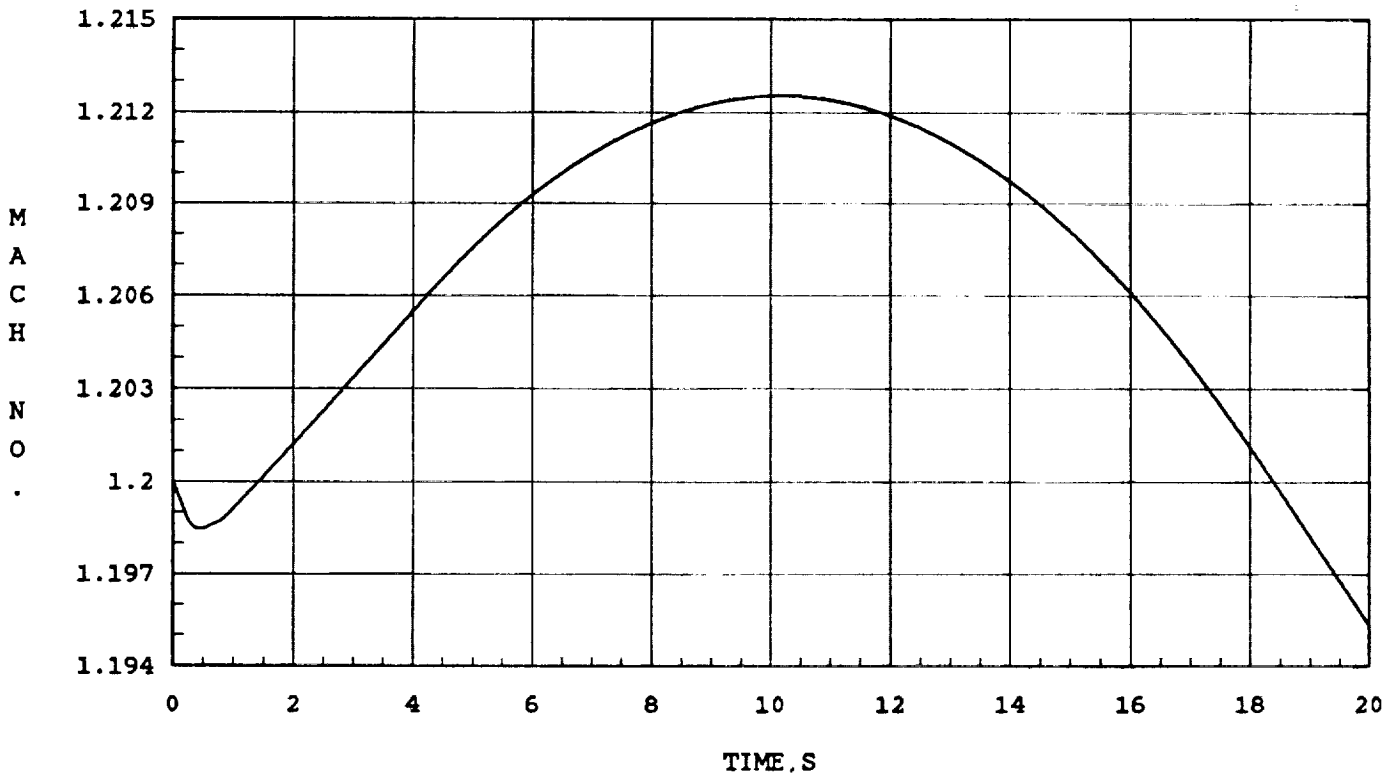


Figure 3.28. Mach Number vs. Time along the Constant Thrust Windup Turn Flight Test Trajectory.

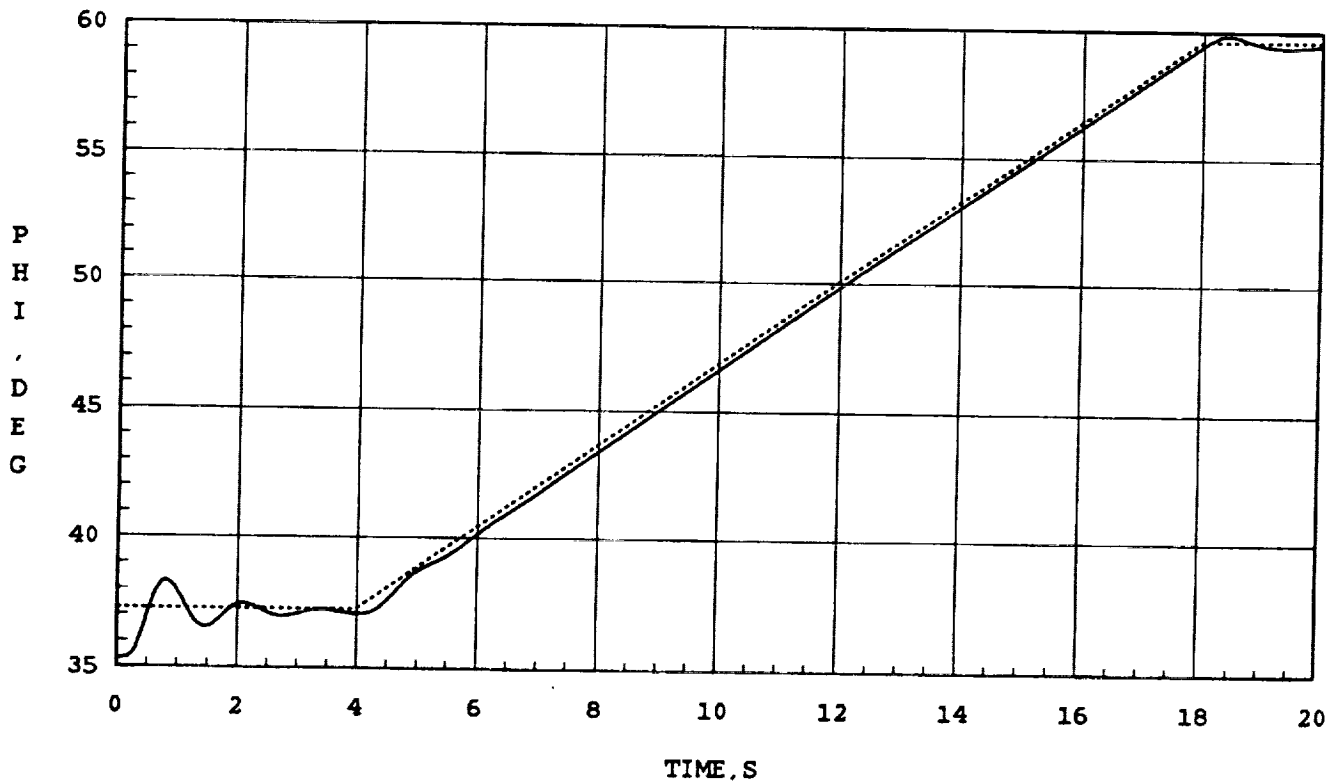
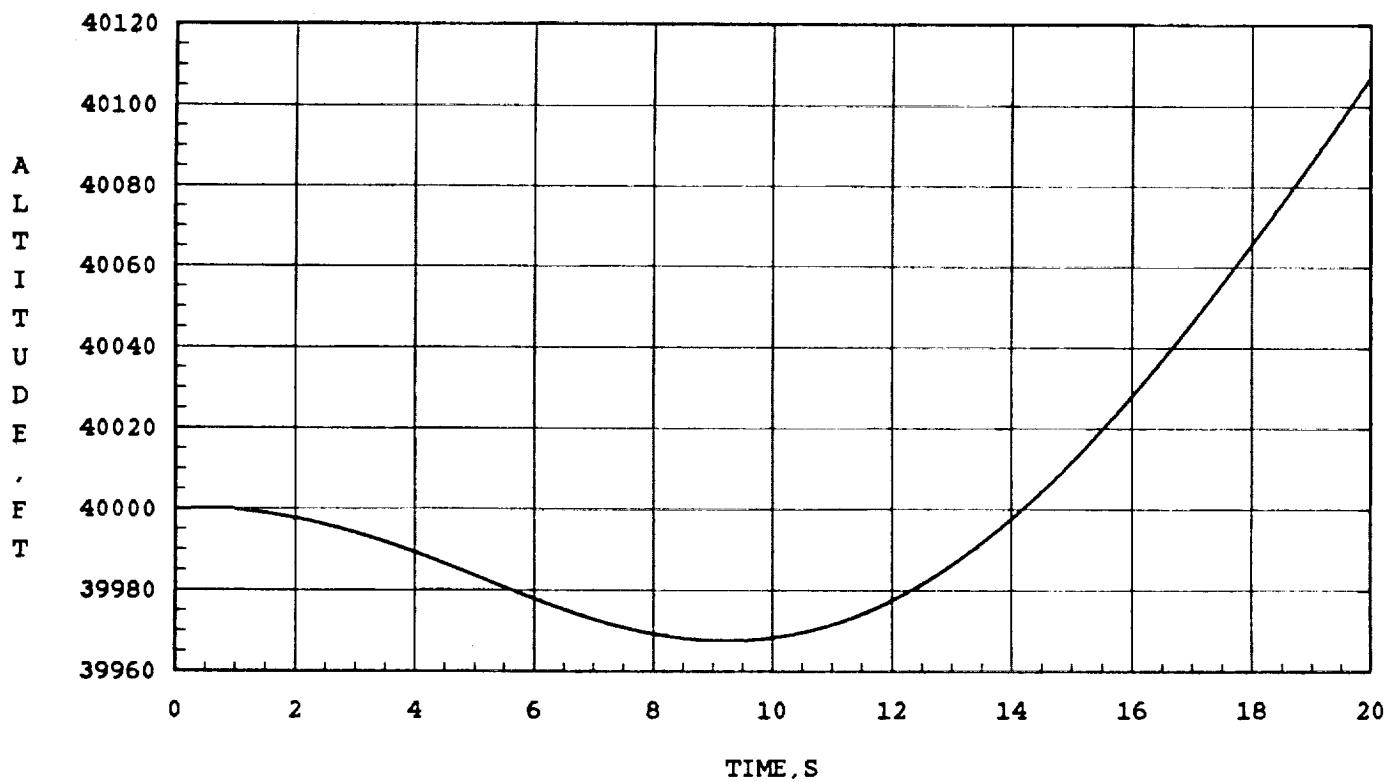


Figure 3.29. Roll Attitude vs. Time along the Constant Thrust Windup Turn Flight Test Trajectory.

Dotted Line: Commanded Roll Attitude.

Solid Line: Actual Roll Attitude.



3.30 Altitude vs. Time along the Constant Thrust Windup Turn Flight Test Trajectory.

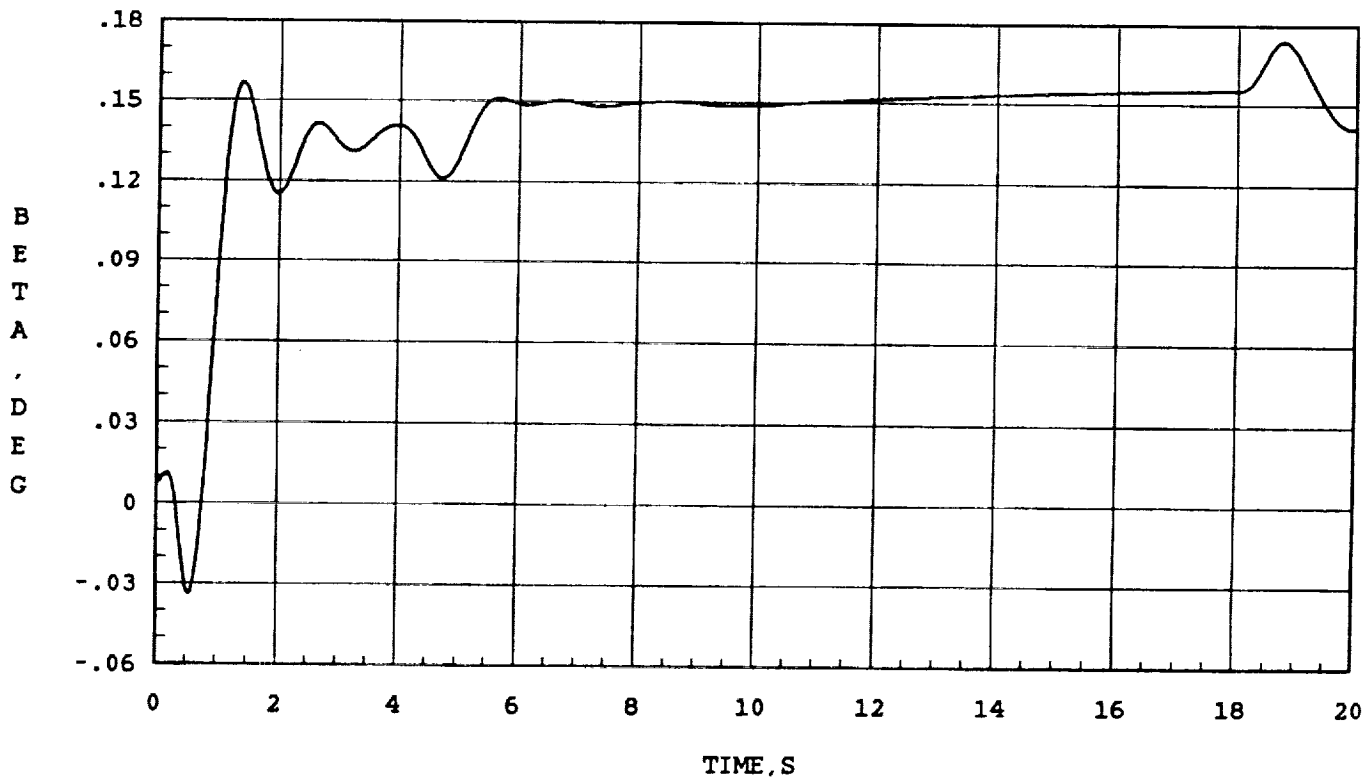


Figure 3.31. Angle of Sideslip vs. Time along the Constant Thrust Windup Turn Flight Test Trajectory.

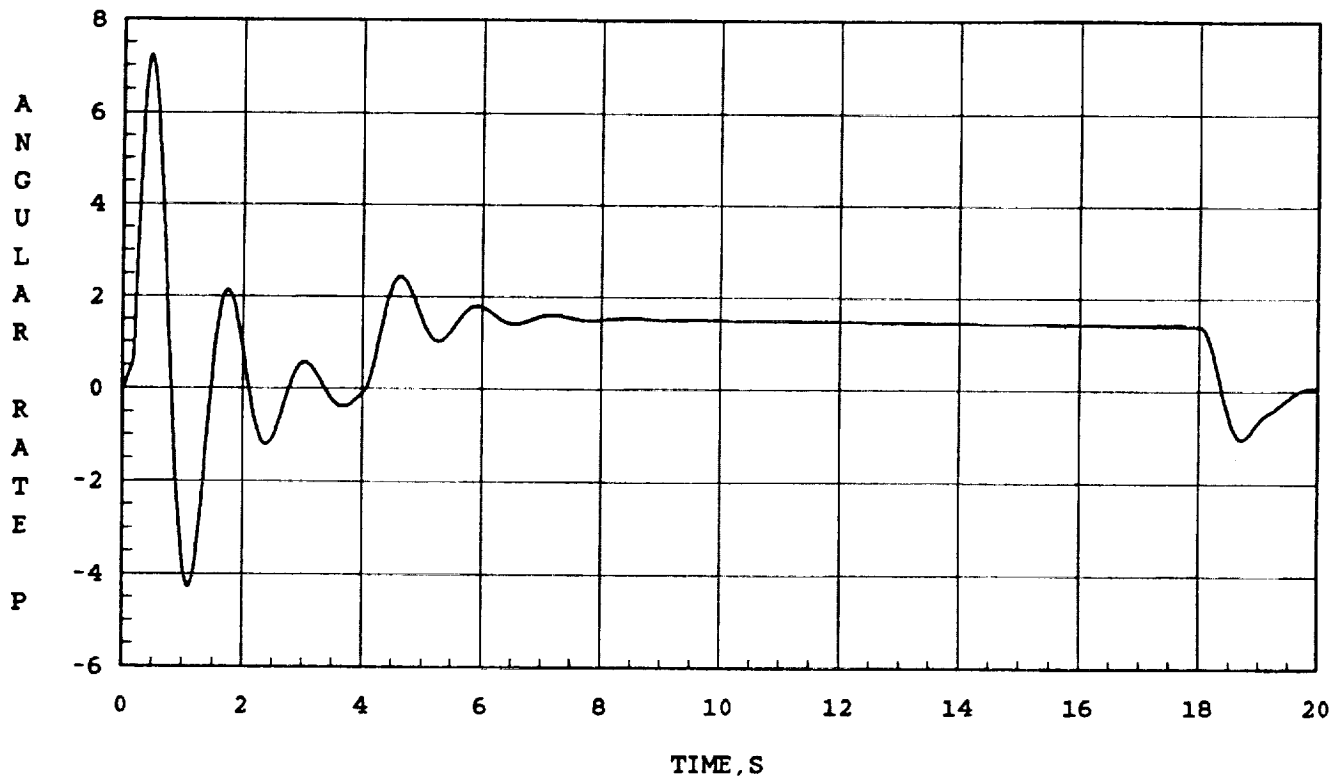


Figure 3.32. Roll Body Rate (Deg/s) vs. Time along the Constant Thrust Windup Turn Flight Test Trajectory.

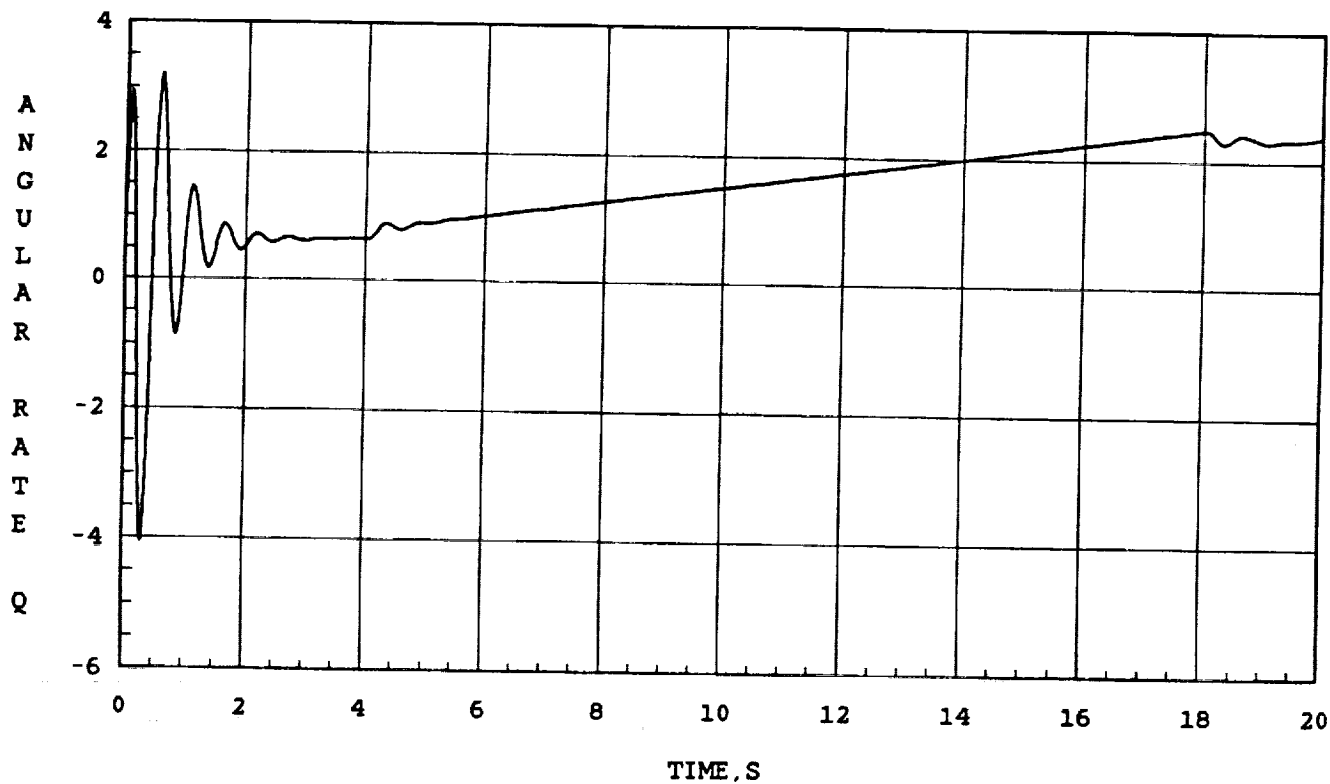


Figure 3.33. Pitch Body Rate (Deg/s) vs. Time along the Constant Thrust Windup Turn Flight Test Trajectory.

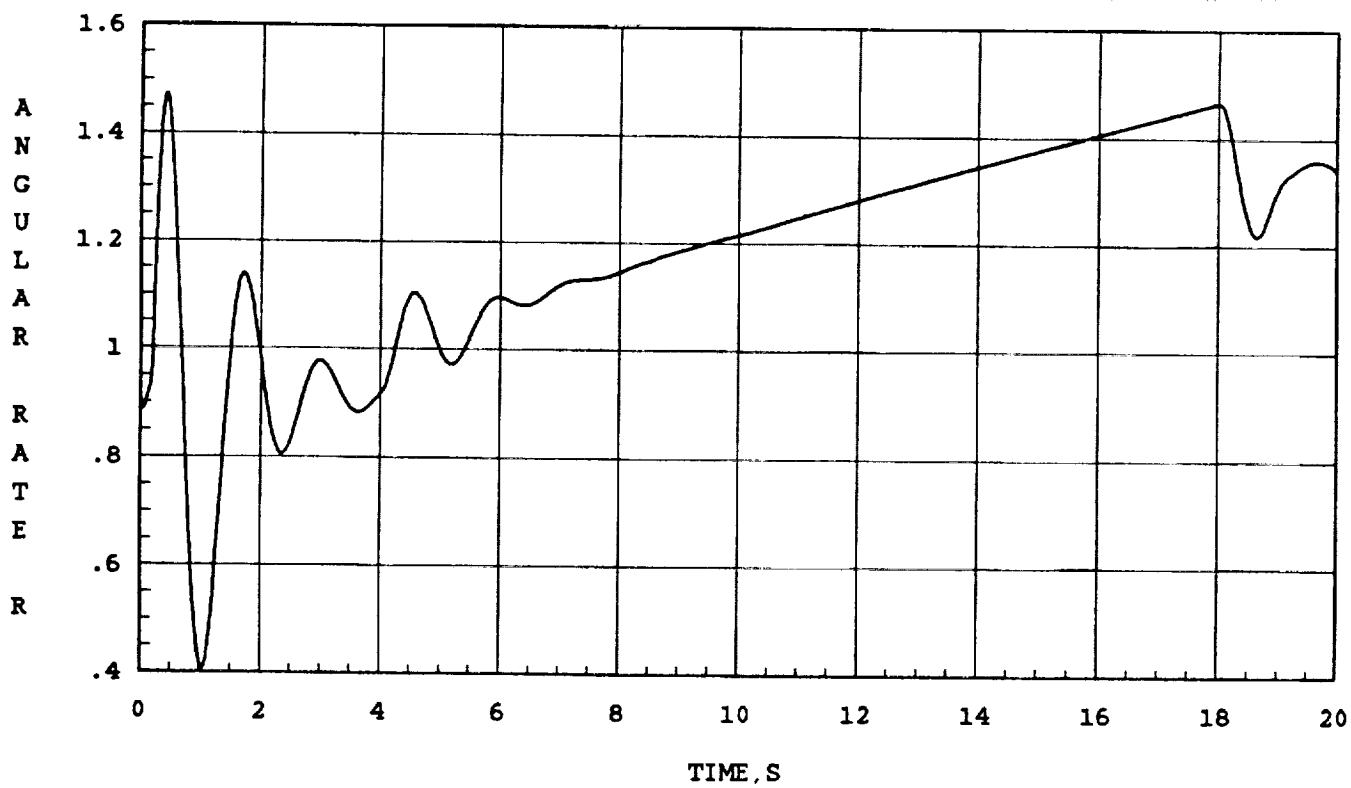


Figure 3.34. Yaw Body Rate (Deg/S) vs. Time along the Constant Thrust Windup Turn Flight Test Trajectory.

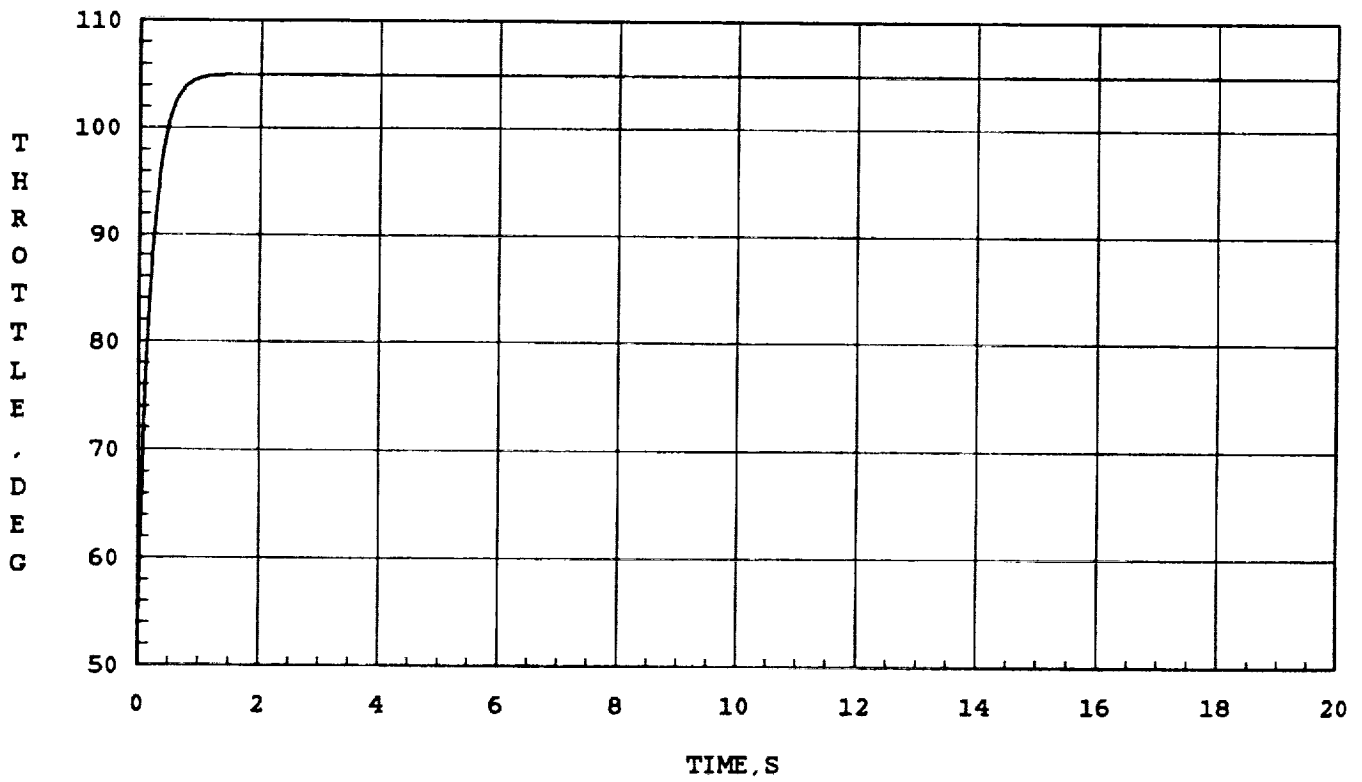


Figure 3.35. Throttle Setting vs. Time along the Constant Thrust Windup Turn Flight Test Trajectory.

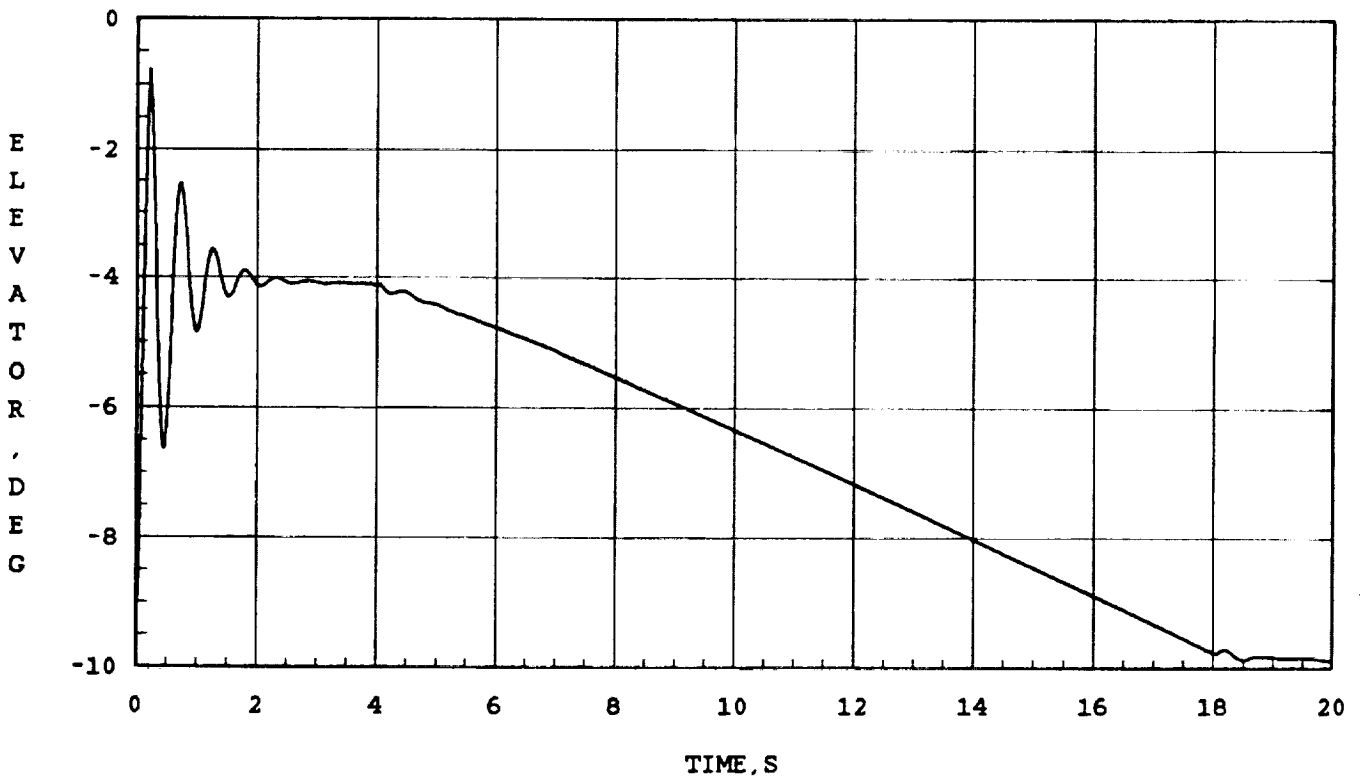


Figure 3.36. Elevator Deflection vs. Time along the Constant Thrust Windup Turn Flight Test Trajectory.

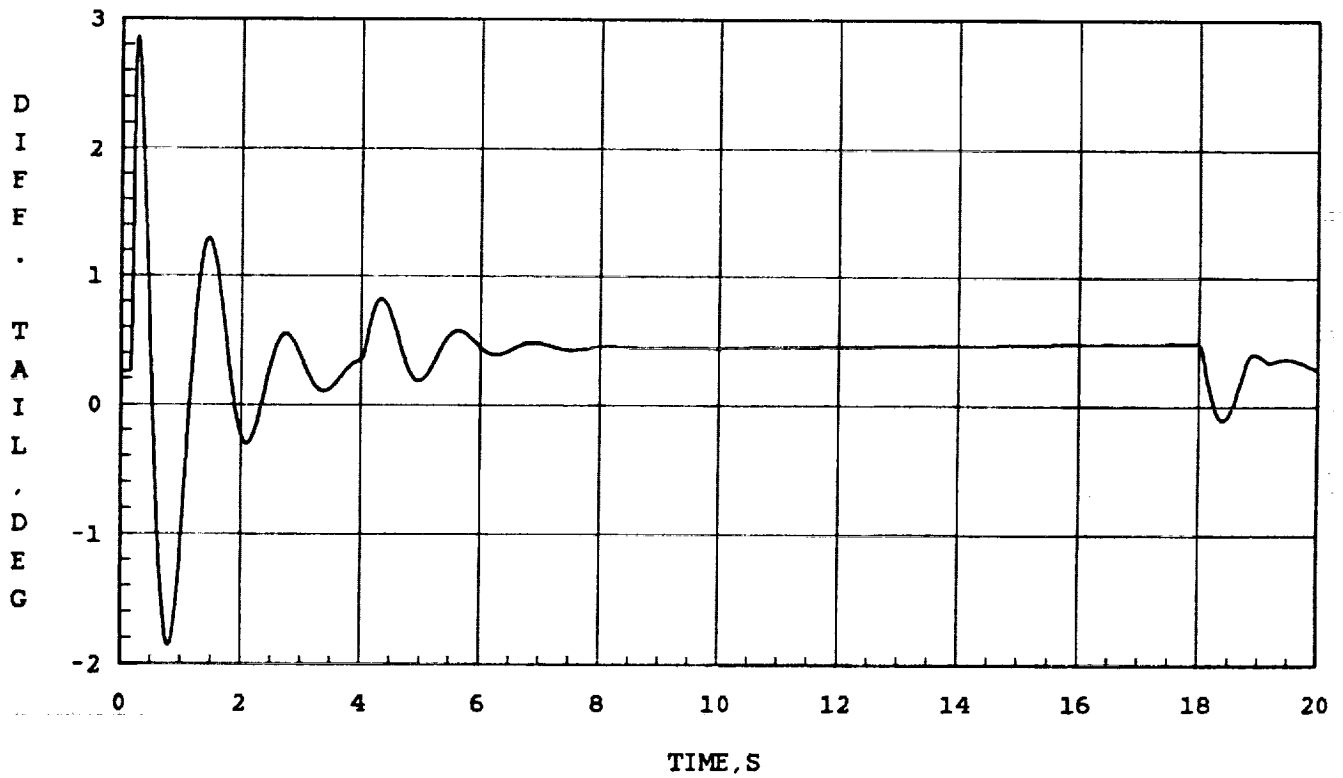


Figure 3.37. Differential Tail Deflection vs. Time along the Constant Thrust Windup Turn Flight Test Trajectory.

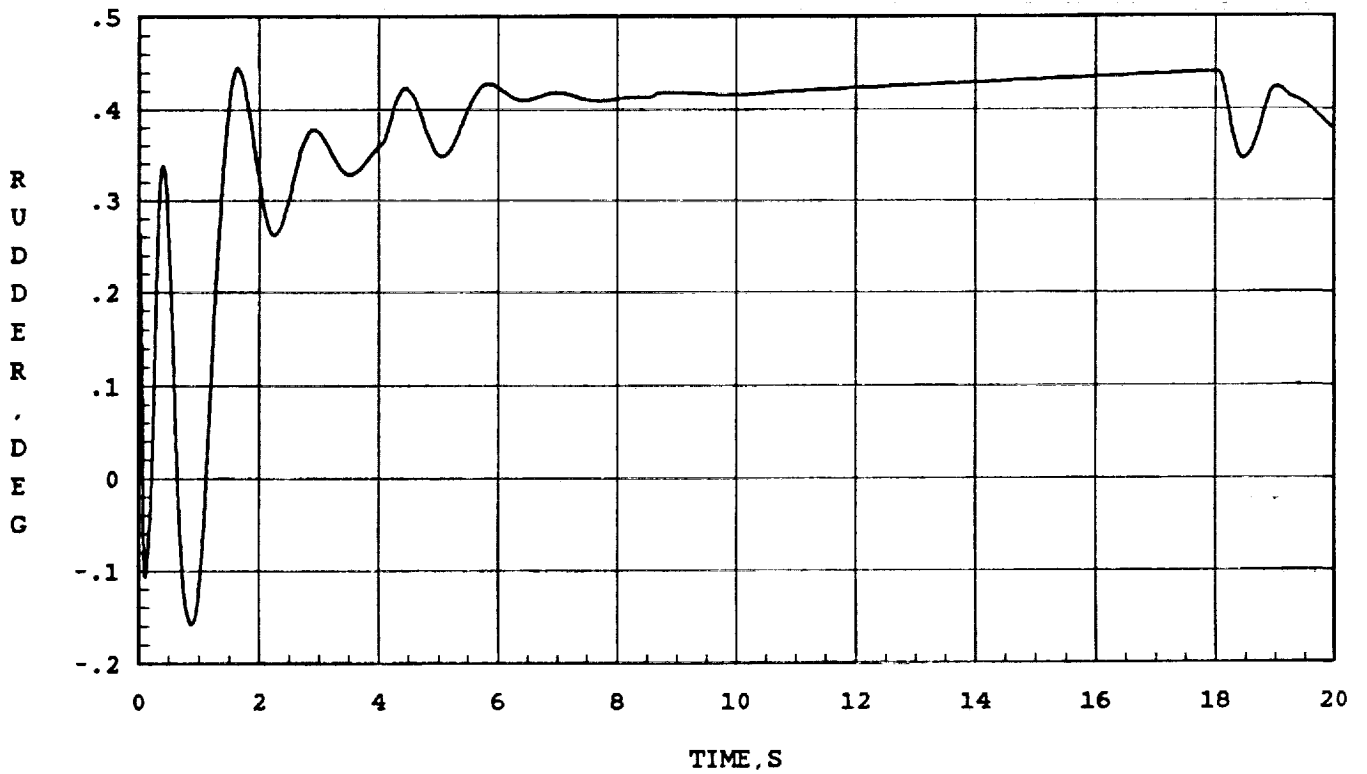


Figure 3.38. Rudder Deflection vs. Time along the Constant Thrust windup Turn Flight Test Trajectory.

the atmospheric density gradient is fixed. For a detailed analysis of this maneuver, see [6]. The maneuver autopilot for this trajectory consists of the airspeed controller given by the expressions (2.13), (2.14), (2.16), and the altitude controller given by (2.25), (2.26), (2.29), (2.30) in conjunction with the roll attitude controller (2.40), (2.41) and (2.43).

Similar to the excess thrust windup turn and constant thrust windup turn flight test trajectories, in the present work, this maneuver is implemented using the controllers for airspeed, angle of attack and roll attitude for simplicity.

The controller performance along the constant dynamic pressure, constant load factor trajectory is given in Figures 3.39 through 3.51. From Figure 3.41, it can be seen that the dynamic pressure has been maintained constant within 0.8% throughout the trajectory. The flight test trajectory began at 10 seconds in the present case, and the load factor is maintained within 0.05 of the required value, as can be seen from Figure 3.42. As noted in the two earlier maneuvers, there is a hang-off error in the angle of attack channel. During the initial transient region, there is a saturation in the elevator and differential tail due to the control deflection authority limits. The overall performance of the controller is well within the performance specifications.

3.4. Conclusions

The closed loop simulation reveals that the initial assumption with regard to the speed of the CAS is valid. This system is indeed stable and sufficiently fast. The second conclusion that emerges from the present analysis is that the nonlinear Maneuver Autopilot is sufficiently robust with respect to modeling inaccuracies since a simpler model than that implemented in the simulation could control the aircraft with a high degree of accuracy. If the CAS and aircraft models are close to the actual, one would expect a satisfactory control system response during the actual flight test also.

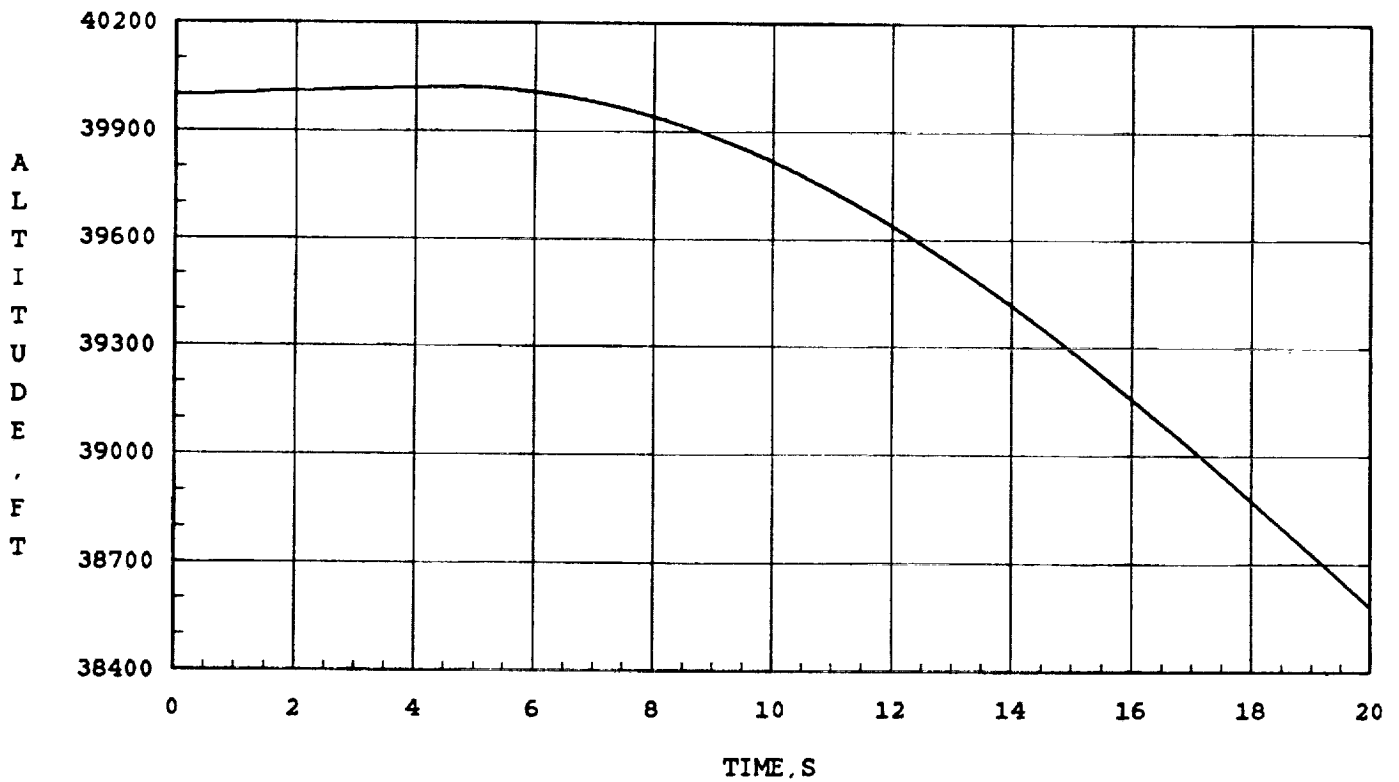


Figure 3.39. Altitude vs. Time along the Constant Dynamic Pressure/ Constant Load Factor Flight Test Trajectory.

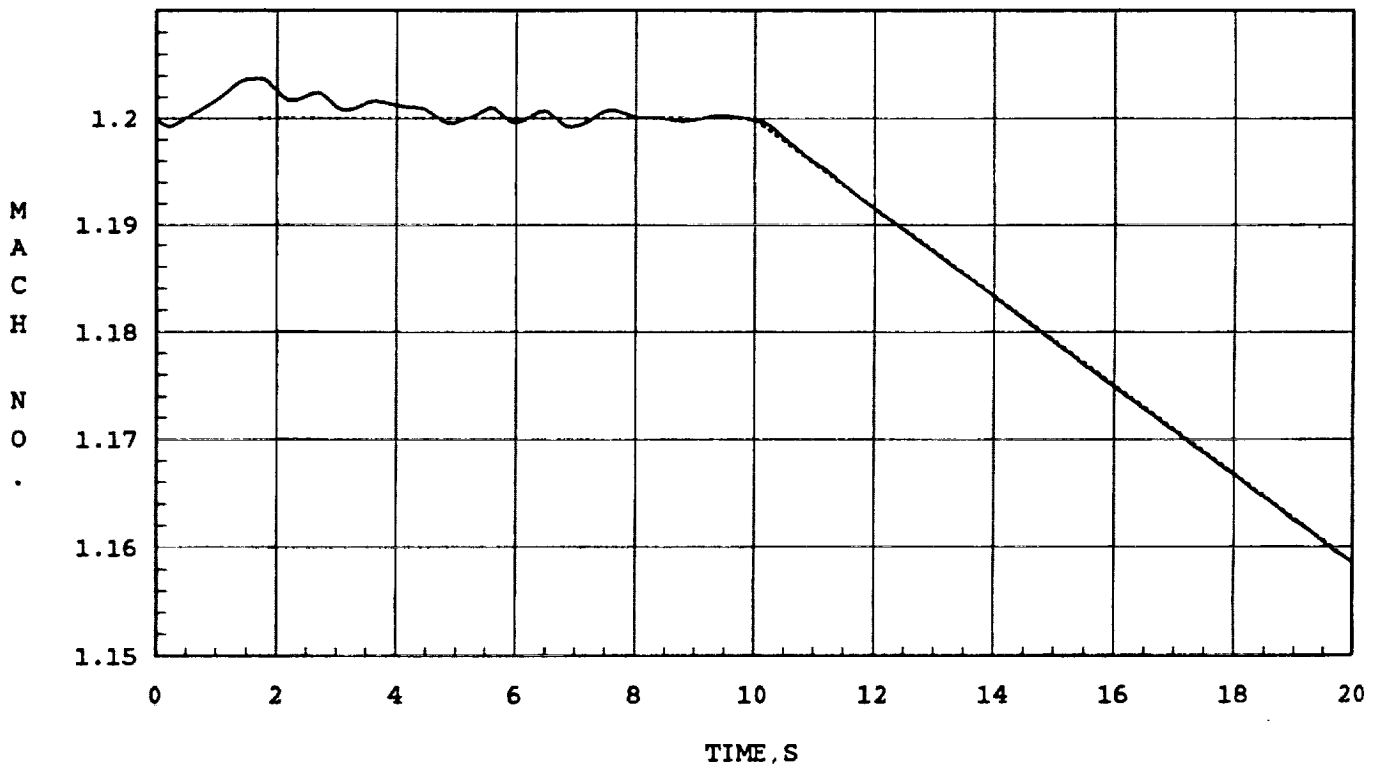


Figure 3.40. Mach number vs. Time along the Constant Dynamic Pressure /Constant Load Factor Flight Test Trajectory.

Dotted Line: Commanded Mach Number.
 Solid Line: Actual Mach Number.

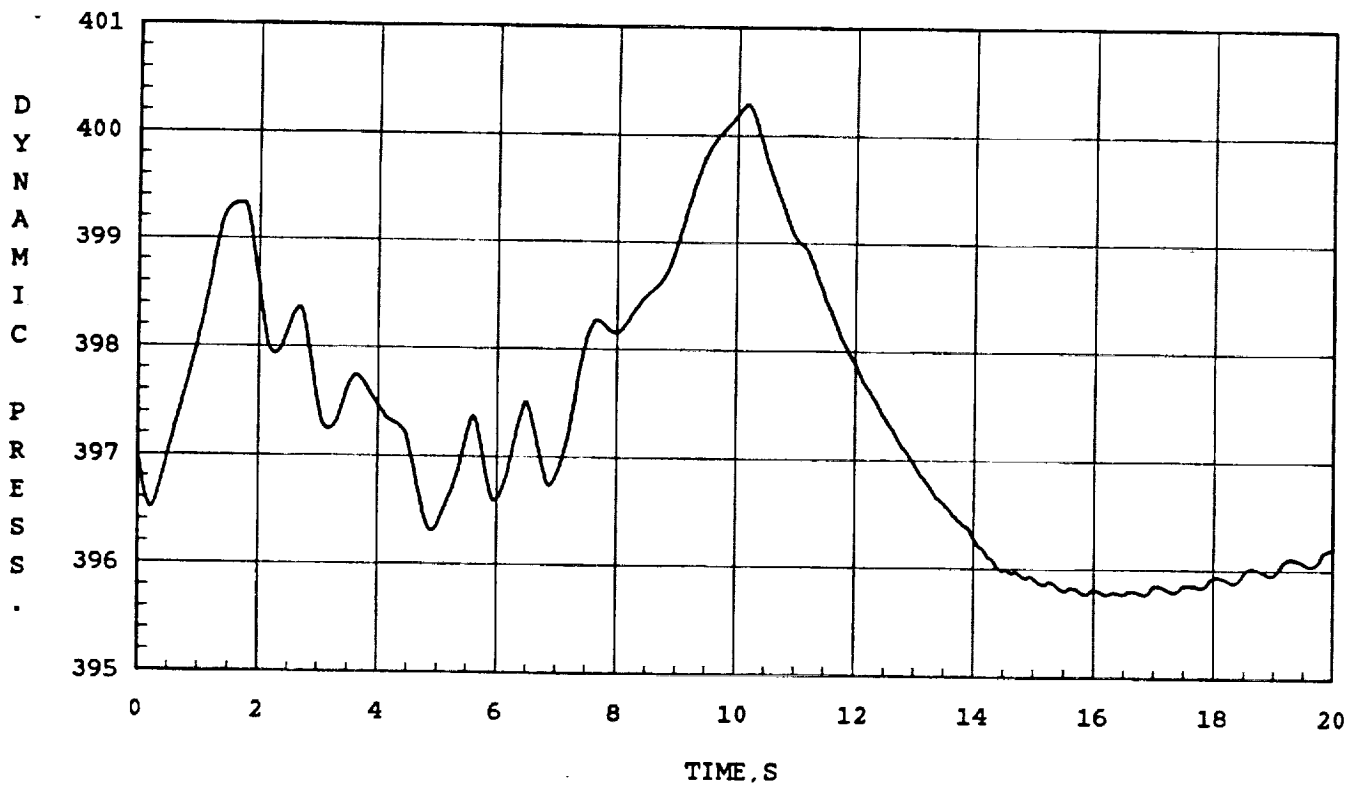


Figure 3.41. Dynamic Pressure vs. Time along the Constant Dyanmic Pressure/Constant Load Factor Flight Test Trajectory.

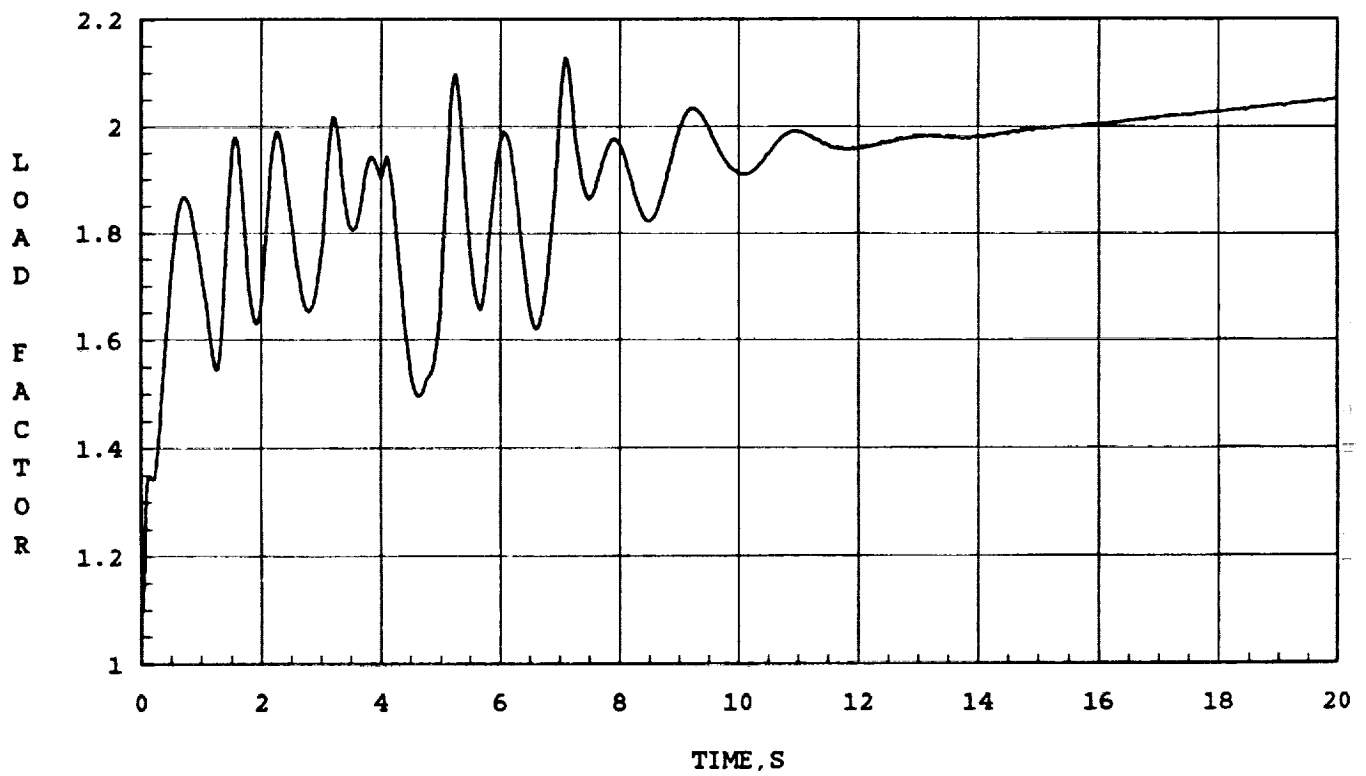


Figure 3.42. Load Factor vs. Time along the Constant Dynamic Pressure /Constant Load Factor Flight Test Trajectory.

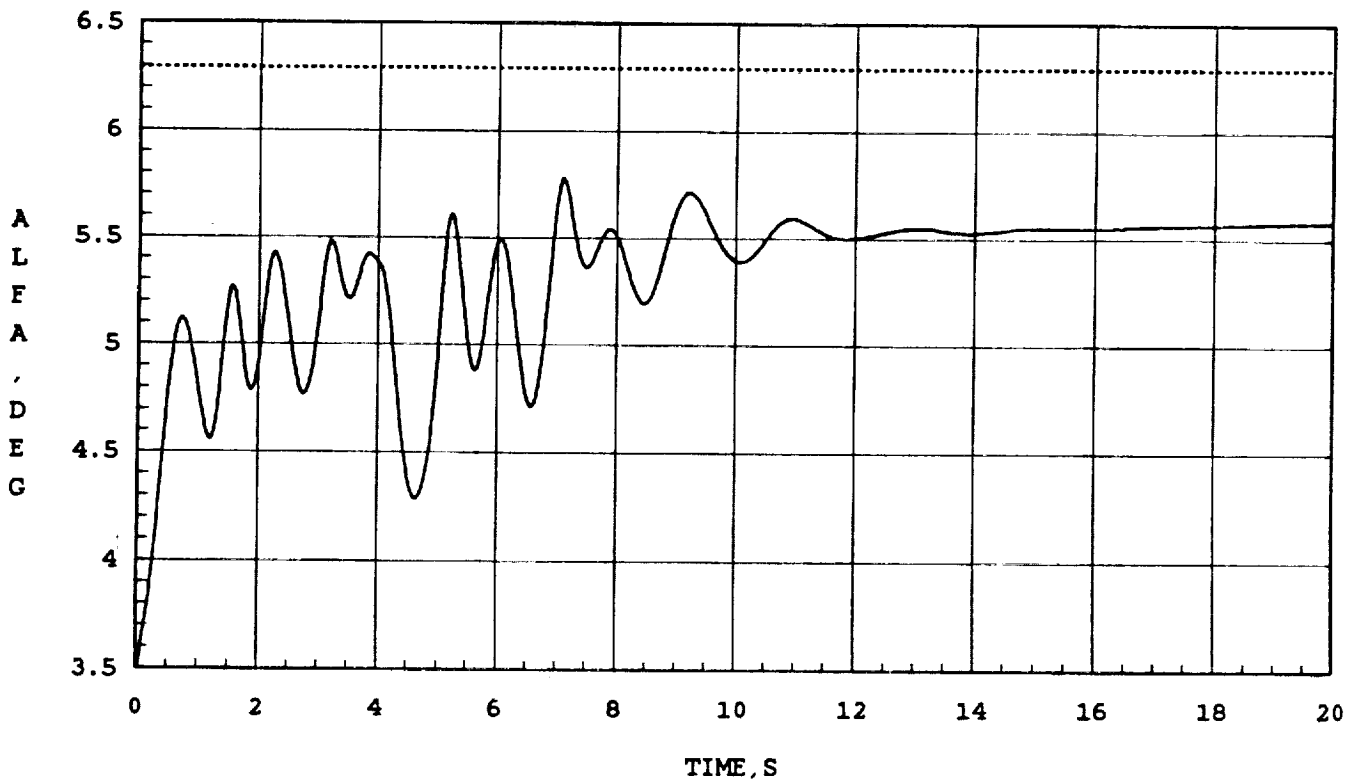


Figure 3.43. Angle of Attack vs. Time along the Constant Dynamic Pressure/Constant Load Factor Flight Test Trajectory.

**Dotted Line: Commanded Angle of Attack.
 Solid Line: Actual Angle of Attack.**

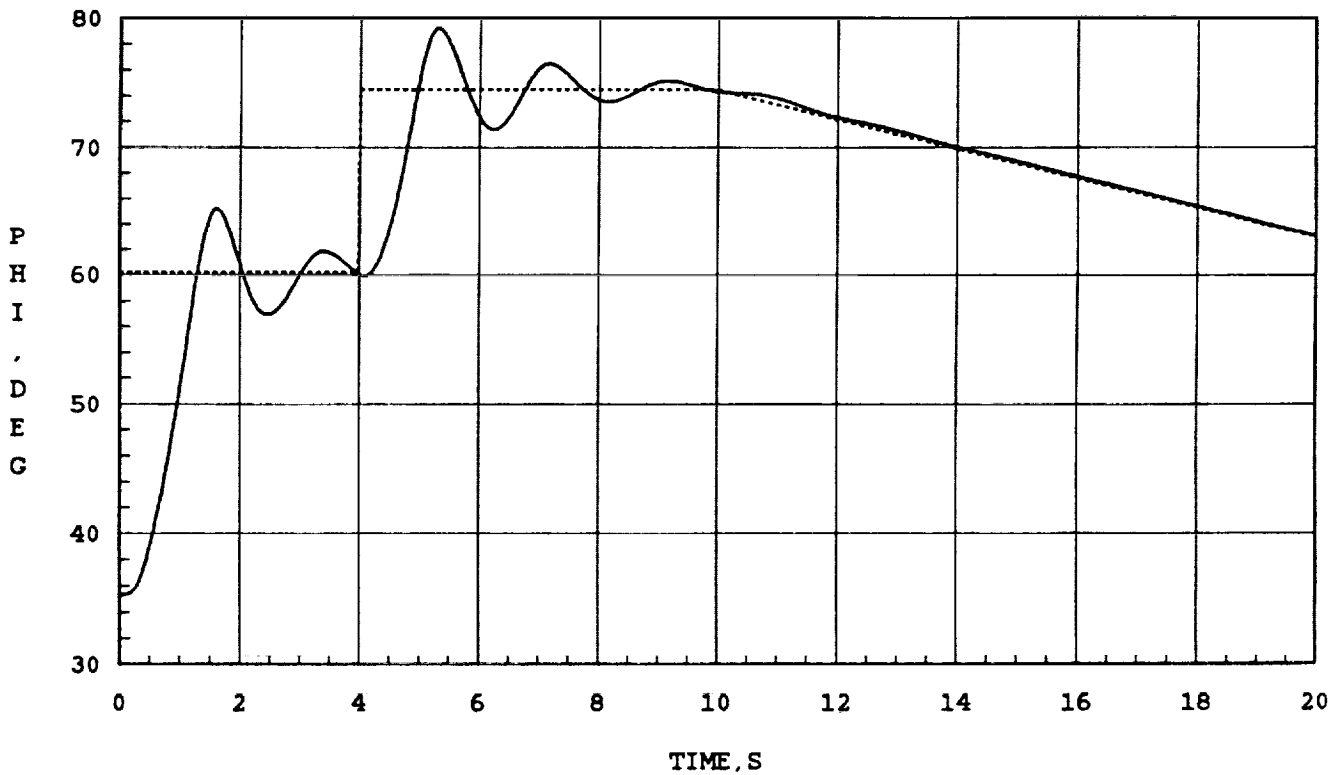


Figure 3.44. Roll Attitude vs. Time along the Constant Dynamic Pressure/Constant Load Factor Flight Test Trajectory.

Dotted line: Commanded Roll Attitude.

Solid line: Actual Roll Attitude.

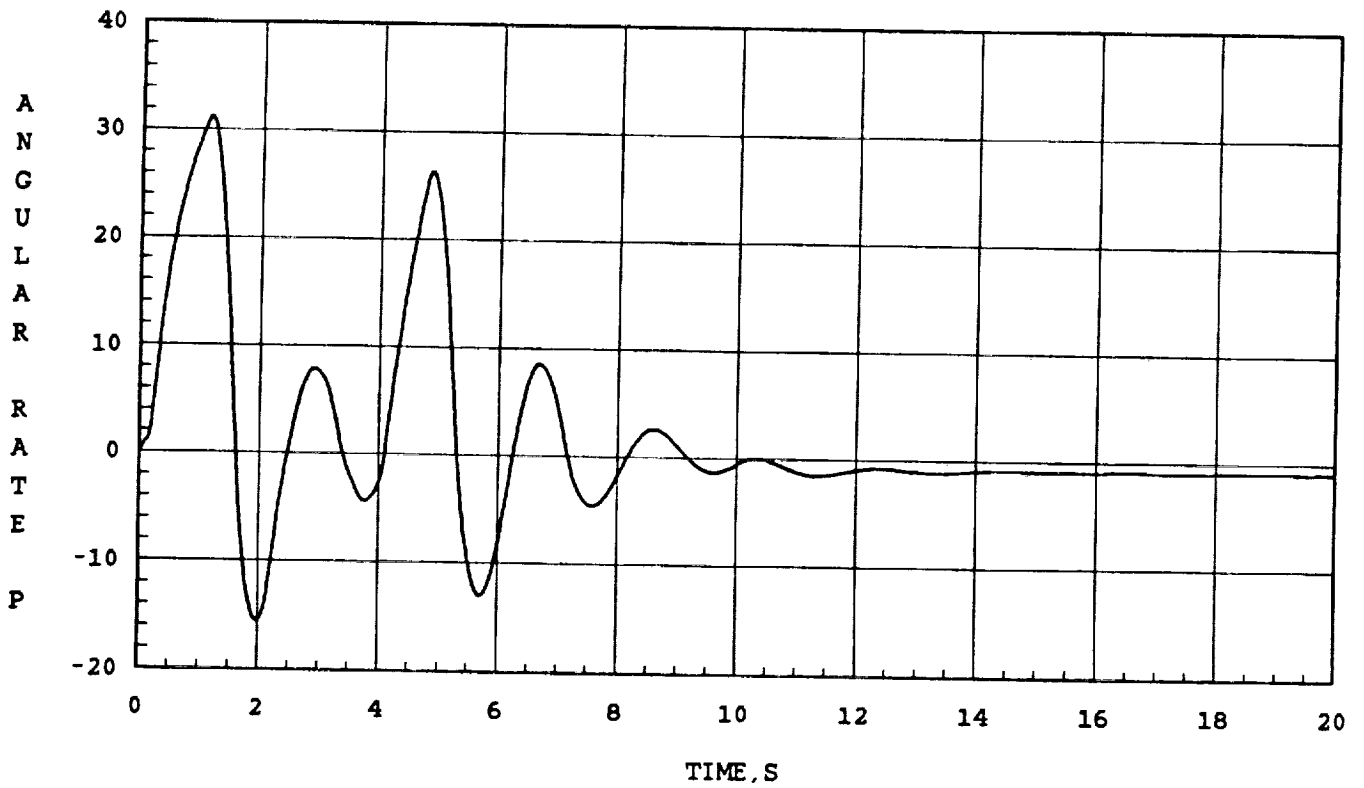


Figure 3.45 Roll Body Rate (Deg/s) vs. Time along the Constant Dyanmic Pressure/Constant Load Facotr Flight Test Trajectory.

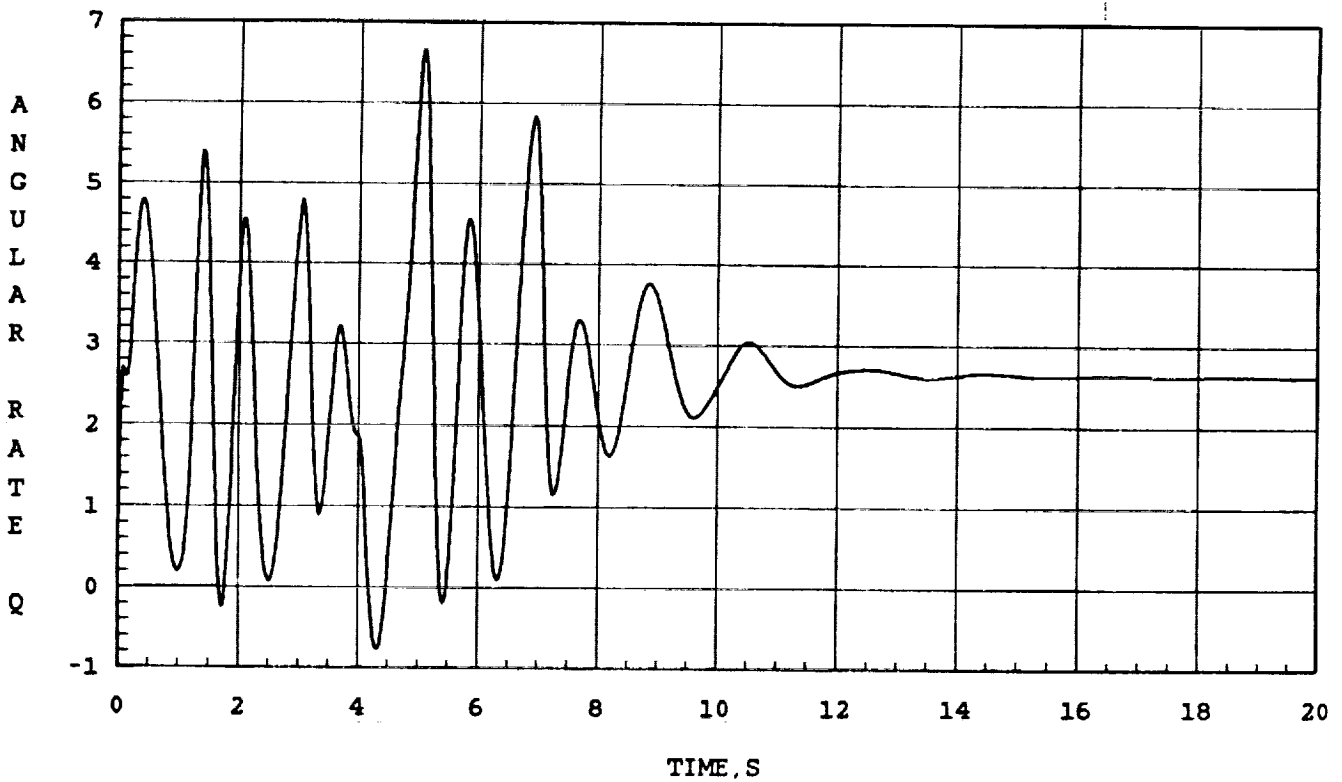


Figure 3.46. Pitch Body Rate (Deg/s) vs. Time along the Constant Dynamic Pressure/Constant Load Factor Flight Test Trajectory.

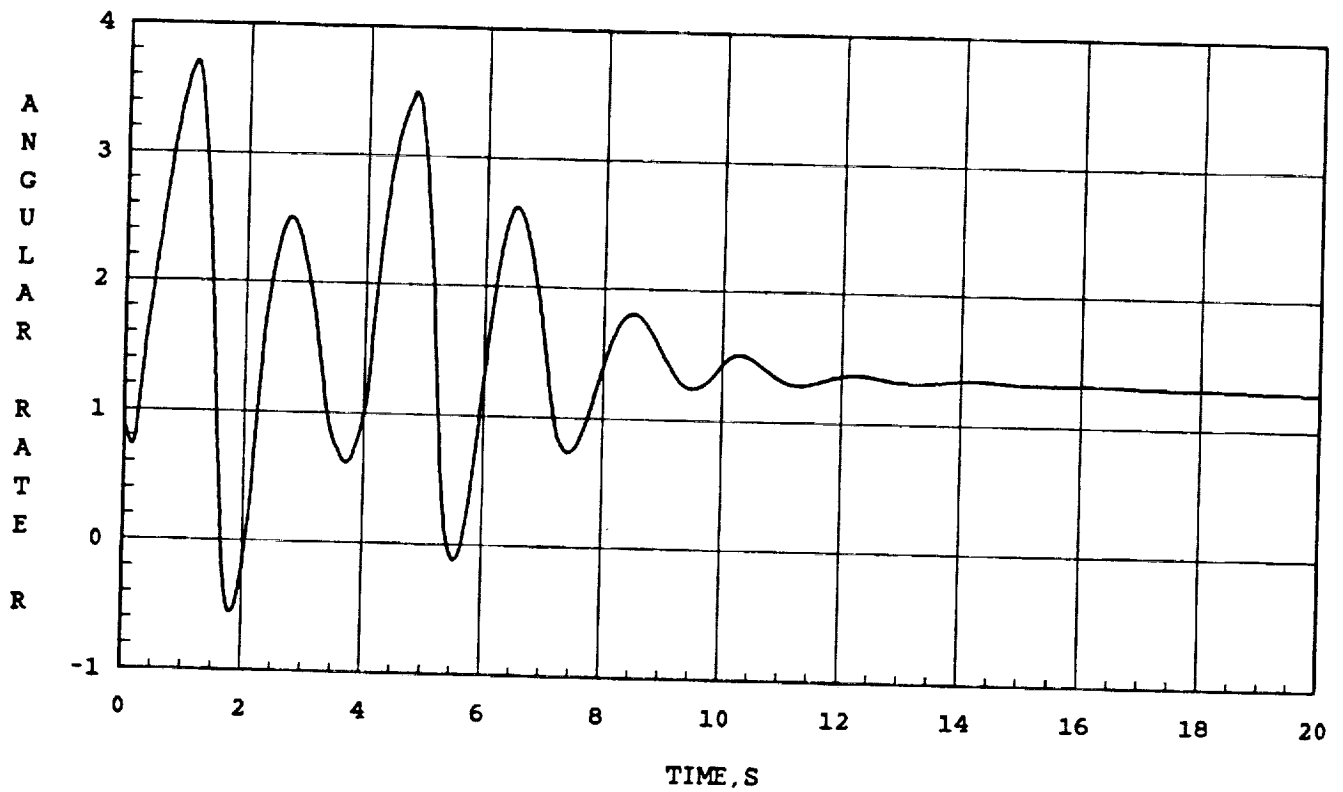


Figure 3.47. Yaw Body Rate (Deg/s) vs. Time along the Constant Dynamic Pressure/Constant Load Factor Flight Test Trajectory.

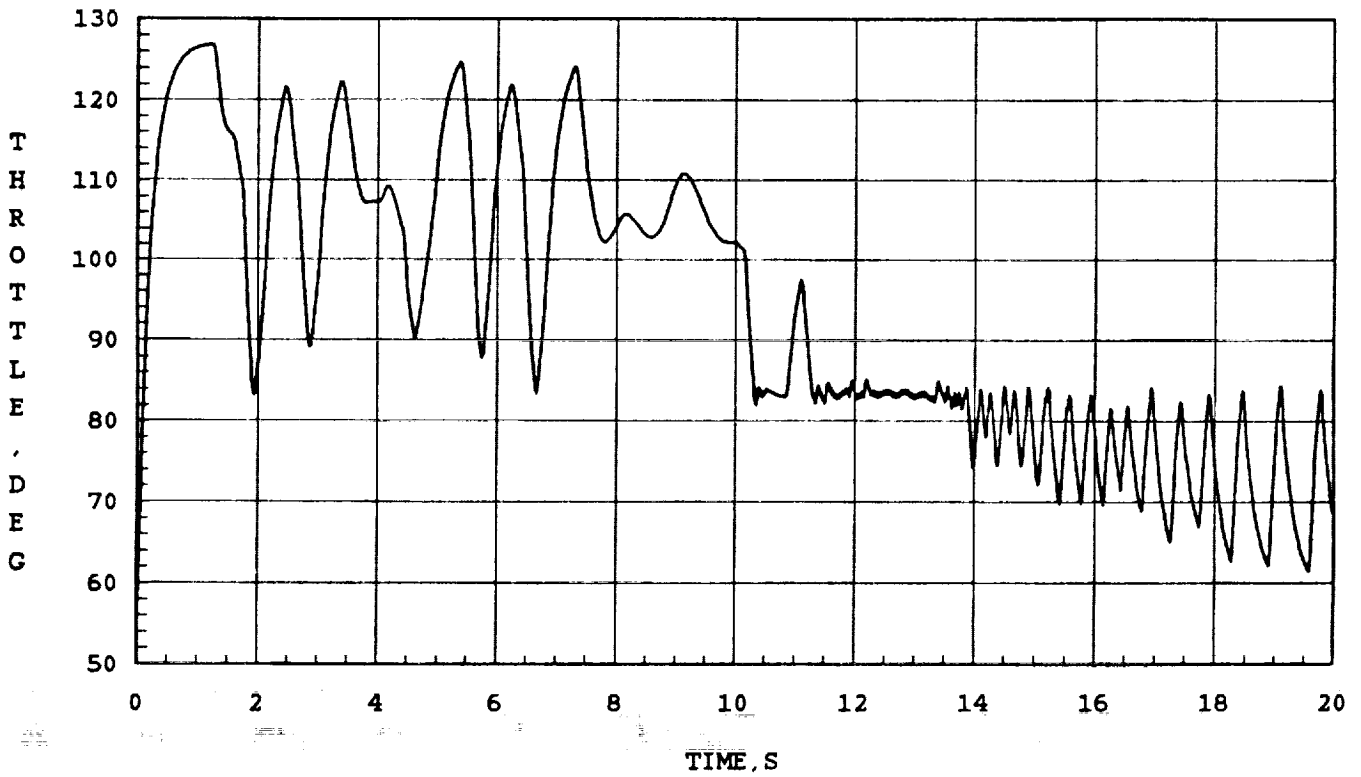


Figure 3.48. Throttle Setting vs. Time along the Constant Dynamic Pressure/Constant Load Factor Flight Test Trajectory.

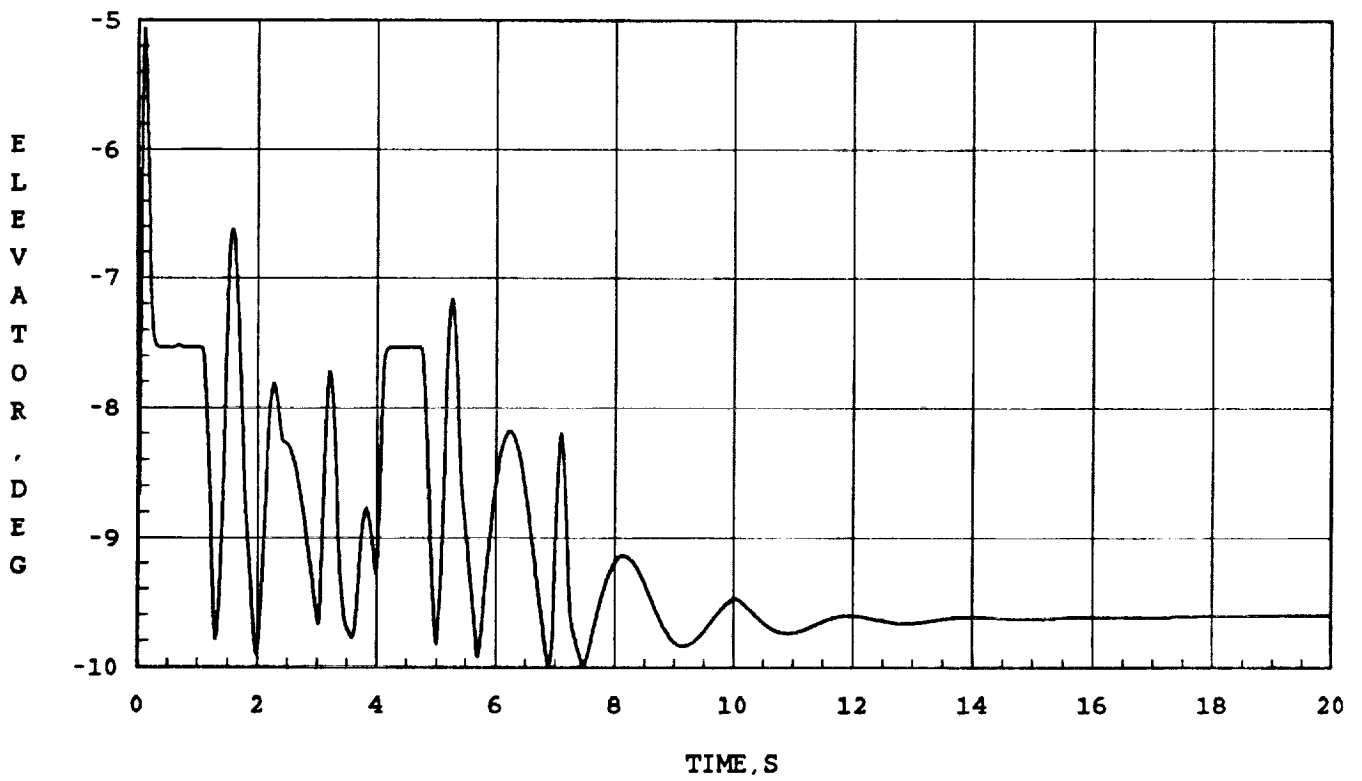
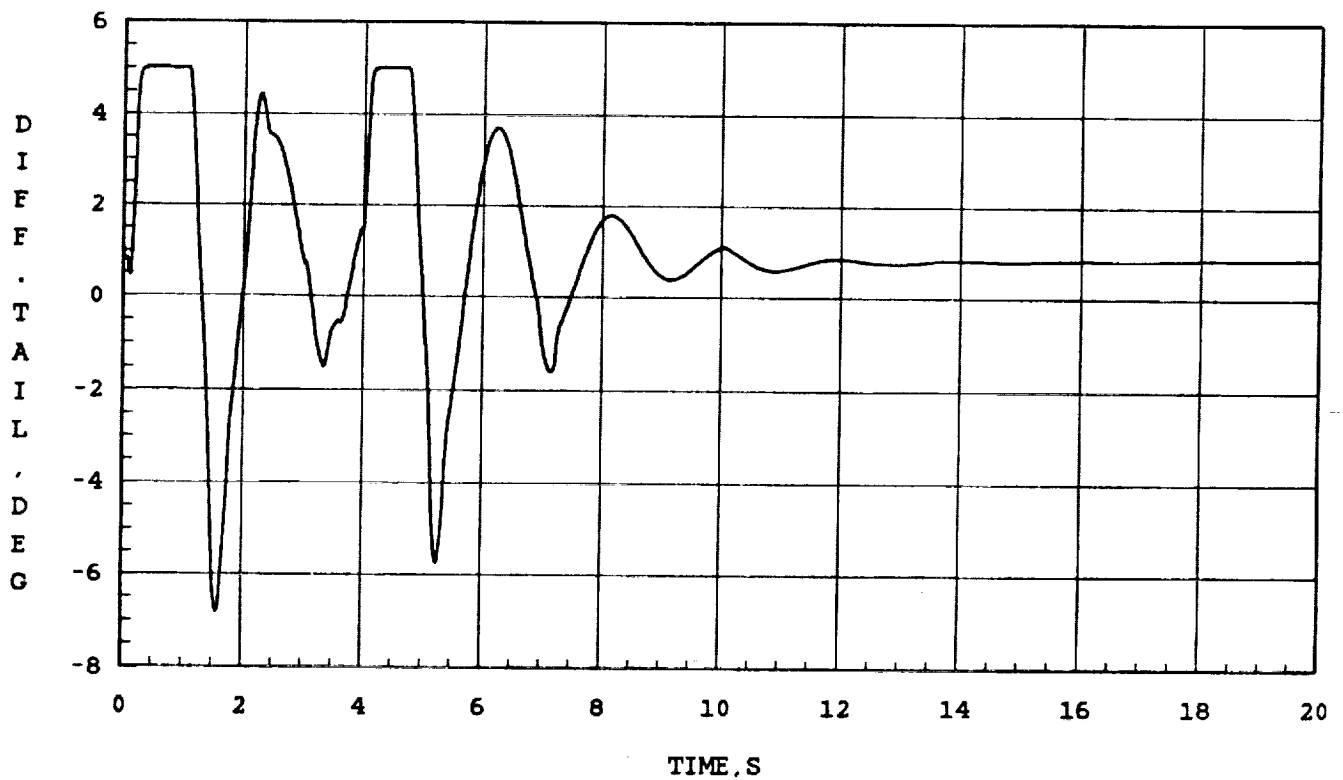


Figure 3.49. Elevator Deflection vs. Time along the Constant Dynamic Pressure/Constant Load Factor Flight Test Trajectory.



Figur 3.50. Differential Tail Deflection vs. Time along the Constant Dynamic Pressure/Constant Load Factor Flight Test Trajectory.

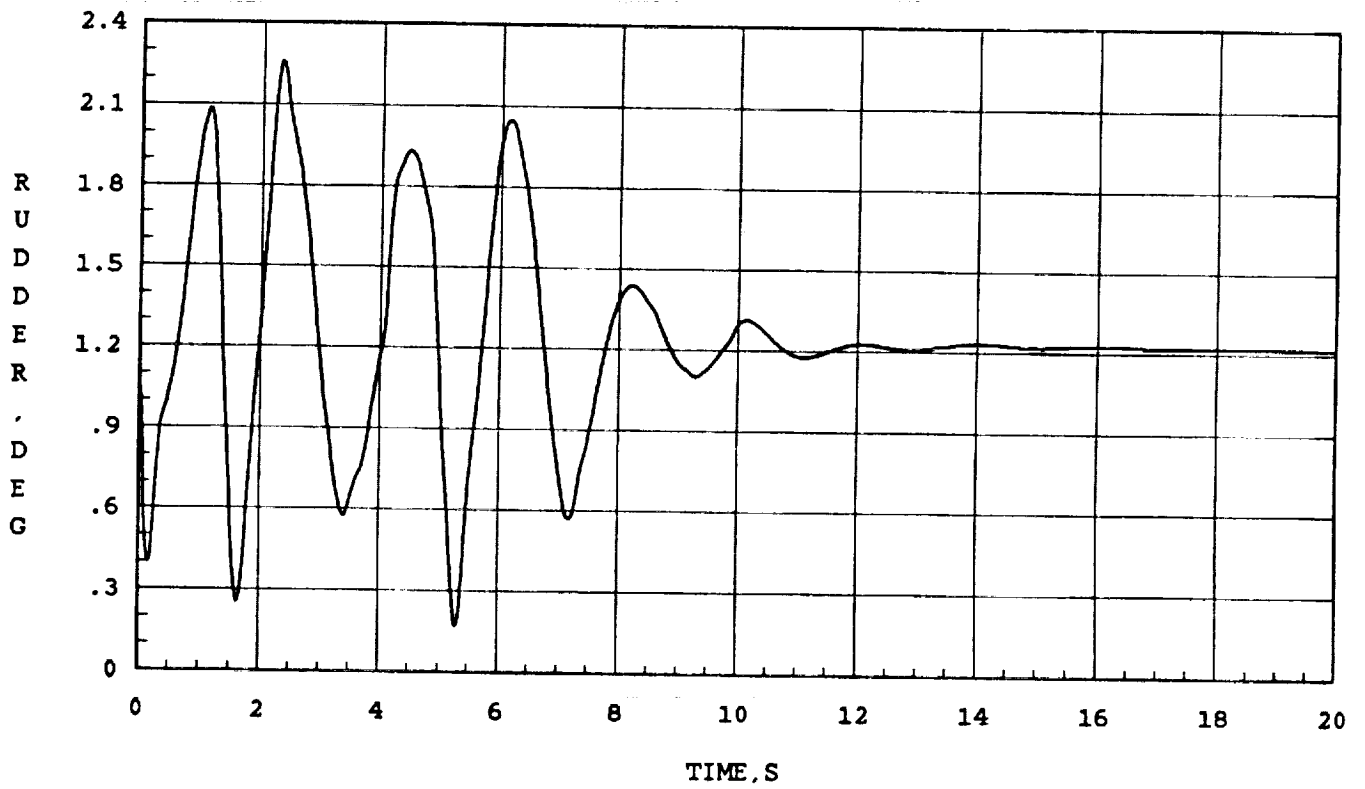


Figure 3.51. Rudder Deflection vs. Time along the Constant Dynamic Pressure/Constant Load Factor Flight Test Trajectory.

Chapter IV

Conclusions and Future Work

This report dealt with the development of nonlinear flight test trajectory controllers for a high performance fighter aircraft. This work employed the singular perturbations arguments to reduce the order of the system and the recently developed theory of prelinearizing transformations to generate explicit nonlinear controllers. Appropriate dynamic compensators were incorporated in this controller to ensure a measure of insensitivity to modeling inaccuracies. The modifications of these nonlinear controllers to permit manual control have been indicated. This would involve the use of a lead-lag filter to compensate for the dynamics of the human pilot.

The closed-loop performance of the nonlinear controller along the six desired flight test trajectories were demonstrated through a complete simulation of the aircraft and CAS system along with the controller. The controller performance has been found meet all the specifications along the six flight test maneuvers. In the next project phase, these controllers will be implemented in a manned simulation of the flight test trajectory control system in order to evaluate it more completely.

The development of a nonlinear controller for a generic aircraft is given in the Appendix A. This approach is useful in developing nonlinear controllers for tracking arbitrary command histories.

4.1. Future Work

The controller development discussed here has a much wider application than the flight test trajectory control problem alone. For example, recently there is a strong interest at NASA and USAF in cockpit automation. The problem of automatic flight guidance is likely to be central issue here. The methods developed in the present work can yield efficient schemes for manual or automatic tracking of guidance commands, such as those generated by Calise and Moerder [21]. Indeed, one of the early applications of the prelinearization technique was in synthesizing an automatic scheme for landing on an aircraft carrier, see [22] for details.

These and other related problems will be of future interest.

REFERENCES

- [1] Duke, E.L., "Automated Flight Test Maneuvers: The Development of a New Technique", *Flight Testing Technology-A-State-of-the-Art Review*, pp. 101-119, *Proceedings of the Society of Flight Test Engineers 13th Annual Symposium*, New York, N.Y., September 1982.
- [2] Duke, E.L., Swann, M.R., Enevoldson, E.K., and Wolf, T.D., "Experience with Flight Test Trajectory Guidance", *Journal of Guidance, Control, and Dynamics*, pp. 393-398 Vol 6., Sept. - Oct. 1983.
- [3] "Final Report, HiMAT Maneuver Autopilot", TRA 29255-1, Teledyne Ryan Aeronautical, February 1981.
- [4] Walker, R.A., and Gupta, N.K., "Flight Test Trajectory Control Analysis", NASA CR 170395 February 1983.
- [5] Menon, P.K.A., Saberi, H.A., Walker, R.A. and Duke, E.L., "Flight Test Trajectory Controller Synthesis with Eigenstructure Assignment", *1985 American Control Conference*, June 19-21, Boston, MA, paper No. FA1.
- [6] Menon, P.K.A. and Walker, R.A., "Aircraft Flight Test Trajectory Control", ISI Report 56, Prepared for NASA Ames-Dryden Flight Research Facility under contract NAS2-11877, Oct. 1985.
- [7] Meyer, G. and Cicolani, S., "A Formal Structure for Advanced Automatic Flight Control Systems", NASA TN D-7940, 1975.
- [8] Smith, G.A. and Meyer, C., "Total Aircraft Flight-Control System - Balanced Open - and Closed-Loop Control with Dynamic Trim Maps", *Proceedings of the Third Digital Avionics Systems Conference*, Ft. Worth, Texas, Nov. 1979, IEEE Catalog No. 79CH1518-0.
- [9] Smith, G.A. and Meyer, G., Application of the Concept of Dynamic Trim Control to Automatic Landing of Carrier Aircraft. NASA TP-1512, 1980.
- [10] Hunt, L.R., and Su, R., Control of Nonlinear Time-Varying Systems, *IEEE Conference on Decision and Control*, 1981, pp. 558-563.
- [11] Hunt, L.R., Su, R., and Meyer, G., Global Transformations of Nonlinear Systems, *IEEE Transactions on Automatic Control*, January 1983, pp. 24-31.

- [12] Hunt, L.R., Su, R., and Meyer, G., Multi Input Nonlinear Systems, in *Differential Geometric Control Theory Conference*, Birkhauser, Boston, Cambridge, Mass., 1982.
- [13] Meyer, G., Su, R. and Hunt, L.R., "Application of Nonlinear Transformations to Automatic Flight Control" *Automatica*, Vol 20, pp. 103-107, 1984.
- [14] Brockett, R.W., "Nonlinear Systems and Differential Geometry", *Proceedings of the IEEE*, Vol. 64, February 1976, pp 61-72.
- [15] Guggenheimer, H.W., *Differential Geometry*, Dover, New York, 1977.
- [16] Cicolani, L.S., Sridhar, B., and Meyer, G., " Configuration Management and Automatic Control of an Augmentor Wing Aircraft with Vectored Thrust", NASA TP-1222, March 1979.
- [17] Menon, P.K.A., Badgett, M.E., Walker, R.A., and Duke, E.L., "Nonlinear Flight Test Trajectory Controllers for Aircraft", *AIAA Guidance and Control Conference*, Snowmass, CO., Aug. 19-21, Paper No. AIAA-85-1890-CP.
- [18] Gerald, C.F., *Applied Numerical Analysis*, Addison-Wesley, Reading, MA. , 1978.
- [19] Walker, R.A., Shah, S.C., and Gupta, N.K., "Computer - Aided Engineering (CAE) for System Analysis", *Proceedings of the IEEE*, Vol. 72, Dec. 1984, pp 1732-1745.
- [20] Gupta, N.K., Varvell, D.B., and Walker, R.A., "SYSTEM_BUILD : A New Interactive Model Building and Simulation CAE Tool", *1985 Summer Computer Simulation Conference*, July 22-26, 1985, Chicago, Ill.
- [21] Calise, A.J., and Moerder, D.D., "Singular Perturbation Techniques for Real Time Aircraft Trajectory Optimization and Control", NASA CR-3597, August 1982.
- [22] Smith, G.A., and Meyer, G., "Application of the Concept of Dynamic Trim Control to Automatic Landing of Carrier Aircraft", NASA TP-1512, 1980.

APPENDIX - A

NONLINEAR FLIGHT TEST TRAJECTORY
CONTROLLERS FOR AIRCRAFT

By

P.K.A MENON, M.E. BADGETT,
R.A. WALKER AND E.L. DUKE

PAPER PRESENTED AT THE AIAA GUIDANCE AND
CONTROL CONFERENCE, AUGUST 19-21, 1985
SNOW MASS, CO PAPER NO. AIAA-85-1890-CP

NONLINEAR FLIGHT TEST TRAJECTORY
CONTROLLERS FOR AIRCRAFT

By

P.K.A. Menon*, M.E. Badgett**, R.A. Walker***

INTEGRATED SYSTEMS, INC.
101 University Avenue
Palo Alto, CA 94301

And

E.L. Duke⁺⁺

NASA Ames-Dryden Flight Research Facility/OFDC
Edwards, CA 93523

ABSTRACT

Flight test trajectory control systems are designed to enable the pilot to follow complex trajectories for evaluating an aircraft within its known flight envelope and to explore the boundaries of its capabilities. Previous design approaches were based on linearized aircraft models necessitating a large amount of data storage along with gain schedules. In this paper, the synthesis of nonlinear flight test trajectory controllers for a fixed wing aircraft is described. This approach uses singular perturbations theory and the recently developed theory of prelinearizing transforms. These controllers do not require gain scheduling for satisfactory operation, can be used in arbitrarily nonlinear maneuvers, and are mechanized with a direct, non-iterative analytic solution.

NOMENCLATURE

D drag force

e_1, e_2, e_3 Control surface influence coefficients for the moments about the roll body axis (X)

f_1, f_2, f_3 Control surface influence coefficients for the moments about the pitch body axis (Y)

g_1, g_2, g_3 Control surface influence coefficients for the moments about the yaw body axis (Z)

H altitude rate

h altitude

I_x X body axis moment of inertia

I_{xy} X-Y body axis product of inertia

I_{xz} X-Z body axis product of inertia

I_y Y body axis moment of inertia

I_{yz} Y-Z body axis product of inertia

I_z Z body axis moment of inertia

k_1T Component of thrust along the X body axis

k_2T Component of thrust along the Y body axis

k_3T Component of thrust along the Z body axis.

L lift force

M Mach number

m Aircraft mass

P roll body rate

q pitch body rate

r yaw body rate

P total aerodynamic and thrust moment about the X body axis not including the control moments

Q total aerodynamic and thrust moment about the Y body axis, not including the control moments

R total aerodynamic and thrust moment about the Z body axis, not including the control moments

* Research supported by NASA Ames-Dryden Flight Research Facility under Contract NAS2-11877
©1985 by Integrated Systems Inc. Published by the American Institute of Aeronautics and Astronautics, Inc., with permission

*Research Scientist, Member AIAA
**Research Engineer
***Manager, Aircraft and robotics Division, Member AIAA
++ Aerospace Engineer, Member AIAA

S	side force
T	engine thrust
V	total velocity
α	angle of attack
β	angle of sideslip
δ_a	Aileron Deflection
δ_e	Elevator Deflection
δ_r	Rudder Deflection
ϕ	roll attitude
θ	pitch attitude
.	indicates derivative with respect to time.
-	an underbar indicates the transpose of a vector
-	denotes the fast variables in the slow-time scale
-	denotes the slow variables in the fast-time scale

INTRODUCTION

The motivation for the development of flight test trajectory controllers is well documented in the literature¹⁻⁶. The primary objective is to enable the pilot to follow complex flight test trajectories consistently and accurately. Two versions of these controllers have been employed, viz a closed-loop automatic system and an open-loop system providing manual piloting information. Originally, the open loop flight test trajectory guidance algorithms were developed on-line in a piloted simulation using cut and try techniques. This approach was not only manpower intensive, but often produced less than desirable controllers. Closed-loop system designs based on linearized aircraft models⁴⁻⁶ required the generation of large amounts of numerical data to arrive at satisfactory designs. Further, gain scheduling was found to be essential for acceptable performance.

The present paper deals with the synthesis of nonlinear flight test trajectory controllers using the recent results⁷⁻¹⁵ in the prelinearizing transformation theory⁷⁻¹⁵ and the singular perturbations theory¹⁶⁻¹⁹. The application of singular perturbation theory to this problem simplifies the linearizing transformation considerably, in addition to providing a consistent means for eliminating ignorable state variables. In this framework, the state variables in the original nonlinear problem are retained, while the control variables are transformed. This is advantageous from an implementation point of view. Splitting the dynamics based on speed of state variable evolution generates a controller in which certain control loops can be computed at a slower rate than others on the flight control computer. It is interesting to note that in Reference 9, even though the controller development did not make use

of singular perturbation theory, the time-scale separation formed a basis for implementation on the flight control computer. Note, however, that the flight test trajectory control problem discussed here is distinct from those described in references 7-10, since in those investigations, the trajectory to be followed consisted of three position components specified as a function of time.

The flight test trajectory controller synthesis for a fixed wing high performance fighter aircraft without VTOL or hover capabilities will be discussed in this paper. Though specific engine and airframe models are required for implementation, these will not be discussed as they are not central to the material to be presented. It will be assumed that the aircraft under consideration has the four usual controls throttle, aileron, rudder and elevator. It is further assumed that the aircraft has no direct force generation devices other than the engine thrust without thrust vectoring capabilities. The task of the flight test trajectory controller is to track the given commands in airspeed, angle of attack, angle of side slip and altitude in the presence of disturbances and modeling uncertainties.

The next section will discuss the aircraft modeling and time-scale separation. The details of prelinearization and slow-fast controller synthesis will be given in Section 3. Simulation results using the nonlinear flight test trajectory controllers will be presented in Section 4.

MODELING AND TIME-SCALE SEPARATION:

The equations of motion for an aircraft flight over flat, nonrotating earth with zero ambient winds is given by²⁰

$$\dot{V} = [-D \cos\beta + S \sin\beta + (k_1 \cos\alpha \cos\beta + k_2 \sin\alpha \cos\beta)T - mg (\sin\theta \cos\alpha \cos\beta - \cos\theta \sin\phi \sin\beta - \cos\theta \cos\phi \sin\alpha \cos\beta)]/m \quad (1)$$

$$\dot{\alpha} = [-L + (k_3 \cos\alpha - k_4 \sin\alpha)T + mg (\cos\theta \cos\phi \cos\alpha + \sin\theta \sin\alpha)]/mV \cos\beta + q - \tan\beta (p \cos\alpha + r \sin\alpha) \quad (2)$$

$$\dot{\beta} = [D \sin\beta + S \cos\beta - (k_1 \cos\alpha \sin\beta + k_2 \sin\alpha \sin\beta)T + mg (\sin\theta \cos\alpha \sin\beta + \cos\theta \sin\phi \cos\beta \cos\theta \cos\phi \sin\alpha \sin\beta)]/mV + p \sin\alpha - r \cos\alpha \quad (3)$$

$$\dot{\eta} = V(\cos\beta \cos\alpha \sin\theta - \sin\beta \sin\phi \cos\theta - \cos\beta \sin\alpha \cos\phi \cos\theta) \quad (4)$$

$$\dot{\phi} = p + q \sin\phi \tan\theta + r \cos\phi \tan\theta \quad (5)$$

$$\dot{\theta} = q \cos\phi - r \sin\phi \quad (6)$$

$$\begin{aligned} \epsilon \dot{p} = & [PI_1 + RI_1 + e_1 I_1 \delta_e + c_2 I_1 \delta_a + e_2 I_1 \delta_r \\ & + pq(I_{xz} I_1 - D_z I_1) - qr \\ & (D_x I_1 + I_{xz} I_1)]/I \end{aligned} \quad (7)$$

$$\begin{aligned} \epsilon \dot{q} = & [QI_2 + f_1 I_2 \delta_e + f_2 I_2 \delta_a + f_3 I_2 \delta_r \\ & + p I_{xz} I_2 - pr D_y I_2 + r I_{xz} I_2]/I \end{aligned} \quad (8)$$

$$\begin{aligned} \epsilon \dot{r} = & [PI_3 + RI_3 + g_1 I_3 \delta_e + g_2 I_3 \delta_a + g_3 I_3 \delta_r \\ & + pq(I_{xz} I_3 - D_z I_3) - qr (D_x I_3 + I_{xz} I_3)]/I \end{aligned} \quad (9)$$

with

$$\begin{aligned} I_1 &= I_y I_z \\ I_2 &= I_y I_{xz} \\ I_3 &= I_x I_z - I_{xz}^2 \\ I_4 &= I_x I_y \\ D_x &= I_z - I_y \\ D_y &= I_x - I_z \end{aligned}$$

$$D_z = I_y - I_x$$

$$I = I_x I_y I_z - I_x I_y^2 - I_y I_x^2$$

$I_{xy} = I_{yz} = 0$ for the Aircraft under consideration

The X, Y positions and yaw attitude ψ are ignorable in the flight test trajectory problem under consideration. Consequently the equations describing their dynamics have been eliminated. The interpolation parameter ϵ introduced on the left-hand-side of equation (7)-(9) is motivated from the forced singular perturbation theory and serves to indicate the difference in time-scale between the expressions (1)-(6) and the body rate equations (7)-(9). Thus, with $\epsilon=0$, one obtains the slow-time scale problem, while $\epsilon=1$ yields the complete system. Assuming that the control surface deflections have a relatively small effect on lift, drag and sideforce, with $\epsilon=0$, the fast variables p , q and r appear 'control like' in the system (1) (6) with three nonlinear algebraic equations relating them to control surface deflections.

This approach runs into difficulty however, since the expression (4) does not contain p , q , r components explicitly. To remedy this situation, the expression (4) is differentiated once with respect to time and substituting for $\dot{\phi}$, $\dot{\theta}$ from expressions (5) and (6) one obtains

$$\dot{h} = H \quad (10)$$

$$\dot{H} = b_0 \dot{V} + b_1 \dot{\beta} + b_2 \dot{\alpha} + a_0 p + a_1 q + a_2 r \quad (11)$$

where

$$a_0 = b_0$$

$$a_1 = b_1 \cos\phi + b_2 \sin\phi \tan\theta$$

$$a_2 = b_1 \cos\phi \tan\theta - b_2 \sin\phi$$

and

$$b_0 = (\cos\beta \cos\alpha \sin\theta - \sin\beta \sin\phi \cos\theta - \cos\beta \sin\alpha \cos\phi \cos\theta)$$

$$b_1 = V(-\sin\beta \cos\alpha \sin\theta - \cos\beta \sin\phi \cos\theta + \sin\beta \sin\alpha \cos\phi \cos\theta)$$

$$b_2 = V(-\cos\beta \sin\alpha \sin\theta - \cos\beta \cos\alpha \cos\phi \cos\theta)$$

$$b_3 = V(\cos\beta \cos\alpha \cos\theta + \sin\beta \sin\phi \sin\theta + \cos\beta \sin\alpha \cos\phi \sin\theta)$$

$$b_4 = V(-\sin\beta \cos\phi \cos\theta + \cos\beta \sin\alpha \sin\phi \cos\theta)$$

In order to illustrate the singular perturbation procedure, the expressions (1)-(3), (5)-(11) are next expressed in a compact form as

$$\dot{\bar{x}} = A_1(\bar{x}) + B_1(\bar{x}) \bar{z} + C_1(\bar{x}) u_1 \quad (12)$$

$$\epsilon \dot{\bar{z}} = A_2(\bar{x}, u_1, \bar{z}) + B_2(\bar{z}) + C_2(\bar{x}) u_2 \quad (13)$$

with

$$\bar{x} = [V, \alpha, \beta, \theta, \phi, h, H],$$

$$u_1 = T$$

$$\bar{z} = [p, q, r]$$

$$u_2 = [\delta_e, \delta_a, \delta_r]$$

A nonlinear controller for the system (12), (13) can be designed by transforming it into Brunovsky's canonical form¹². But this would involve the computation of partial derivatives of the terms $A_1(\bar{x})$, $B_1(\bar{x})$ and $C_1(\bar{x})$. This difficulty is avoided by invoking the assumption that the body rates p , q and r evolve faster than other variables.

In the following, slow - fast controller synthesis using singular perturbation theory is discussed without any theoretical development. Setting $\epsilon=0$ in the system (12), (13) one obtains the slow system as

$$\dot{\bar{x}} = A_1(\bar{x}) + B_1(\bar{x}) \bar{z} + C_1(\bar{x}) u_1 \quad (14)$$

$$0 = A_2(\bar{x}, u_1, \bar{z}) + B_2(\bar{z}) + C_2(\bar{x}) \bar{u}_2 \quad (15)$$

\bar{z} are the values of fast state variables in the slow-time scale. Ideally, as in ref. 16, one should solve for \bar{z} in terms of u_1 from the expression (15) and substitute in the equations (14) to obtain a system independent of \bar{z} . This is

difficult in the aircraft trajectory control problem due to the nature of the functions A_2 and B_2 . Alternatively, a nonlinear controller can be synthesized for the dynamic system (14) with \bar{z} and u_1 as the controls to track the required \bar{x} commands, see ref. 16 for example. Next the \bar{z} obtained from this exercise can be substituted in (15) to solve for \bar{u}_2 , provided that $C_2(\bar{x})$ is invertible. This completes the design of slow time scale system.

To derive the fast-time scale controller, one assumes that the slow variables are constant in the fast-time scale dynamics. Subtracting (15) from (13) and putting

$$\Delta \bar{z} = \bar{z} - \bar{z}, \Delta u = u_2 - \bar{u}_2$$

one has

$$\Delta \dot{\bar{z}} = A_2(\bar{x}, \bar{u}_1, \Delta \bar{z}) + B_2(\Delta \bar{z}) + C_2(\bar{x}) \Delta u \quad (16)$$

\bar{x} , \bar{u}_1 are values of slow state variables in the fast-time scale problem. A nonlinear feedback controller can again be designed for the system (16) to maintain $\Delta \bar{z}$ close to zero. As long as the body rate dynamics remain faster than other dynamics, one would expect a satisfactory performance from this controller. The time scale separation similar to the one discussed here has been employed in the past for flight control system design and is known to be valid in most situations. If the actuator dynamics are to be included in the control system synthesis, they can be handled in an additional time scale. Thus, with time scale separation, the flight test trajectory controller will be of the form given in Figure 1.

In summary, the singular perturbation scheme described relies on the fact that the force generation mechanisms on the airframe are slower than moment generation processes.

NONLINEAR CONTROLLER DESIGN

The main specification on the flight test trajectory controller is that it should track given time histories of V , h and α . While there are no direct specifications on the angle of side slip β , it is desirable to maintain it close to zero throughout a given maneuver. In the following the slow and fast time scale controllers for tracking these will be discussed separately with specific details.

slow-time Scale Controller:

Setting the interpolation parameter to zero the slow-time scale dynamics given by the expressions (1)-(3), (5), (6) and (10), (11) can be written as

$$\dot{V} = c_0 + c_1 T \quad (17)$$

with

$$c_0 = [-D \cos \beta + S \sin \alpha - mg (\sin \theta \cos \alpha \cos \beta - \cos \theta \sin \phi \sin \beta - \cos \theta \cos \phi \sin \alpha \cos \beta)]/m$$

$$c_1 = (k_1 \cos \alpha \cos \beta + k_2 \sin \alpha \cos \beta)/m$$

and

$$\dot{\alpha} = c_2 + c_3 T + c_4 \bar{p} + c_5 \bar{q} + c_6 \bar{r} \quad (18)$$

with

$$c_2 = [-L + mg (\cos \theta \cos \phi \cos \alpha + \sin \theta \sin \alpha)]/mV \cos \beta$$

$$c_3 = (k_3 \cos \alpha - k_4 \sin \alpha)/mV \cos \beta$$

$$c_4 = -\cos \alpha \tan \beta$$

$$c_5 = 1$$

$$c_6 = -\tan \beta \sin \alpha$$

and

$$\dot{\beta} = d_0 + d_1 T + d_2 \bar{p} + d_3 \bar{r} \quad (19)$$

with

$$d_0 = [D \sin \beta + S \cos \beta + mg (\sin \theta \cos \alpha \sin \beta + \cos \theta \sin \phi \cos \beta - \cos \theta \cos \phi \sin \alpha \sin \beta)]/Vm$$

$$d_1 = (-k_1 \cos \alpha \sin \beta - k_2 \sin \alpha \sin \beta)/Vm$$

$$d_2 = \sin \alpha$$

$$d_3 = -\cos \alpha$$

$$\dot{\phi} = d_4 \bar{p} + d_5 \bar{q} + d_6 \bar{r} \quad (20)$$

$$\dot{\theta} = d_7 \bar{q} + d_8 \bar{r} \quad (21)$$

with

$$d_4 = 1$$

$$d_5 = \sin \phi \tan \theta$$

$$d_6 = \cos \phi \tan \theta$$

$$d_7 = \cos \phi$$

$$d_8 = -\sin \phi$$

ORIGINAL PAGE IS
OF POOR QUALITY

$$\dot{h} = H \quad (22)$$

$$\dot{H} = \ddot{h} = b_0 \dot{V} + b_1 \dot{\beta} + b_2 \dot{\alpha} + a_0 \bar{p} + a_1 \bar{q} + a_2 \bar{r} \quad (23)$$

$$0 = [\bar{p}I_1 + \bar{r}I_2 + e_1 I_1 \bar{\delta}_e + e_2 I_1 \bar{\delta}_a + e_3 I_1 \bar{\delta}_r + \bar{p} \bar{q} (I_{xz} I_1 - D_z I_2) - \bar{q} \bar{r} (D_x I_1 + I_{xz} I_2)]/I \quad (24)$$

$$0 = [\bar{q}I_3 + f_1 I_1 \bar{\delta}_e + f_2 I_1 \bar{\delta}_a + f_3 I_1 \bar{\delta}_r + \bar{p}^2 I_{xz} I_1 - \bar{p} \bar{r} D_y I_1 + \bar{r}^2 I_{xz} I_1]/I \quad (25)$$

$$0 = [\bar{r}I_4 + \bar{q}I_5 + g_1 I_1 \bar{\delta}_e + g_2 I_1 \bar{\delta}_a + g_3 I_1 \bar{\delta}_r + \bar{p} \bar{q} (I_{xz} I_3 - D_z I_4) - \bar{q} \bar{r} (D_x I_3 + I_{xz} I_4)]/I \quad (26)$$

The system (17)-(26) describes the slow-time scale dynamics with control variables \bar{p} , \bar{q} , \bar{r} and T , the body rates and the engine thrust. Since there are seven state variables and four control variables, only four of these states can be completely controlled.

The variables of interest in the present flight test trajectory control problem can be broadly grouped into two sets i.e., tracking the variables

$$(i) \quad V, h, \alpha, \beta$$

or

$$(ii) \quad V, h, \beta, \phi$$

Consequently, the number of states to be controlled is equal to the number of controls. The other state variables are treated as free. The discussions in the following will be limited to Case (i). Case (ii) can be handled in an entirely analogous manner. Since there are four state-variables to be tracked and four control variables, the slow-time scale system can be put in the following form by defining four new pseudo-controls U_1, U_2, U_3, U_4 .

$$\begin{aligned} \dot{h} &= H \\ \dot{H} &= U_1 \\ \dot{V} &= U_2 \\ \dot{\alpha} &= U_3 \\ \dot{\beta} &= U_4 \end{aligned} \quad (27)$$

Next, four independent linear controllers can be designed for this system to ensure zero tracking errors for ramp commands. Typically, the airspeed angle of attack and angle of side slip will have proportional plus integral control while the altitude loop will have a proportional plus derivative control. The form of these pseudo controller loops is given in Figure 2 and 3.

It can be verified that except for the altitude loop, all other controllers will have zero steady state errors for ramp commands. Moreover, the natural frequencies and damping ratios of these control loops are

(i) airspeed loop:

$$\omega_{n_V} = \sqrt{k_2}, \quad \xi_V = \frac{k_1}{2\sqrt{k_2}}$$

(ii) Angle of attack loop:

$$\omega_{n_\alpha} = \sqrt{k_4}, \quad \xi_\alpha = \frac{k_3}{2\sqrt{k_4}}$$

(iii) Angle of side slip:

$$\omega_{n_\beta} = \sqrt{k_6}, \quad \xi_\beta = \frac{k_5}{2\sqrt{k_6}}$$

(iv) Altitude loop:

$$\omega_{n_h} = \sqrt{k_7}, \quad \xi_h = \frac{k_6}{2\sqrt{k_7}}$$

Hence, two time response specifications can be set for each of these control loops. Note, however, that the extent to which these specifications are met would depend on the actuator saturation levels and the tracking commands.

The remaining task in the slow-time scale control problem is that of converting the four pseudo controls to the four real controls. Thus, from (17)-(19) and (23), one has

$$T = (U_2 - c_0)/c_1 \quad (28)$$

$$\begin{bmatrix} a_0 & a_1 & a_2 \\ c_4 & c_5 & c_6 \\ d_2 & 0 & d_3 \end{bmatrix} \begin{bmatrix} \bar{p} \\ \bar{q} \\ \bar{r} \end{bmatrix} = \begin{bmatrix} U_1 - (b_0 U_2 + b_1 U_3 + b_2 U_4) \\ U_2 - c_2 - c_3 T \\ U_3 - d_0 - d_1 T \end{bmatrix} \quad (29)$$

It is assumed here that the required thrust given by the expression (28) can be converted into the throttle setting using tabular data. The set of linear equations (29) can be solved for \bar{p} , \bar{q} , \bar{r} . If the aircraft is in symmetric flight, the 3x3 matrix premultiplying \bar{p} , \bar{q} , \bar{r} vector will have less than three rank. This is because under these conditions, in the reduced order problem, there are three longitudinal state variables to be controlled while there are only two available controls, viz; the thrust T and the pitch body rate \dot{q} . Hence one can precisely control the airspeed and altitude or the airspeed and angle of attack or the angle of attack and altitude. However, if a linear combination of any two of these three variables is formed, then that linear combination can be controlled exactly along with the remaining variable. The situation in the lateral channel is reverse under the symmetric

flight condition, i.e., there are two control variables, \tilde{r} and \tilde{p} available while there is just one state, β , to be controlled. Thus, in the lateral channel, the angle of side slip can be maintained zero either by the yaw body rate \tilde{r} or the roll body rate \tilde{p} or by a linear combination of these. The approach adopted in the present work is to use \tilde{r} to control β while using \tilde{p} to maintain the roll attitude zero.

Once the expressions (28) and (29) have been solved, the \tilde{p} , \tilde{q} , \tilde{r} values and thrust can be substituted in equations (24)-(26) to compute the control surface deflections δ_e , δ_a , δ_r along the "outer" solution.

Fast-time scale controller:

In the fast-time scale, the slow-time scale variables h , V , α , β are assumed to remain constant. The fast-time scale controller attempts to maintain the body rates p , q , r close to their values in the "outer" solution. Subtracting the expressions (24)-(26) from (7)-(9), and putting

$$\Delta p = p - \tilde{p}, \Delta q = q - \tilde{q}, \Delta r = r - \tilde{r}$$

one obtains

$$\begin{aligned} \dot{\Delta p} = & [(P - \tilde{P})I_1 + (R - \tilde{R})I_1 + e_1 I_1 (\delta_e - \tilde{\delta}_e) \\ & + e_2 I_1 (\delta_a - \tilde{\delta}_a) + e_3 I_1 (\delta_r - \tilde{\delta}_r) + \\ & (\Delta p \cdot \Delta q + \tilde{p} \cdot \Delta q + \tilde{q} \cdot \Delta p) (I_{xz} I_1 - D_z I_1) \\ & - (\Delta q \cdot \Delta r + \tilde{q} \cdot \Delta r + \tilde{r} \cdot \Delta q) (D_x I_1 + I_{xz} I_1)] / I \end{aligned} \quad (30)$$

$$\begin{aligned} \dot{\Delta q} = & [(Q - \tilde{Q})I_1 + f_1 I_1 (\delta_e - \tilde{\delta}_e) + f_2 I_1 (\delta_a - \tilde{\delta}_a) \\ & + f_3 I_1 (\delta_r - \tilde{\delta}_r) + (\Delta p + \Delta p \cdot \tilde{p}) I_{xz} I_1 \\ & - (\Delta p \cdot \Delta r + \Delta r \cdot \tilde{p} + \Delta p \cdot \tilde{r}) D_y I_1 \\ & + (\Delta r + \Delta r \cdot \tilde{r}) I_{xz} I_1] / I \end{aligned} \quad (31)$$

$$\begin{aligned} \dot{\Delta r} = & [(P - \tilde{P})I_1 + (R - \tilde{R})I_1 + g_1 I_1 (\delta_e - \tilde{\delta}_e) \\ & + g_2 I_1 (\delta_a - \tilde{\delta}_a) + g_3 I_1 (\delta_r - \tilde{\delta}_r) - (\Delta p \cdot \Delta r \\ & + \tilde{q} \cdot \Delta r + \tilde{r} \cdot \Delta q) (D_x I_1 + I_{xz} I_1)] / I \end{aligned} \quad (32)$$

The fast-time scale controller maintains Δp , Δq , Δr close to zero throughout a given maneuver. Since there are three independent controls available, three pseudo controls are next defined such that the system (30)-(32) takes the form

$$\begin{aligned} \dot{\Delta p} &= U_s \\ \dot{\Delta q} &= U_e \\ \dot{\Delta r} &= U_r \end{aligned} \quad (33)$$

Three independent control loops can be designed in pseudo controls U_s , U_e , U_r such that the system (33) has a much faster time constant than the slow-time scale system (17)-(26). Integral feedbacks are not necessary for these control loops since

there are no explicit tracking requirements. The real controls can be obtained from pseudo controls as

$$\begin{bmatrix} e_1 I_1 & e_2 I_1 & e_3 I_1 \\ f_1 I_1 & f_2 I_1 & f_3 I_1 \\ g_1 I_1 & g_2 I_1 & g_3 I_1 \end{bmatrix} \begin{bmatrix} (\delta_e - \tilde{\delta}_e) \\ (\delta_a - \tilde{\delta}_a) \\ (\delta_r - \tilde{\delta}_r) \end{bmatrix} = \begin{bmatrix} f_s \\ f_e \\ f_r \end{bmatrix} \quad (34)$$

where

$$\begin{aligned} f_s = & IU_s - (P - \tilde{P})I_1 - (R - \tilde{R})I_1 - (\Delta p \cdot \Delta q + \tilde{p} \cdot \Delta q \\ & + \tilde{q} \cdot \Delta p) (I_{xz} I_1 - D_z I_1) - (\Delta q \cdot \Delta r \\ & + \tilde{q} \cdot \Delta r + \tilde{r} \cdot \Delta q) (D_x I_1 + I_{xz} I_1) \end{aligned}$$

$$\begin{aligned} f_e = & IU_e - (Q - \tilde{Q})I_1 - (\Delta p + \Delta p \cdot \tilde{p}) I_{xz} I_1 \\ & + (\Delta p \cdot \Delta r + \Delta r \cdot \tilde{p} + \Delta p \cdot \tilde{r}) D_y I_1 \\ & - (\Delta r + \Delta r \cdot \tilde{r}) I_{xz} I_1 \end{aligned}$$

$$\begin{aligned} f_r = & IU_r - (P - \tilde{P})I_1 - (R - \tilde{R})I_1 + (\Delta q \cdot \Delta r + \tilde{q} \cdot \Delta r \\ & + \tilde{r} \cdot \Delta q) (D_x I_1 + I_{xz} I_1) \end{aligned}$$

The set of linear algebraic equations (34) can be solved for $(\delta_e - \tilde{\delta}_e)$, $(\delta_a - \tilde{\delta}_a)$ and $(\delta_r - \tilde{\delta}_r)$. Note that the matrix multiplying these quantities has full rank everywhere on the flight envelope and a unique solution always exists. Since $\tilde{\delta}_e$, $\tilde{\delta}_a$, $\tilde{\delta}_r$ are known from the outer solution, the actual control surface deflections can be computed.

NONLINEAR CONTROLLER EVALUATION

In order to test the performance of the nonlinear controller synthesized in Section 3, it is implemented on a six-degrees-of-freedom simulation of a high performance fighter aircraft including a first order engine dynamics. Two symmetric flight test maneuvers were executed, viz, a level acceleration trajectory and a pushover-pullup trajectory.

The level acceleration trajectory is a wings level, constant altitude maneuver with a ramp Mach number command. This maneuver is initiated at 20000' and Mach 0.9. The objective is to accelerate the aircraft at about 10ft/sec for 5 seconds. An initial constant Mach number leg is included in the command history to provide adequate time for damping out the effect of inexact trim conditions. The Mach number command as well as the response of the aircraft are given in Fig. 4. The altitude history is given in Fig. 5, and the throttle setting is in Fig. 6. The Mach number tracking error is less than ± 0.001 during most of the acceleration phase. The altitude is maintained within ± 0.2 feet. This maneuver required the after-burner thrust as can be seen from the throttle history in Fig. 6.

A pushover-pullup trajectory is executed next. This flight test trajectory is a wings level, constant Mach number maneuver in which the angle of attack is varied a specified increment about the trim value at some specified rate. Fig. 7 depicts

the commanded and the actual angle of attack. The angle of attack tracking error is well within $\pm 0.1^\circ$. The Mach number was maintained within ± 0.006 throughout the maneuver as can be observed from Fig. 8. A transient appearing at 20 seconds in the Mach number history is due to the throttle-thrust characteristics of the engine. For this aircraft engine, there is small core thrust saturation region approximately between 83 and 98 degrees of throttle setting. This region is illustrated on the throttle setting curve in Fig. 9. Note that in this maneuver, the altitude is not controlled and it is free to change as it may throughout the trajectory. In Fig. 10, the resulting altitude is given. During the initial negative angle of attack rate region as well as for some positive angle of attack rate, the aircraft loses as much as 2000 feet. During the second half of this maneuver, the aircraft gains altitude and overshoots the initial altitude by almost 700 feet. If desired, the commanded angle of attack history can be tailored to return the aircraft to initial straight and level conditions at the end of the maneuver.

Summarizing the results presented so far, the nonlinear controller performance for these two maneuvers has been found very good. Currently, work is underway to evaluate the controller performance along several other maneuvers.

CONCLUSIONS:

Nonlinear controllers for tracking flight test trajectory commands were described. The controller development employed singular perturbation theory and the recent results for a class of nonlinear systems. The synthesized controllers do not require gain scheduling and can be implemented at

different rates on the flight control computer. The approach presented here can be extended for tracking three position components and velocity for example, as in an autoland task. The synthesized control laws have a general character in the sense that their form remains invariant for any conventional aircraft. However, the time-scale separation presented must be valid for the maneuver under consideration.

Acknowledgement:

The first author would like to thank Dr. G Meyer of NASA Ames Research Center for kindly furnishing us with the copies of his papers and reports. We thank Mr. Robert Antoniewicz of NASA Ames-Dryden Flight Research for help in the controller implementation.

References:

[1] Duke, E.L., "Automated Flight Test Maneuvers: The Development of a New Technique", Flight Testing Technology-A State-of-the-Art Review, pp. 101-119, Proceedings of the Society of Flight Test Engineers 13th Annual Symposium, New York, N.Y., September 1982.

- [2] Duke, E.L., Swann, M.R., Enevoldson, E.K., and Wolf, T.D., "Experience with Flight Test Trajectory Guidance", J. Guidance, Control, and Dynamics, pp. 393-398 Vol 6., Sept.-Oct. 1983.
- [3] "Final Report, HiMAT Maneuver Autopilot", TRA 29255-1, Teledyne Ryan Aeronautical, February 1981.
- [4] Walker, R.A., and Gupta, N.K., "Flight Test Trajectory Control Analysis", NASA CR 170395 February 1983.
- [5] Menon, P.K.A., Saberli, H.A., Walker, R.A. and Duke, E.L., "Flight Test Trajectory Controller synthesis with Eigenstructure Assignment", 1985 American Control Conference, June 19-21, Boston, MA, paper #FA1.
- [6] Menon, P.K.A. and Walker, R.A., "Aircraft Flight Test Trajectory Control", ISI Report 56, Prepared for NASA Ames-Dryden Flight Research Facility under contract NAS2-11877, March 1985.
- [7] Meyer, G. and Cicolani, S., "A Formal Structure for Advanced Automatic Flight Control Systems". NASA TN D-7940, 1975.
- [8] Brockett, R.W., 'Nonlinear systems and Differential Geometry', proceedings of the IEEE, vol. 64, Feb. 1976, pp 61-72.
- [9] Smith, G.A. and Meyer, G., "Total Aircraft Flight-Control System - Balanced Open - and Closed-Loop Control With Dynamic Trim Maps. Proceedings of the Third Digital Avionics Systems Conference, Ft. Worth, Texas. Nov. 1979, IEEE Catalog No 79CH1518-0.
- [10] Smith, G.A. and Meyer, G., Application of the Concept of Dynamic Trim Control to Automatic Landing of Carrier Aircraft. NASA TP-1512, 1980.
- [11] Hunt, L.R., and Su, R., Control of Nonlinear Time-Varying Systems. IEEE Conference on Decision and Control, 1981, pp. 558-563.
- [12] Hunt, L.R., Su, R., and Meyer, G., Global Transformations of Nonlinear Systems. IEEE Trans. on Auto. Control, vol. Jan 1983, pp. 24-31.
- [13] Hunt, L.R., Su, R., and Meyer, G., Multi-Input Nonlinear Systems, in Differential Geometric Control Theory Conference, Birkhauser, Boston, Cambridge, Mass., 1982.
- [14] Meyer, G., Su, R. and Hunt, L.R., "Application of Nonlinear Transformations to Automatic Flight Control" Automatica, Vol 20, pp. 103-107, 1984.
- [15] Dwyer, T.A.W., "Exact Nonlinear Control of Large Angle Rotational Maneuvers", IEEE Trans. Auto. Control, Vol AC-29, No 9, September 1984, pp. 769-774.
- [16] Chow, J.H. and Kokotovic, P.V., "Two-Time-Scale Feedback Design of a class of Nonlinear Systems", IEEE Trans. Auto. Control, Vol AC-23, June 1978, pp. 438-443.

ORIGINAL PAGE IS
OF POOR QUALITY

- [17] Chow, J.H., and Kokotovic, P.V., "A Decomposition of Near-optimum Regulators for Systems with Slow and Fast-modes", IEEE Trans. Auto. Control, Vol. 21, pp. 701-705, October 1976.
- [18] Khalil, H.K., "Linear Quadratic Gaussian Estimation and Control of Singularly Perturbed Systems", in Singular Perturbations in Systems and Control, M.D. Ardema (Ed.) Springer-Verlag, Wien-New York CISM courses and Lectures No 280, 1984.
- [19] Kelley, H.J., "Aircraft Maneuver Optimization by Reduced order Approximation", in Control and Dynamic Systems, Vol. 10., C.T. Leondes (Ed.), Academic press, New York, 1973, pp 131-178.
- [20] Etkin, B., Dynamics of Atmospheric Flight, John Wiley and Sons, 1972.

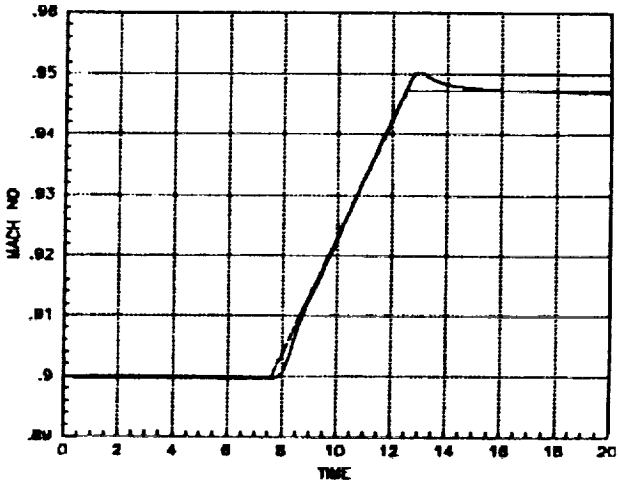
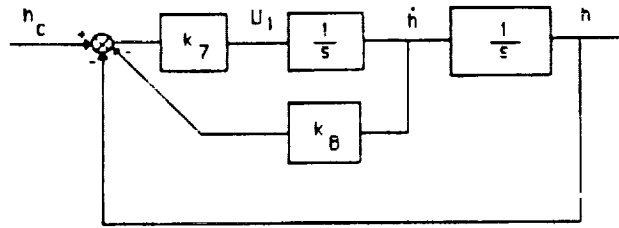


Figure 4. Mach Number Evolution Along The Level Acceleration Flight Test Trajectory
 - - - Commanded Mach Number
 ——— Actual Mach Number

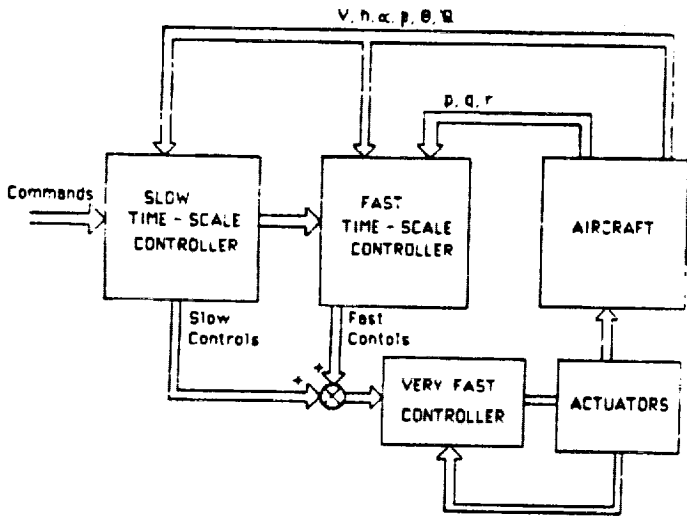
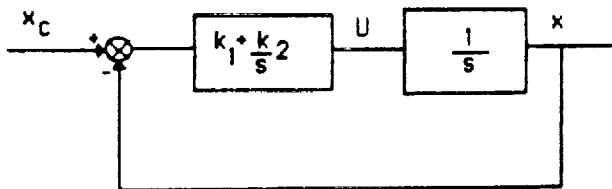


Figure 1. SP Nonlinear Flight Test Trajectory Controller



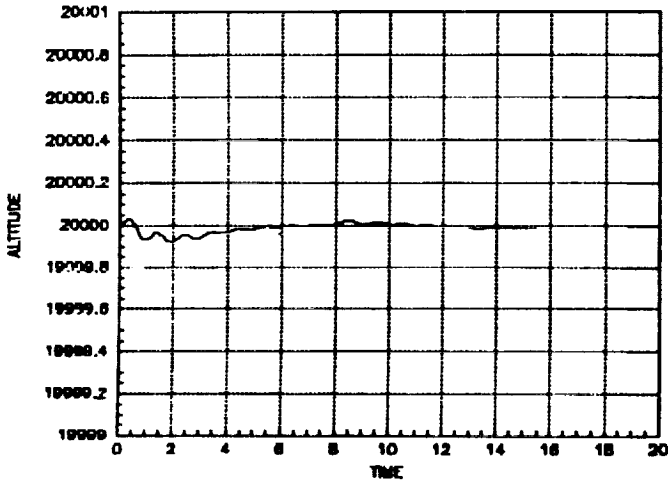


Figure 5. Altitude History Along The Level Acceleration Flight Test Trajectory (seconds, feet)

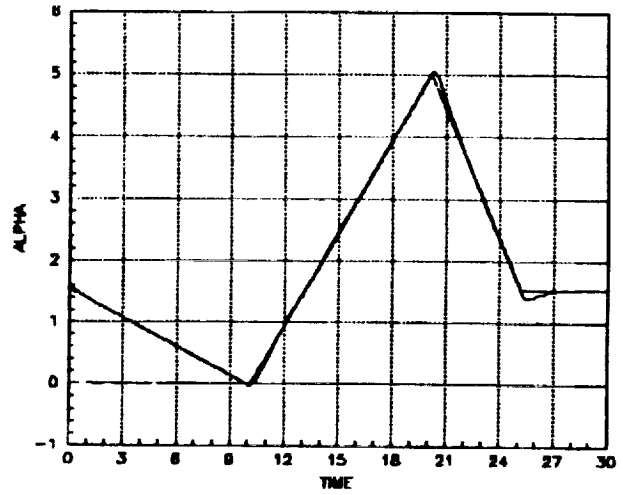


Figure 7. Angle of Attack Along The Pushover-Pullup Flight Test Trajectory (seconds, degrees)

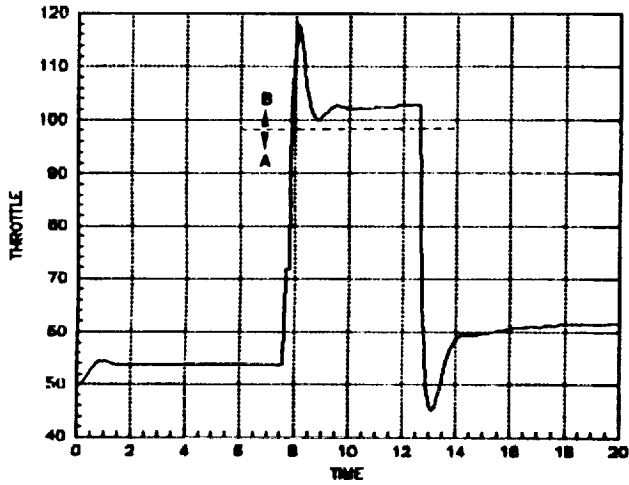


Figure 6. Throttle Setting Along The Level Acceleration Flight Test Trajectory

- A: Core Thrust
- B: Augmentor Thrust

- - - Commanded Angle of Attack
- Actual Angle of Attack

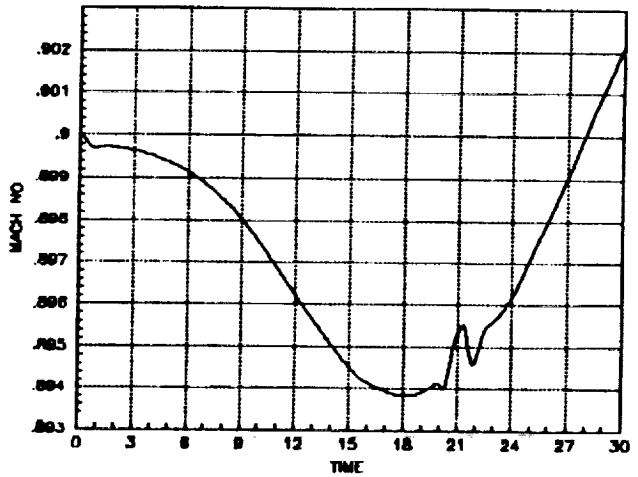


Figure 8. Mach Number Evolution Along The Pushover-Pullup Flight Test Trajectory

ORIGINAL PAGE IS
OF POOR QUALITY

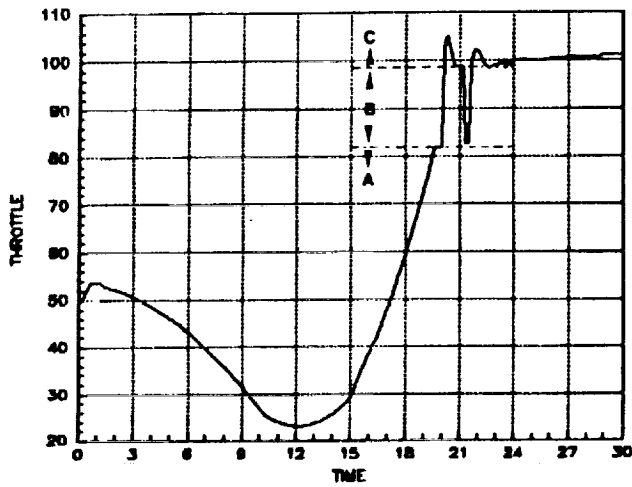


Figure 9. Throttle Setting Along The Pushover-Pullup Flight Test Trajectory

A: Core Thrust
 B: Core Thrust Saturation Region
 C: Augmentor Thrust

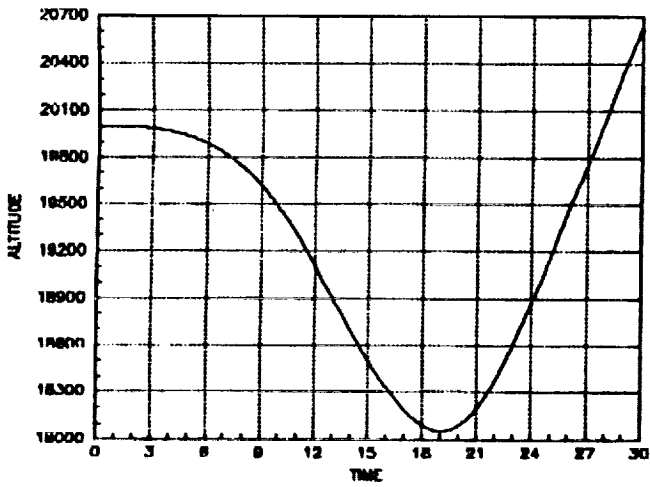


Figure 10. Altitude Evolution Along The Pushover-Pullup Flight Test Trajectory (seconds, feet)



Report Documentation Page

1. Report No. NASA CR-179442		2. Government Accession No.		3. Recipient's Catalog No.	
4. Title and Subtitle Nonlinear Maneuver Autopilot for the F-15 Aircraft				5. Report Date June 1989	
				6. Performing Organization Code	
7. Author(s) P.K.A. Menon, M.E. Badgett, and R.A. Walker				8. Performing Organization Report No. H-1541	
				10. Work Unit No. RTOP 505-66-71	
9. Performing Organization Name and Address Integrated Systems, Inc. 101 University Avenue Palo Alto, California 94301-1695				11. Contract or Grant No. NAS 2-11877	
				13. Type of Report and Period Covered Contractor Report - Final	
12. Sponsoring Agency Name and Address National Aeronautics and Space Administration Washington, DC 20546				14. Sponsoring Agency Code	
15. Supplementary Notes NASA Technical Monitor: E. Lee Duke, Ames Research Center, Dryden Flight Research Facility, Edwards, California 93523-5000					
16. Abstract This report describes a methodology for the development of flight test trajectory control laws based on singular perturbation methodology and nonlinear dynamic modeling. The control design methodology is applied to a detailed nonlinear six-degree-of-freedom simulation of the F-15 and results for a level accelerations, pushover/pullup maneuver, zoom and pushover maneuver, excess thrust windup turn, constant thrust windup turn, and a constant dynamic pressure/constant load factor trajectory are presented.					
17. Key Words (Suggested by Author(s)) Expert systems Fault detection Fault isolation Control systems			18. Distribution Statement Unclassified — Unlimited Subject category 63		
19. Security Classif. (of this report) Unclassified		20. Security Classif. (of this page) Unclassified		21. No. of pages 97	22. Price A05

